VOLUME II
FLYING QUALITIES PHASE

# CHAPTER 7
# LATERAL-DIRECTIONAL STATIC STABILITY



OCTOBER 1990

USAF TEST PILOT SCHOOL
EDWARDS AFB CA

# DISCLAIMER NOTICE

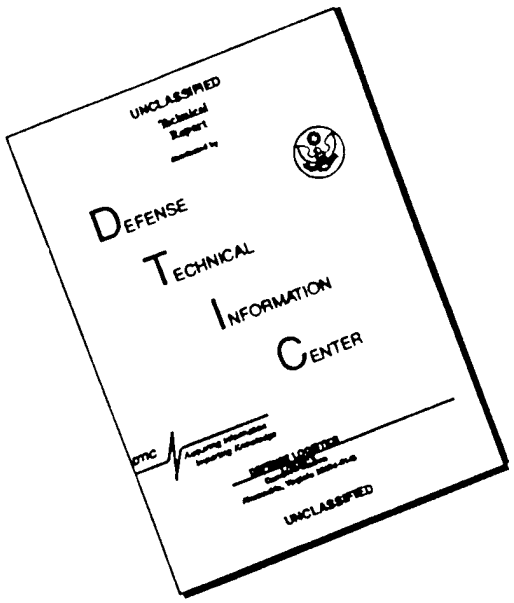


THIS DOCUMENT IS BEST QUALITY AVAILABLE. THE COPY FURNISHED TO DTIC CONTAINED A SIGNIFICANT NUMBER OF PAGES WHICH DO NOT REPRODUCE LEGIBLY.

## 7.1 INTRODUCTION

Your study of flying qualities to date has been concerned with the stability of the airplane flying in equilibrium on symmetrical flight paths. More specifically, you have been concerned with the problem of providing control over the airplane's angle of attack and thereby its lift coefficient, and with ensuring static stability of this angle of attack.

This course considers the characteristics of the airplane when its flight path no longer lies in the plane of symmetry. This means that the relative wind will make some angle to the aircraft centerline which we define as $\beta$. The motions which result from $\beta$ being applied to the airplane are motion along the y-axis and motion about the x and z axes. These motions can be described by the following equations of aircraft lateral-directional motion

$$F_y = m\dot{v} + m\,r\,U - p\,w\,m \tag{7.1}$$

$$G_x = \dot{p}I_x + qr\,(I_z - I_y) - (\dot{r} + pq)\,I_{xz} \tag{7.2}$$

$$G_z = \dot{r}I_z + pq\,(I_y - I_x) + (qr - \dot{p})\,I_{xz} \tag{7.3}$$

where the right side of the equation represents the response of an aircraft to the applied forces and moments on the left side. These applied forces and moments are composed primarily of contributions from aerodynamic forces and moments, direct thrust, gravity, and gyroscopic moments. Since the aerodynamic forces and the moments are by far the most important, we shall consider the other contributions as negligible or as having been eliminated through proper design.

It has been shown in Equations of Motion that when operating under a small disturbance assumption, aircraft lateral-directional motion can be considered independent of longitudinal motion and can be considered as a function of the following variables

$$(Y,\ L,\ N) = f\,(\beta,\ \dot{\beta},\ p,\ r,\ \delta_a,\ \delta_r) \tag{7.4}$$

The ensuing analysis is concerned with the question of lateral-directional static stability or the initial tendency of an airplane to return to stabilized flight after being perturbed in sideslip or roll. This will be determined by the values of the yawing and rolling moments (N and L). Since the side force equation governs only the aircraft translatory response and has no effect on the angular motion, the side force equation will not be considered.

The two remaining aerodynamic functions can be expressed in terms of non-dimensional stability derivatives, angular rates and angular displacements

$$C_n = C_{n_\beta}\beta + C_{n_{\dot\beta}}\frac{\dot\beta b}{2U_o} + C_{n_p}\frac{pb}{2U_o} + C_{n_r}\frac{rb}{2U_o} + C_{n_{\delta_a}}\delta_a + C_{n_{\delta_r}}\delta_r \quad (7.5)$$

$$C_l = C_{l_\beta}\beta + C_{l_{\dot\beta}}\frac{\dot\beta b}{2U_o} + C_{l_p}\frac{pb}{2U_o} + C_{l_r}\frac{rb}{2U_o} + C_{l_{\delta_a}}\delta_a + C_{l_{\delta_r}}\delta_r \quad (7.6)$$

The analysis of aircraft lateral-directional motion is based on these two equations. A cursory examination of these two equations reveals that they are "cross-coupled." That is, $C_{n_p}$ and $C_{n_{\delta_a}}$ are found in Equation 7.5, while $C_{l_r}$ and $C_{l_{\delta_r}}$ are present in the lateral Equation 7.6. It is for this reason that aircraft lateral and directional motions must be considered together - each one influences the other.

## 7.2 TERMINOLOGY

Since considerable confusion can arise if the terms sideslip and yaw are misunderstood, we shall define them before proceeding further.

Sideslip is defined as the angle the relative wind makes with the XZ plane of the aircraft. From Figure 7.1, we see that the angle of sideslip, $\beta$, is equal to the arcsin (v/V), or for the small angles normally encountered in flight, $\beta \equiv v/V$. By definition, $\beta$ is positive when the relative wind is to the right of the geometric longitudinal axis of the airplane (i.e., when wind is in the right ear).

Yaw angle, $\psi$, is defined as the angular displacement of the airplane's longitudinal axis in the horizontal plane from some arbitrary direction taken as zero at some instant in time (Figure 7.1). Note that for a curved flight path, yaw angle does not equal sideslip angle. For example, in a 360° turn, the airplane yaws through 360°, but may not develop any sideslip during the maneuver, if the turn is perfectly coordinated.

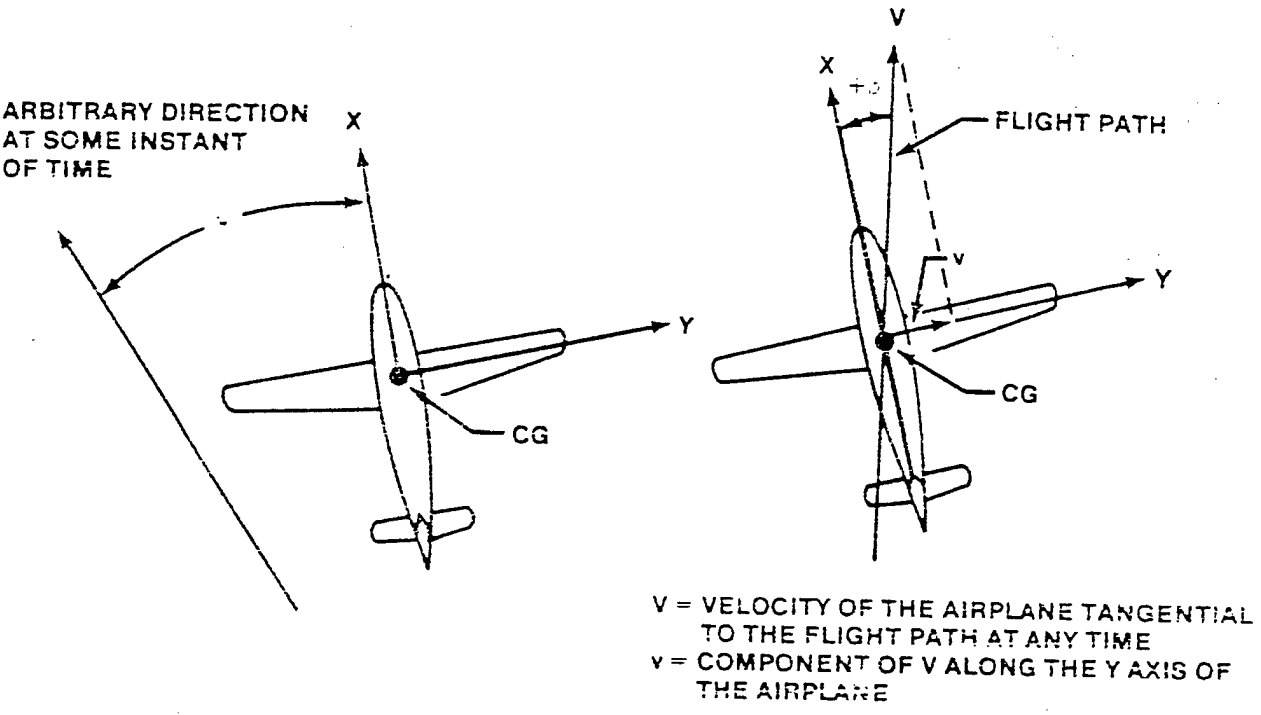


FIGURE 7.1. YAW AND SIDESLIP ANGLE

With these definitions of yaw and sideslip in mind, each of the stability derivatives comprising Equations 7.5 and 7.6 may be analyzed.

## 7.3 DIRECTIONAL STABILITY

In general, it is advantageous to fly an airplane at zero sideslip, and the easier it is for a pilot to do this, the better he will like the flying qualities of his airplane. The problem of directional stability and control, then, is first to ensure that the airplane will tend to remain in equilibrium at zero sideslip, and second to provide a control to maintain zero sideslip during maneuvers that introduce moments tending to produce sideslip. The stability derivatives which contribute to static directional stability are those comprising Equation 7.5. A summary of these derivatives is shown in Table 7.1.

TABLE 7.1
DIRECTIONAL STABILITY AND CONTROL DERIVATIVES

| DERIVATIVE | NAME | SIGN FOR A STABLE AIRCRAFT | CONTRIBUTING PARTS OF AIRCRAFT |
|---|---|---|---|
| $C_{n_\beta}$ | Static Directional Stability or Weathercock Stability | (+) | Tail, Fuselage, Wing |
| $C_{n_{\dot\beta}}$ | Lag Effects | (-) | Tail |
| $C_{n_p}$ | Cross-Coupling | (+) | Wing, Tail |
| $C_{n_r}$ | Yaw Damping | (-) | Tail, Wing, Fuselage |
| $C_{n_{\delta_a}}$ | Adverse or Proverse (complimentary) Yaw | "O" or slightly (-) | Lateral Control |
| $C_{n_{\delta_r}}$ | Rudder Power | (+) | Rudder Control |

### 7.3.1 $C_{n_\beta}$ Static Directional Stability or Weathercock Stability

Static directional stability is defined as the initial tendency of an aircraft to return to, or depart from, its equilibrium angle of sideslip (normally zero) when disturbed. Although the static directional stability of an aircraft is fully described by Equation 7.5, $C_{n_\beta}$ is often referred to as "static directional stability" because it is the predominant term.

When an aircraft is placed in a sideslip, aerodynamic forces develop which create moments about all three axes. The moments created about the z-axis tend to turn the nose of the aircraft into or away from the relative wind. The aircraft has positive directional stability if the moments created by a sideslip angle tend to align the nose of the aircraft with the relative wind.

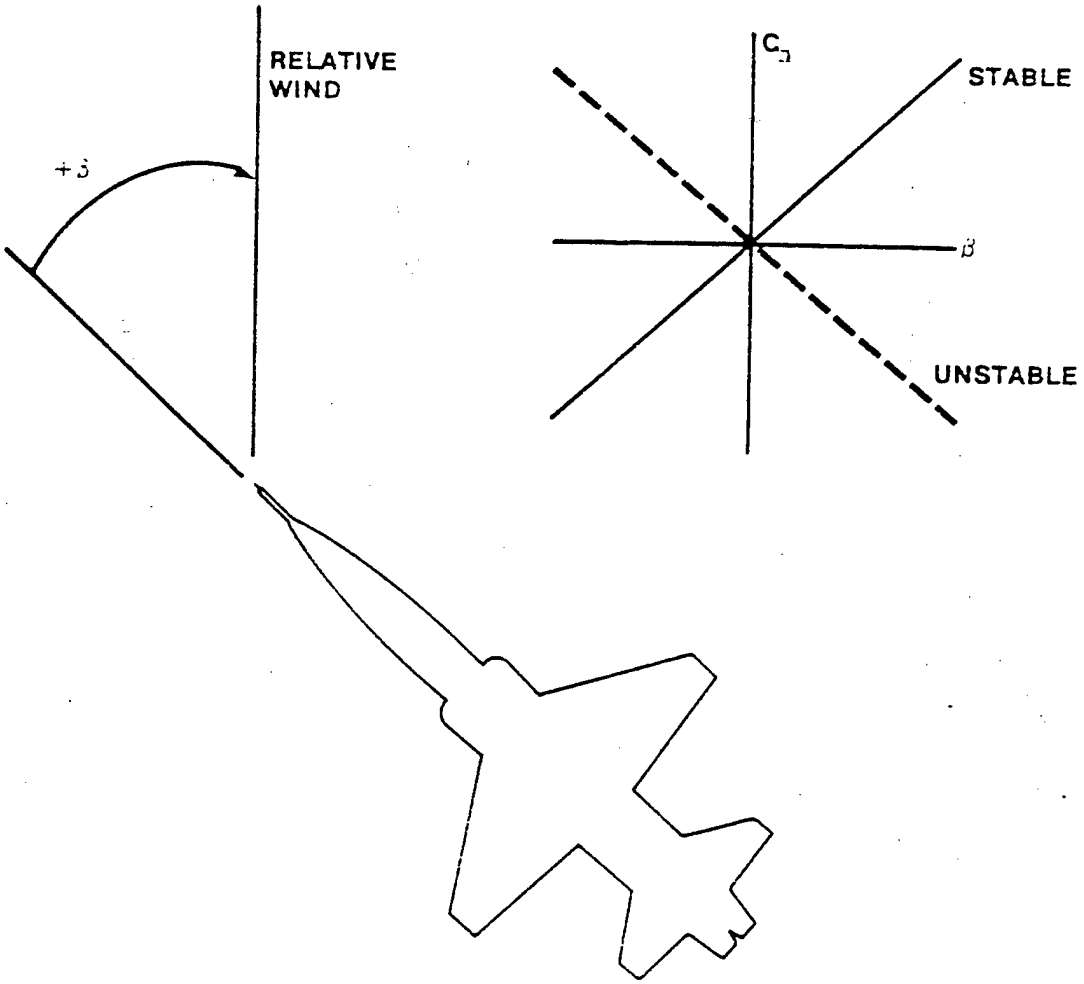


FIGURE 7.2. STATIC DIRECTIONAL STABILITY

In Figure 7.2 the aircraft is in a right sideslip. It is statically stable if it develops yawing moments that tend to align it with the relative wind, or in this case, right (positive) yawing moments. Therefore, an aircraft is statically directionally stable if it develops positive yawing moments with a positive increase in sideslip. Thus, the slope of a plot of yawing moment coefficient, $C_n$, versus sideslip, $\beta$, is a quantitative measure of the static directional stability that an aircraft possesses. This plot would normally be determined from wind tunnel results.

The total value of the directional stability derivative, $C_{n_\beta}$, at any sideslip angle, is determined primarily by contributions from the vertical tail, the fuselage, and the wing. These contributions will be discussed separately.

7.3.1.1 Vertical Tail Contribution to $C_{n_\beta}$. The vertical tail is the primary source of directional stability for virtually all aircraft. When the aircraft is yawed, the angle of attack of the vertical tail is changed. This change of angle of attack produces a change in lift on the vertical tail, and thus a yawing moment about the Z-axis.

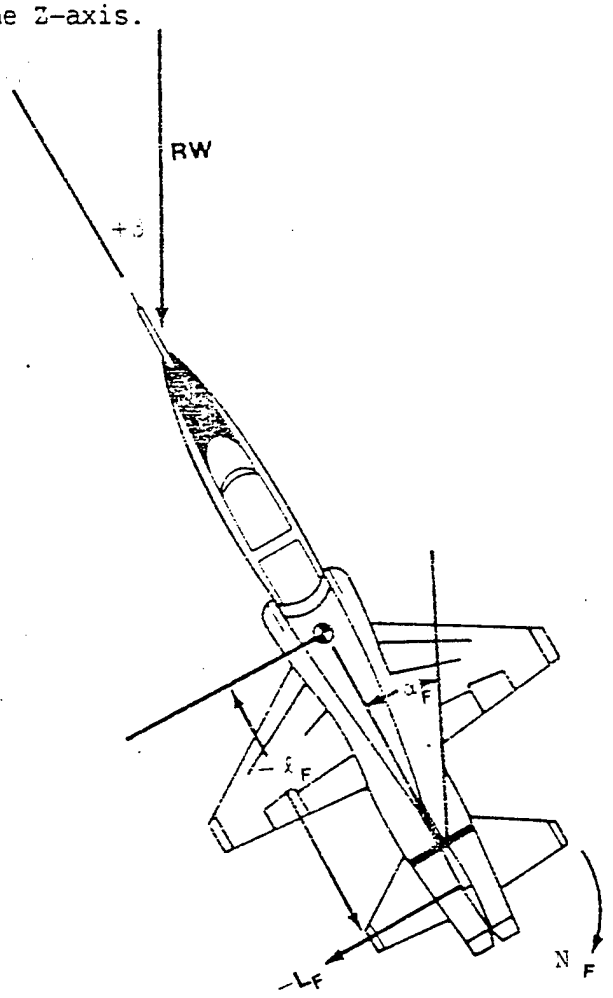


FIGURE 7.3. VERTICAL TAIL CONTRIBUTION TO $C_{n_\beta}$

Referring to Figure 7.3, the yawing moment produced by the tail is

$$N_F = (-l_F)(-L_F) = l_F L_F \tag{7.7}$$

The minus signs in this equation arise from the use of the sign convention adopted in the study of aircraft equations of motion. Forces to the left and distances behind the aircraft cg are negative.

As in other aerodynamic considerations, it is convenient to consider yawing moments in coefficient form so that static directional stability can be evaluated independent of weight, altitude and speed. Putting Equation 7.7 in coefficient form

$$C_{n_F} = \frac{l_F L_F}{q_w S_w b_w} = \frac{l_F C_{L_F} q_F S_F}{q_w S_w b_w} \quad \text{[where } q = 1/2\ \rho V^2 \text{ and } w = \text{wing]} \tag{7.8}$$

Vertical tail volume ratio, $V_v$, is defined as

$$V_v = \frac{S_F l_F}{S_w b_w} = \frac{(+)(-)}{(+)(+)} = (-) \text{ for tail to the rear aircraft} \tag{7.9}$$

$$= \frac{(+)(+)}{(+)(+)} = (+) \text{ for tail to the front aircraft}$$

Making this substitution into Equation 7.8

$$C_{n_F} = \frac{C_{L_F} q_F V_v}{q_w} \tag{7.10}$$

For a propeller-driven aircraft, $q_w$ may be less than or greater than $q_F$. However, for a jet aircraft, these two quantities are normally equal. Thus, for a jet aircraft, $q_F/q_w = 1$ and Equation 7.10 becomes

$$C_{n_F} = C_{L_F} V_v \tag{7.11}$$

The lift curve for a vertical tail is presented in Figure 7.4.

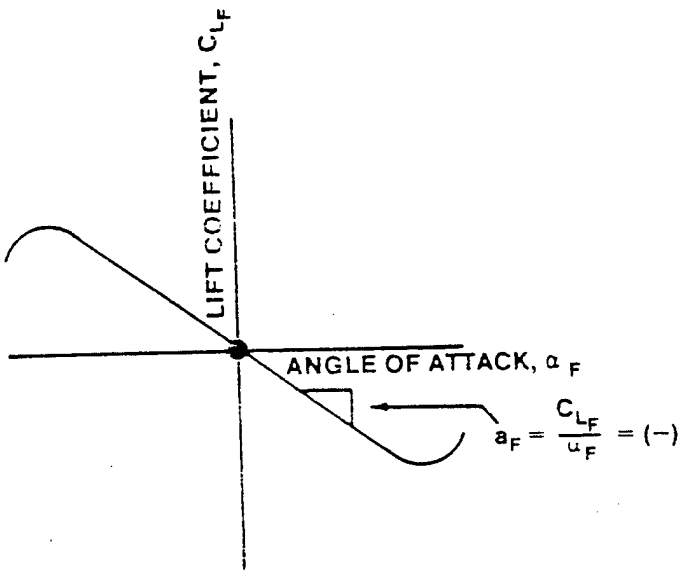


FIGURE 7.4. LIFT CURVE FOR VERTICAL TAIL

The negative slope is a result of the sign convention used (Figure 7.3). When the relative wind is displaced to the right of the fuselage reference line, the vertical tail is placed at a positive angle of attack. However, this results in a lift force to the left, or a negative lift. Thus, the sign of the lift curve slope of a vertical tail, $a_F$, will always be negative below the stall. Substituting $C_{L_F} = a_F \alpha_F$ into Equation 7.11 yields

$$C_{n_F} = a_F \alpha_F V_F \qquad (7.12)$$

The angle of attack of the vertical tail, $\alpha_F$, is not merely $\beta$. If the vertical tail were placed alone in an airstream, then $\alpha_F$ would be equal to $\beta$. However, when the tail is installed on an aircraft, changes in both magnitude and direction of the local flow at the tail take place. These changes may be caused by a propeller slipstream, or by the wing and the fuselage when the airplane is yawed. The angular deflection is allowed for by introducing the sidewash angle, $\sigma$, analogous to the downwash angle, $\varepsilon$. The value of $\sigma$ is very difficult to predict, therefore suitable wind tunnel tests are required. The

sign of $\sigma$ is defined as positive if it causes $\alpha_F$ to be less than $\beta$, which is normally the case since the fuselage tries to straighten the air which causes $\alpha_F$ to be less than $\beta$. Thus,

$$\sigma = \beta - \alpha_F \tag{7.13}$$

Substituting $\alpha_F$ from Equation 7.13 into Equation 7.12

$$C_{n_F} = a_F V_v (\beta - \sigma) \tag{7.14}$$

The contribution of the vertical tail to directional stability is found by examining the change in $C_{n_F}$ with a change in sideslip angle, $\beta$.

$$\frac{\partial C_{n_F}}{\partial \beta} = \left[ C_{n_{\beta(Tail)}} \right]_{Fixed} = V_v \; a_F \left[ 1 - \frac{\partial \sigma}{\partial \beta} \right] \tag{7.15}$$

(−) (−) (+) = (+) for tail to rear aircraft

(+) (−) (+) = (−) for tail to front aircraft

The subscript "fixed" is added to emphasize that, thus far, the vertical tail has been considered as a surface with no movable parts, i.e., the rudder is "fixed."

Equation 7.15 reveals that the vertical tail contribution to directional stability can only be changed by varying the vertical tail volume ratio, $V_v$, or the vertical tail lift curve slope, $a_F$. The vertical tail volume ratio can be changed by varying the size of the vertical tail, or its distance from the aircraft cg. The vertical tail lift curve slope can be changed by altering the basic airfoil section of the vertical tail, or by end plating the vertical fin. An end plate on the top of the vertical tail is a relatively minor modification, and yet it increases the directional stability of the aircraft

significantly at lower sideslip angles. This has been used on the T-38 (Figure 7.5). The entire stabilator on the F-104 acts as an end plate (Figure 7.6) and, therefore, adds greatly to the directional stability of the aircraft.

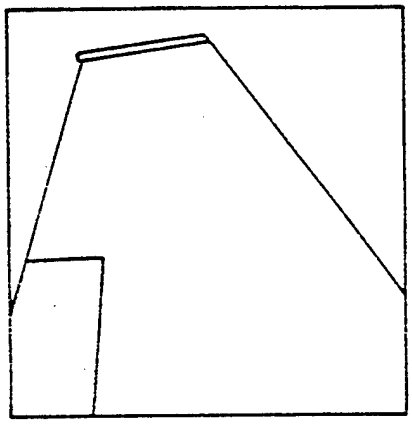

FIGURE 7.5. T-38 END PLATE

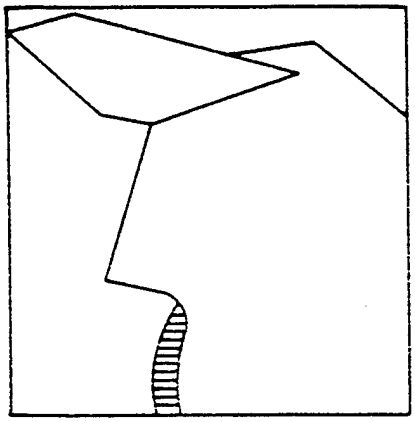

FIGURE 7.6. F-104 END PLATE

The end plate increases the effective aspect ratio of the vertical tail. As with any airfoil, this change in aspect ratio produces a change in the lift curve slope of the airfoil as shown in Figure 7.7.

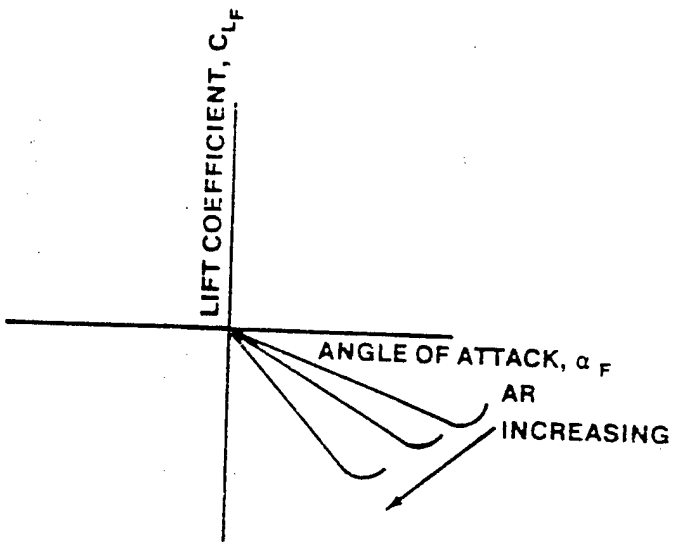


FIGURE 7.7. EFFECTS OF END PLATING

As the aspect ratio is increased, the $\alpha_F$ for stall is decreased. Thus, if the aspect ratio of the vertical tail is too high, the vertical tail will stall at low sideslip angles, and a large decrease in directional stability will occur.

7.3.1.2 Fuselage Contribution to $C_{n_\beta}$. The primary source of directional instability is the aircraft fuselage. This is so because the subsonic aerodynamic center of a typical fuselage usually lies ahead of the aircraft center of gravity. Therefore, a positive sideslip angle will produce a negative yawing moment about the cg causing $C_{n_\beta}$ (fuselage) to be negative or destabilizing (Figure 7.8).

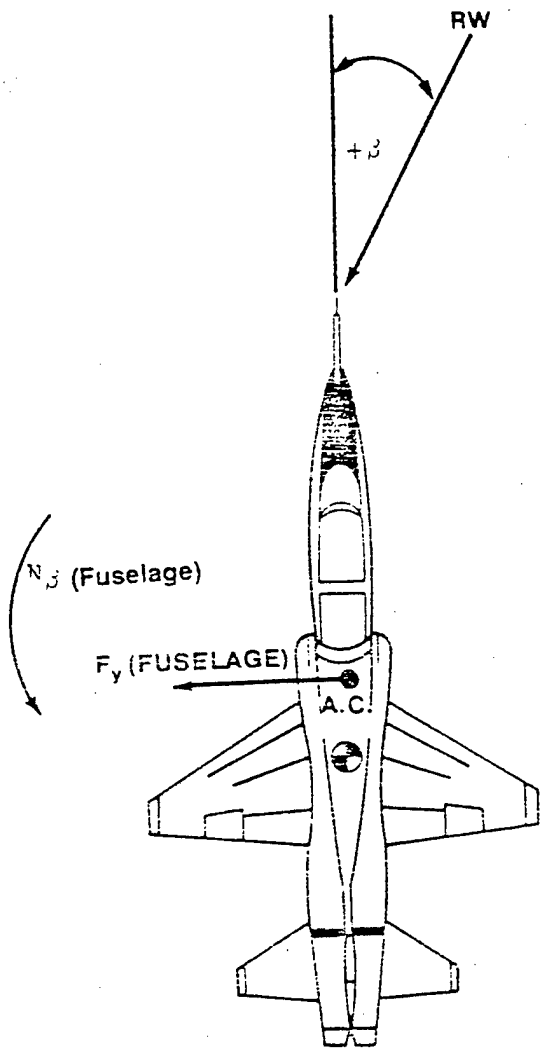


FIGURE 7.8. FUSELAGE CONTRIBUTION TO $C_{n_\beta}$

The destabilizing influence of the fuselage diminishes at large sideslip angles due to a decrease in lift as the fuselage stall angle of attack is exceeded and also due to an increase in parasite drag acting at the center of the equivalent parasite area which is located aft of the cg.

If the overall directional stability of an aircraft becomes too low, the fuselage-tail combination can be made more stabilizing by adding a dorsal fin or a ventral fin. A dorsal fin was added to the C-123, and a ventral fin was added to the F-104 to improve static directional stability.

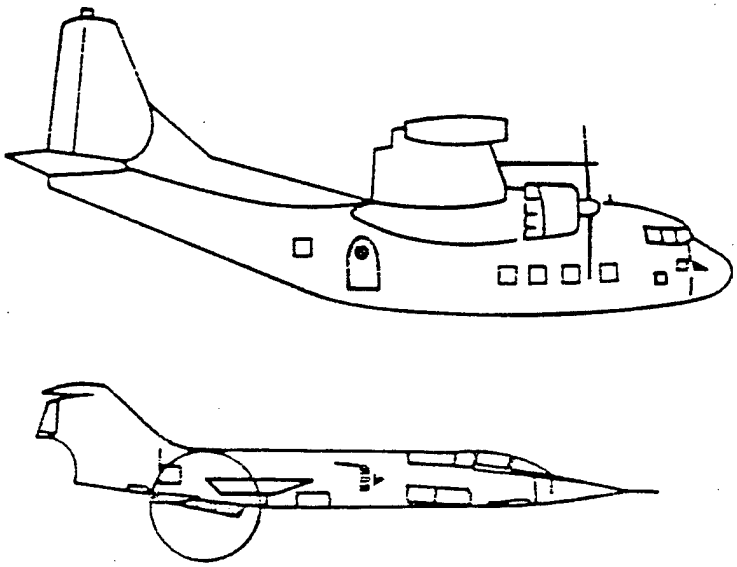

FIGURE 7.9. APPLICATIONS OF DORSAL AND VENTRAL FINS

The addition of a dorsal fin decreases the effective aspect ratio of the tail; therefore, a higher sideslip angle can be attained before the vertical fin stalls. Unfortunately this may occur at the expense of a loss in maximum $C_{L_F}$ (Figure 7.7). However, this loss is usually more than compensated for by the increased area behind the cg. Thus, the overall lift of the fuselage-tail

combination is usually increased ($L_F = C_{L_F} q S$). Therefore, a dorsal fin greatly increases directional stability at large sideslip angles. Figure 7.10 shows the effect of adding a dorsal fin on directional stability.

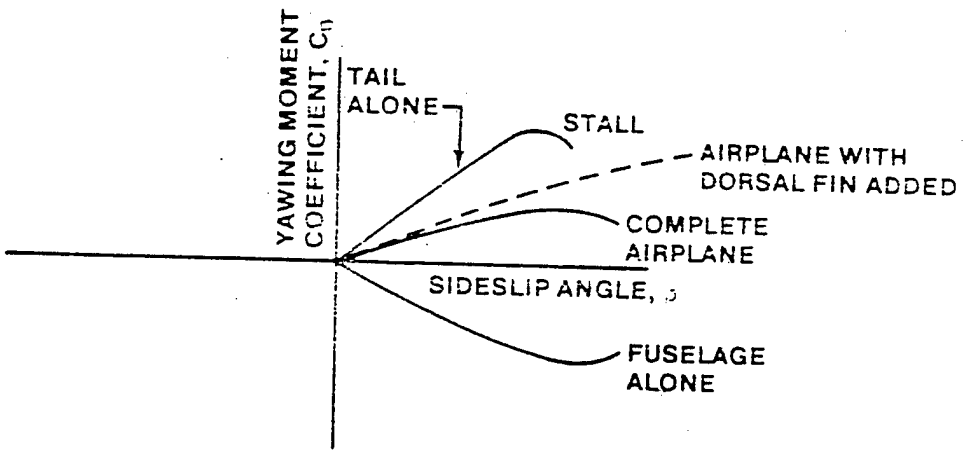


FIGURE 7.10. EFFECT OF ADDING A DORSAL FIN

The addition of a ventral fin is similar to adding another vertical tail. The net effect is an increased surface area and associated lift which produces a greater stabilizing moment.

Another design consideration which minimizes the destabilizing influence of the fuselage is nose shaping/modification. While these fore-body features are usually not put on primarily for directional stability, they do contribute. For example, the fore-body fences on the A-37 were incorporated to attain repeatable spin characteristics, but they also cause the nose to stall at smaller $\beta$ than the same aircraft without the fences, thus diminishing the destabilizing influence of the fuselage (see Figure 7.11).

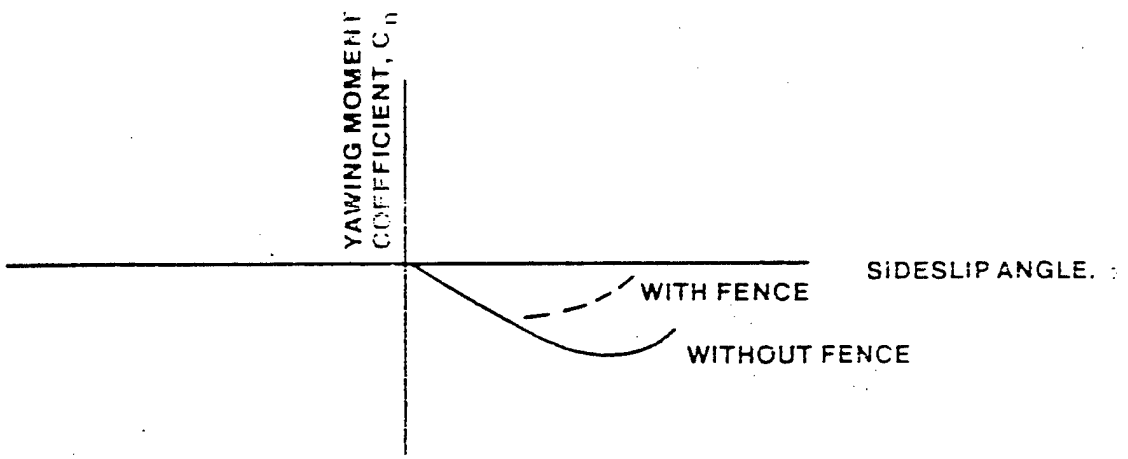


FIGURE 7.11. EFFECTS OF FORE-BODY SHAPING

7.3.1.3 Wing Contribution to $C_{n_\beta}$. The contribution of the wing to the airplane's static directional stability is usually small and is primarily a function of wing sweep ($\Lambda$). Straight wings make a slight positive contribution to static directional stability due to fuselage blanking in a sideslip. Effectively, the relative wind "sees" less of the downwind wing due to fuselage blanking. This reduces the lift of the downwind wing and thus reduces its induced drag. The difference in induced drag between the two wings tends to yaw the aircraft into the relative wind, which is stabilizing.

Swept back wings produce a greater positive contribution to static directional stability than do straight wings. In addition to fuselage blanking effects, it can be seen from Figure 7.12 that the component of free stream velocity normal to the upwind wing is significantly greater than on the downwind wing.

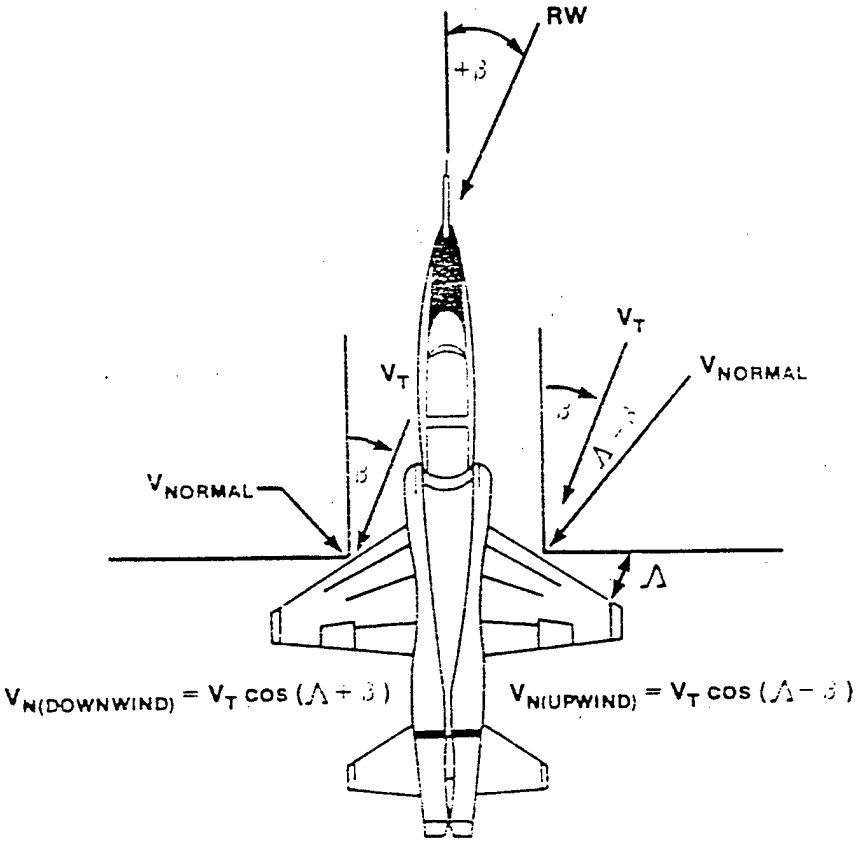


FIGURE 7.12. WING SWEEP EFFECTS ON $C_{n_\beta}$

The difference in normal components creates unbalanced lift and induced drag on the two wings, thus causing a stabilizing yawing moment. Similarly, a forward sweep angle would create an unstable contribution to static directional stability.

7.3.1.4 Miscellaneous Effects on $C_{n_\beta}$. The remaining contributors of significance to $C_{n_\beta}$ are propellers, jet intakes, and engine nacelles.

A propeller can have large effects on an aircraft's static directional stability. The propeller contribution to directional stability arises from the side force component at the propeller disc created as a result of sideslip.

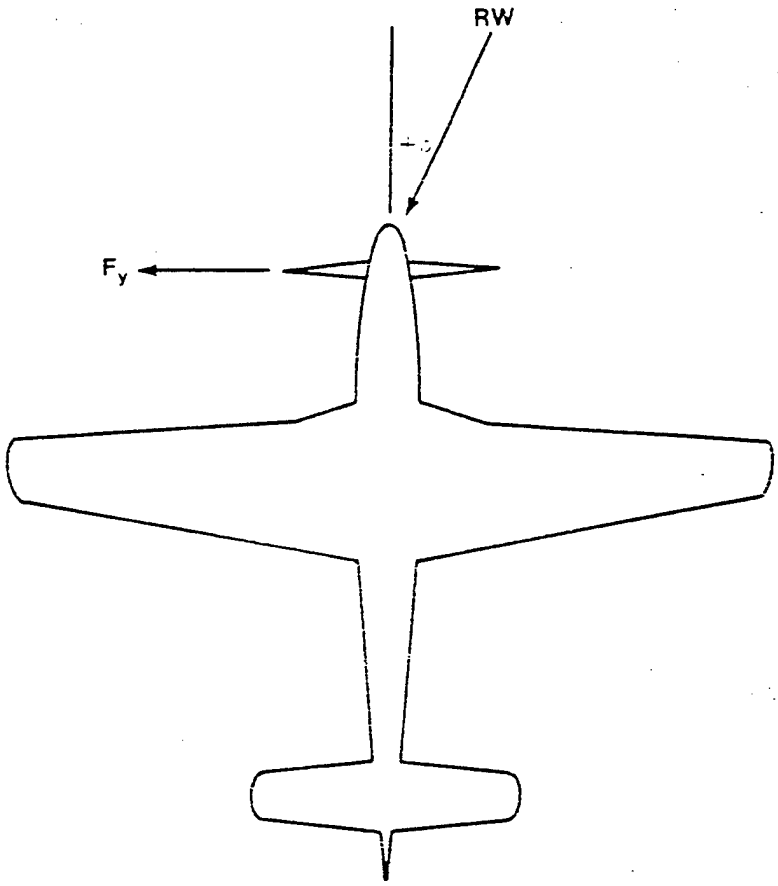


FIGURE 7.13. PROPELLER EFFECTS ON $C_{n_\beta}$

The propeller is destabilizing if a tractor and stabilizing if a pusher (Figure 7.13). Similarly, engine intakes have the same effects if they are located fore or aft of the aircraft cg.

Engine nacelles act like a small fuselage and can be stabilizing or destabilizing depending on whether their cp is located ahead or behind the cg. The magnitude of this contribution is usually small.

Aircraft cg movement is restricted by longitudinal static stability considerations. However, within the relatively narrow limits established by longitudinal considerations, cg movements have no significant effects on static directional stability.

7.3.1.5 $C_{n_\beta}$ Summary. Figure 7.14 summarizes the relative magnitudes of the primary contributor to $C_{n_\beta}$.

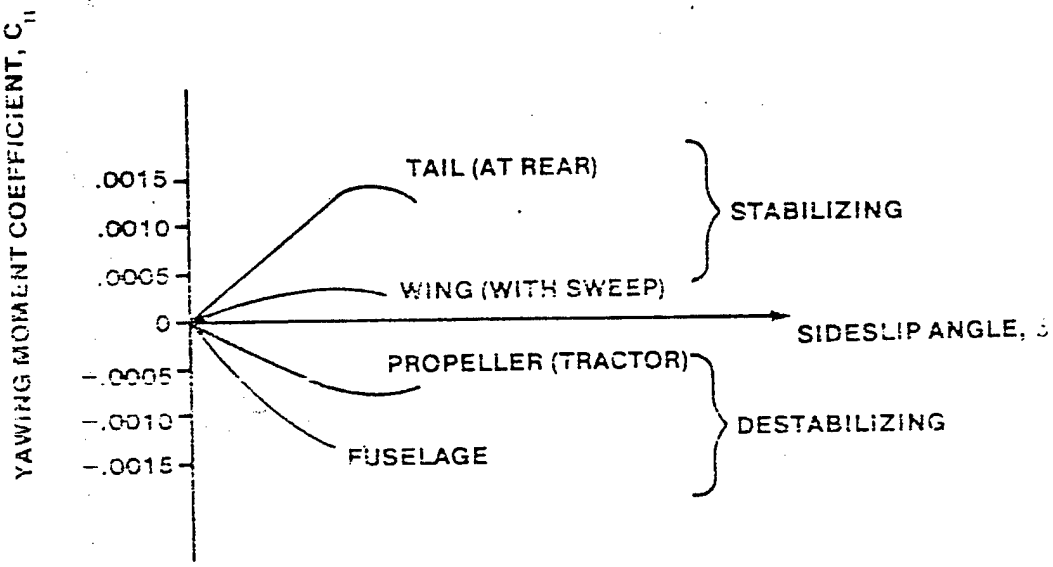


FIGURE 7.14. PRIMARY CONTRIBUTIONS TO $C_{n_\beta}$.

### 7.3.2 $C_{n_{\delta_r}}$ Rudder Power

In most flight conditions, it is desired to maintain zero sideslip. If the aircraft has positive directional stability and is symmetrical, then it will tend to fly in this condition. However, yawing moments may act on the aircraft as a result of asymmetric thrust (one engine inoperative), slipstream rotation, or the unsymmetric flow field associated with turning flight. Under these conditions, sideslip angle can be kept to zero only by the application of a control moment. The control that provides this moment is the rudder.
Recall from Equation 7.12 that

$$C_{n_F} = a_F \alpha_F V_v \tag{7.12}$$

Differentiating with respect to $\delta_r$

$$\frac{\partial C_{n_F}}{\partial \delta_r} = \frac{\partial C_n}{\partial \delta_r} = a_F V_v \frac{\partial \alpha_F}{\partial \delta_r} \tag{7.16}$$

$\partial\alpha_F/\partial\delta_r$ is the equivalent change in effective vertical tail angle of attack per unit change in rudder deflection and is defined as rudder effectiveness, $\tau$. This is a design parameter and ranges in value from zero (with no rudder) to one (in the case of an all moving vertical stabilizer surface). $\tau$ is a measure of how far one would have had to deflect the entire fin to get the same side force change that is obtained just by moving the rudder.
Substituting $\tau = \partial\alpha_F/\partial\delta_r$ into Equation 7.16.

$$\frac{\partial C_n}{\partial \delta_r} = C_{n_{\delta_r}} = a_F V_v \tau \tag{7.17}$$

The derivative, $C_{n_{\delta_r}}$ is called "rudder power" and by definition, its algebraic sign is always positive. This is because a positive rudder deflection, $+\delta_r$ is defined as one that produces a positive moment about the cg, $+C_n$. The magnitude of the rudder power can be altered by varying the size of the vertical tail and its distance from the aircraft cg, by using different airfoils for the tail and/or rudder, or by varying the size of the rudder.

7.3.3 $C_{n_{\delta_a}}$ Yawing Moment Due to Lateral Control Deflection

The next two derivatives which will be studied $\left(C_{n_{\delta_a}} \text{ and } C_{n_p}\right)$ are called "cross derivatives," that is, a lateral input or rate generates a yaw (directional) moment. It is the existence of these cross derivatives that causes the rolling and yawing motions to be so closely coupled.

The first of these cross derivatives to be covered will be $C_{n_{\delta_a}}$, the yawing moment due to lateral control deflection. In order for a lateral control to produce a rolling moment, it must create an unbalanced lift condition on the wings. The wing with the most lift will also produce the most induced drag according to the equation $C_{D_i} = C_L^2 / \pi AR\, e$. Also, any change in the profile of the wing due to a lateral control deflection will cause a change in profile drag. Thus, any lateral control deflection will produce a change in both induced and profile drag. The predominant effect will be dependent on the particular aircraft configuration and the flight condition. If induced drag predominates, the aircraft will tend to yaw away from the direction of roll (negative $C_{n_{\delta_a}}$). This phenomenon is known as "adverse yaw." The sign of $C_{n_{\delta_a}}$ for "proverse" yaw is positive. Both ailerons and spoilers are capable of producing either adverse or proverse yaw. In general, ailerons usually produce adverse yaw and spoilers usually produce proverse yaw. Many aircraft use differential horizontal stabilizer deflections for roll control. When deflected, the horizontal stabilizer on the downgoing side has a region of high pressure above it. This high pressure also acts on the side of the vertical stabilizer, which results in a yawing moment. This yawing moment is normally proverse. To determine which

condition will actually prevail, the particular aircraft configuration and flight condition must be analyzed. If design permits, it is desirable to have $C_{n_{\delta_a}} = 0$ or be slightly negative. A slight negative value may ease the pilot's turn coordination task by eliminating a need to cross control. The designs of some modern fighter-type aircraft make the pilot's task easier by keeping $C_{n_{\delta_a}} = 0$.

### 7.3.4 $C_{n_p}$ Yawing Moment Due to Roll Rate

The second cross derivative is the yawing moment due to roll rate ($C_{n_p}$). Both the wing and vertical tail contribute to this derivative. In this discussion the aircraft will be considered with a roll rate, but no deflection of the control surfaces. It is important that this situation not be confused with yawing moments caused by control surface deflections. This is particularly true in flight tests where it may be difficult or impossible to separate them.

The wing contribution to $C_{n_p}$ arises from two sources: induced drag increase and the change in magnitude and tilting of the lift vectors.

As an aircraft is rolled, the angle of attack on the downgoing wing is increased, while the angle of attack on the upgoing wing is decreased. The increase in angle of attack means that induced drag will be greater on the downgoing wing than on the upgoing wing. This induced drag change results in a positive contribution to $C_{n_p}$.

Since the two wings are at different angles of attack during the roll, their lift vectors will be at different angles. The downgoing wing with a greater angle of attack will tend to have its lift vector increased and tilted more forward. The upgoing wing with a reduced angle of attack will tend to have its lift vector decreased and tilted more aft (Figure 7.15).

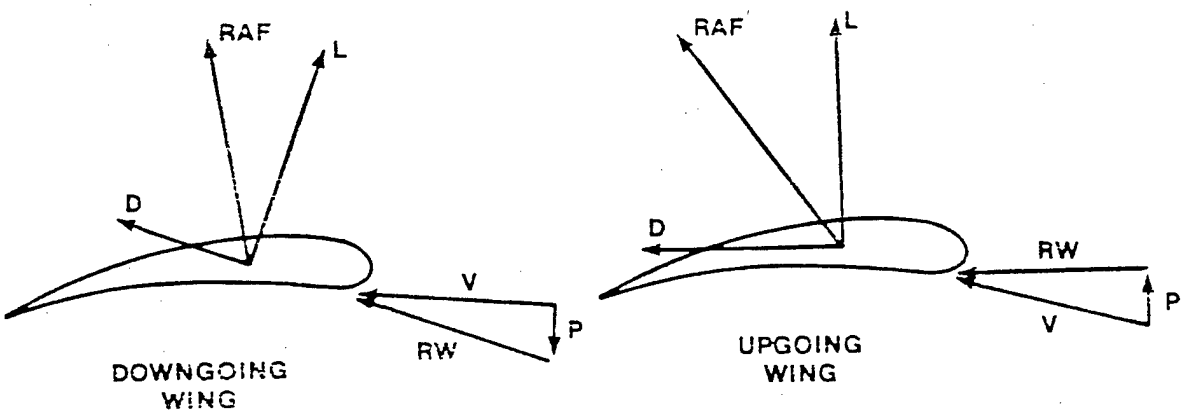


FIGURE 7.15. VECTOR TILT DUE TO ROLL RATE

For a right roll, the left wing will be pulled aft more than the right wing. This causes a negative contribution to $C_{n_p}$. This is true even though the magnitude of the resultant aerodynamic force is greater on the downgoing wing than on the upgoing wing. The contribution caused by tilting of the lift vector is normally greater than the contribution due to induced drag. Therefore, the overall wing contribution to $C_{n_p}$ is usually negative.

Rolling changes the angle of attack on the vertical tail as shown in Figure 7.16. This change in angle of attack on the vertical tail will generate a lift force. In the situation depicted in Figure 7.16, the change in angle of attack will generate a lift force, $L_F$, to the left. This will create a positive yawing moment. Thus, $C_{n_p}$ for the vertical tail is usually positive.

Therefore, the overall value of $C_{n_p}$ is not easily determined. On many aircraft it is both positive and negative, depending upon trim lift coefficient or angle of attack.

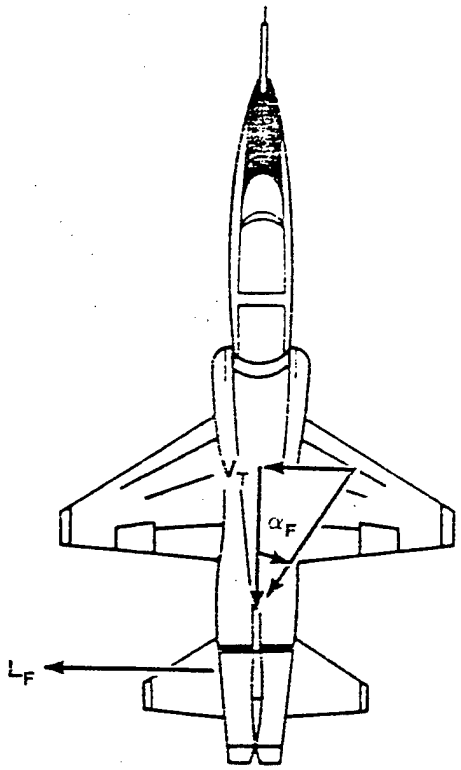


FIGURE 7.16. CHANGE IN ANGLE OF ATTACK OF THE VERTICAL TAIL DUE TO A RIGHT ROLL RATE

Considering both wing and tail, a slight positive value of $C_{n_p}$ is desired to aid in Dutch roll damping.

7.3.5 $C_{n_r}$ Yaw Damping

The derivative $C_{n_r}$ is called yaw damping. It is strongly desired that $C_{n_r}$ be negative. This is so because the forces generated when an airplane is

yawing about its center of gravity should develop moments which tend to oppose the motion.

Figure 7.17 summarizes the major contributors to $C_{n_r}$. In general, the fuselage contributes a negligible amount except when it is very large. The more important contributors are the wing and tail.

The tail contribution to $C_{n_r}$ arises from the fact that there is change in angle of attack on the vertical tail whenever the aircraft is yawed. This change in $\alpha_F$ produces a lift force, $L_F$, that in turn produces a yawing moment that opposes the original yawing moment. The tail contribution to $C_{n_r}$ accounts for 80-90% of the total "yaw damping" on most aircraft.

The wing contribution to $C_{n_r}$ arises from the fact that in a yaw, the outside wing experiences an increase in both induced drag and profile drag due to the increased dynamic pressure on the wing. An increase in drag on the outside wing increases a yawing moment that opposes the original direction of yaw.

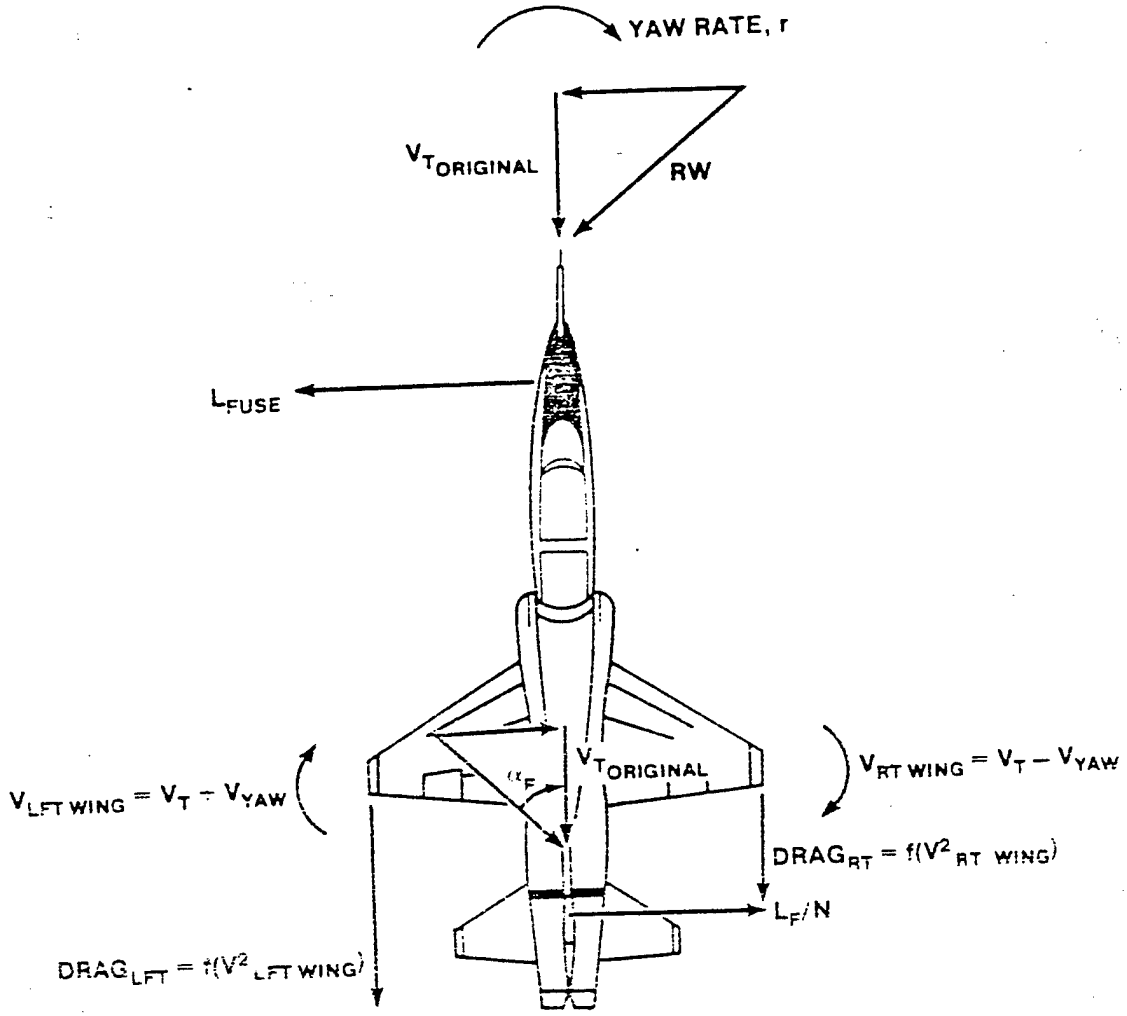


FIGURE 7.17. CONTRIBUTORS TO $C_{n_r}$

### 7.3.6 $C_{n_{\dot{\beta}}}$ Yaw Damping Due to Lag Effects in Sidewash

The derivative $C_{n_{\dot{\beta}}}$ is yaw damping due to lag effects in sidewash, $\sigma$. Very little can be authoritatively stated about the magnitude or algebraic sign of $C_{n_{\dot{\beta}}}$ due to the wide variations of opinion in interpreting the experimental data concerning it.

As an aircraft moves through a certain sideslip angle, the angle of attack of the vertical tail will be less than it would be if the aircraft were allowed to stabilize at that angle of sideslip. This is due to lag effects in sidewash which tends to straighten the flow over the tail. Since this phenomenon reduces the angle of attack of the vertical tail, it also reduces the yawing moment created by the vertical tail. This reduction in yawing moment is, effectively, a contribution to the yaw damping. Figure 7.18 illustrates, "yaw damping due to lag effects in sidewash."

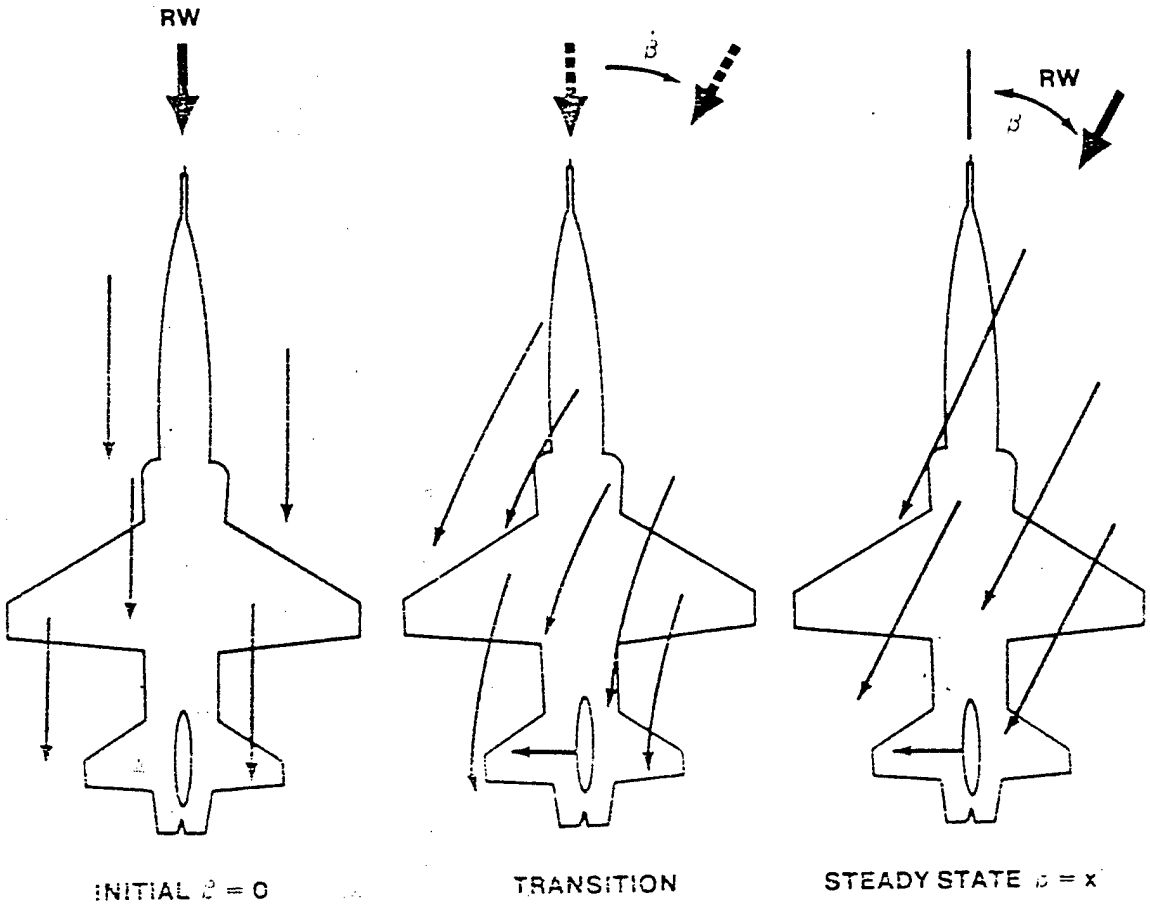


FIGURE 7.18. LAC EFFECTS

7.3.7 High Speed Effects on Static Directional Stability Derivatives

Since most of the directional stability derivatives are dependent on the lift produced by various surfaces, we can generalize the effects of Mach on these derivatives. The effectiveness of an airfoil decreases as the velocity increases supersonically as shown in Figure 7.19.

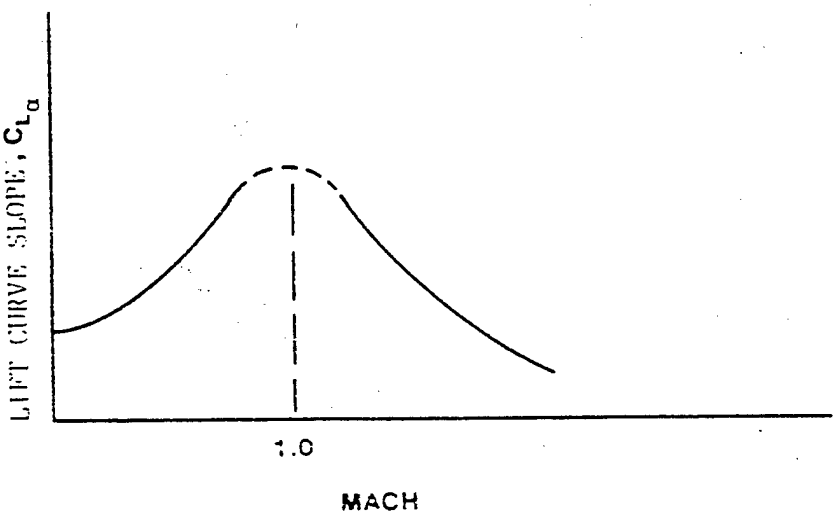


FIGURE 7.19. $C_{L_\alpha}$ VS M

7.3.7.1 $C_{n_\beta}$. Since $C_{n_{\beta_{Fin}}} = f(a_{Fin}, V_v)$ and $a_{Fin} = f(\text{Mach})$, then for a given $\beta$, as Mach increases beyond Mach critical, the restoring moment generated by the tail diminishes. Unfortunately the wing-fuselage combination is destabilizing throughout the flight envelope. Thus, the overall $C_{n_\beta}$ of the aircraft will decrease with increasing Mach, and in fact approaches zero at very high Mach (Figure 7.20).

The requirement for large values of $C_{n_\beta}$ is compounded by the tendency of high speed aerodynamic designs to diverge in yaw due to roll coupling. This problem can be combated by designing an extremely large tail (F-111 and T-38), by endplating the tail (F-104 and T-38), by using ventral fins (F-111 and F-16), by using forebody strakes (SR-71), or by designing twin tails (F-15).

The F-111 employs ventral fins in addition to a sizeable vertical stabilizer to increase supersonic directional stability. The efficiency of

underbody surfaces is not affected by wing wake at high angles of attack, and supersonically, they are located in a high energy compression pattern.

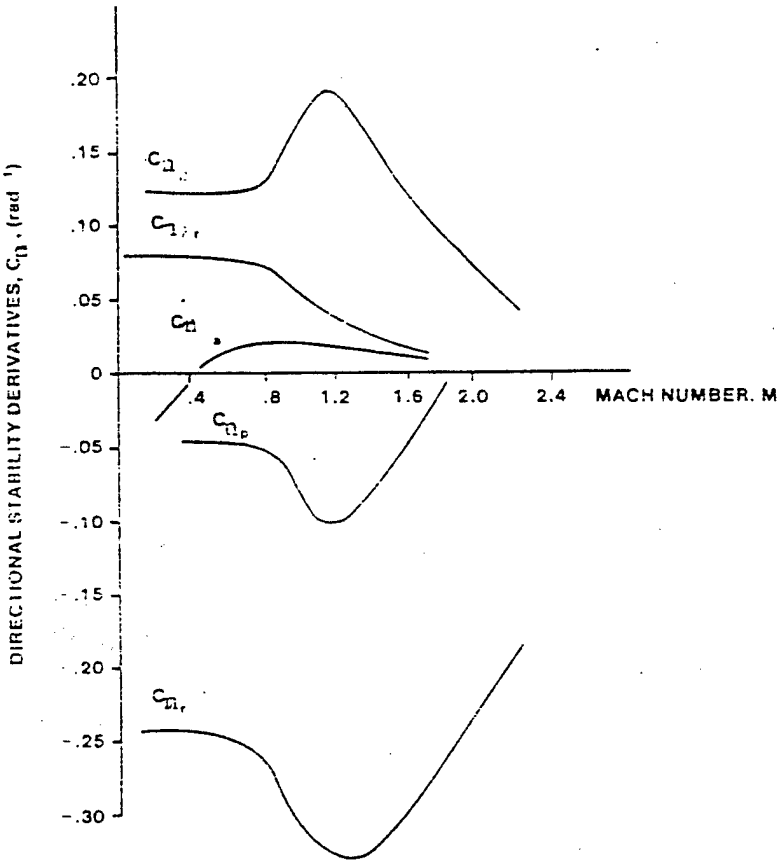


FIGURE 7.20. CHANGES IN DIRECTIONAL STABILITY DERIVATIVES WITH MACH (F-4C)

7.3.7.2 $C_{n_{\delta_r}}$. Flow separation will decrease the effectiveness of any trailing edge control surface in the transonic region. On most aircraft, however, this is offset by an increase in the $C_{L_\alpha}$ curve in the

transonic region. As a result, flight controls are usually the most effective in this region. However, as Mach continues to increase, the $C_{L_\alpha}$ curve decreases, and control surface effectiveness decreases. In addition, once the flow over the surface is supersonic, a trailing edge control cannot influence the pressure distribution on the surface itself, due to the fact that pressure disturbances cannot be transmitted forward in a supersonic environment. Thus, the rudder power will decrease as Mach increases above the transonic region.

7.3.7.3 $C_{n_{\delta_a}}$. For the same reasons discussed under rudder power, a given aileron deflection will not produce as much lift at high Mach as it did transonically. Therefore, induced drag will be less. In addition, the profile drag, for a given aileron deflection, increases with Mach. For some designs, such as roll spoilers or differential ailerons, these changes in drag will combine to cause proverse yaw.

7.3.7.4 $C_{n_r}$. Yaw damping depends on the ability of the wing and tail to develop lift. Thus, as Mach increases and the ability of all surfaces to develop lift decreases, yaw damping will also decrease.

7.3.7.5 $C_{n_p}$. The sign of $C_{n_p}$ for many aircraft is a function of trim lift coefficient and can change signs with Mach.

7.3.7.6 $C_{n_{\dot{\beta}}}$. The effect of Mach on this derivative is not precisely known.

7.3.8 Rudder Fixed Static Directional Stability (Flight Test Relationship)

Now that we have become familiar with the coefficients affecting directional stability, we will develop a flight test relationship to measure the static directional stability of the aircraft. The maneuver we use to determine $C_{n_\beta}$ is the "steady straight sideslip" (Figure 7.21).

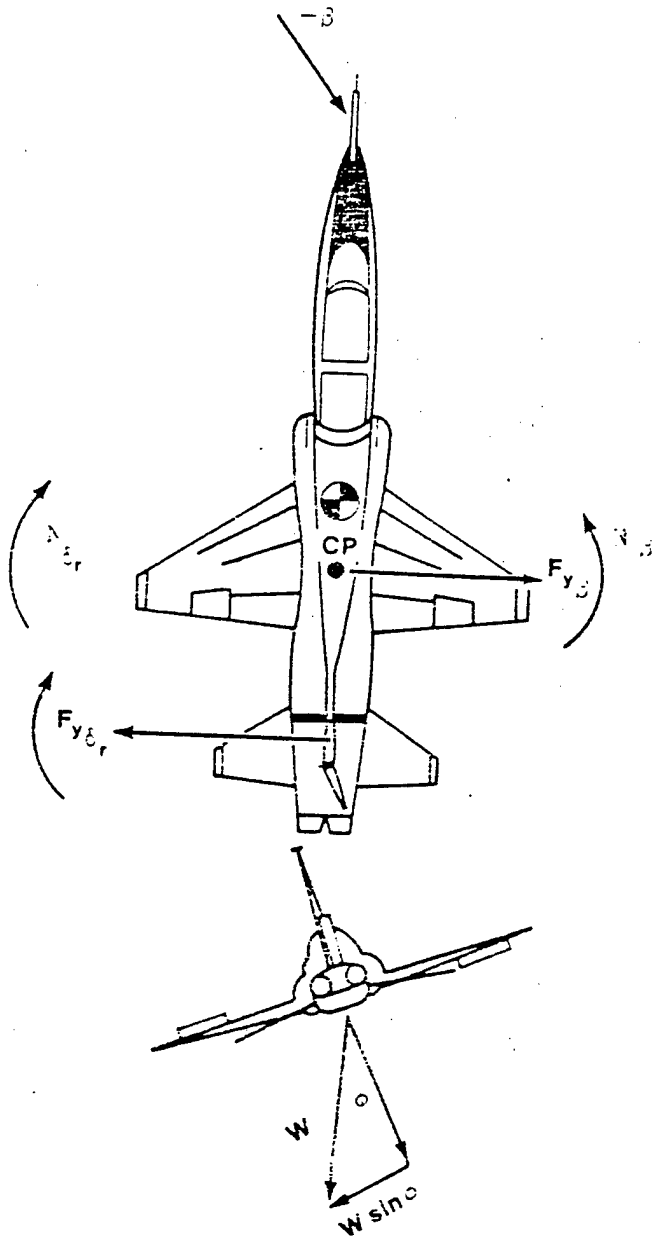


FIGURE 7.21. STEADY STRAIGHT SIDESLIP

Steady straight sideslip requires the pilot to balance the forces and moments generated on the airplane by the sideslip with appropriate lateral and directional control inputs. These control inputs are indicative of the sign (and relative magnitude) of the forces and moments generated.

As its name implies, steady straight sideslip means: $\Sigma F_{xyz} = \Sigma G_{xyz} = 0$. In addition, it implies that no rates are present and, therefore $p = q = r = \dot{\beta} = \dot{p} = \dot{r} = \dot{v} = 0$. Given this information and recalling the static directional equation of motion,

$$C_{n_\beta}\beta + C_{n_{\dot\beta}}\cancel{\frac{\dot\beta b}{2U_o}}^{0} + C_{n_p}\cancel{\frac{pb}{2U_o}}^{0} + C_{n_r}\cancel{\frac{rb}{2U_o}}^{0} + C_{n_{\delta_a}}\delta_a + C_{n_{\delta_r}}\delta_r = \cancel{C_n}^{0}$$

Therefore,

$$C_{n_\beta}\beta + C_{n_{\delta_a}}\delta_a + C_{n_{\delta_r}}\delta_r = 0 \qquad (7.18)$$

Solving for $\delta_r$

$$\delta_r = -\frac{C_{n_\beta}}{C_{n_{\delta_r}}}\beta - \frac{C_{n_{\delta_a}}}{C_{n_{\delta_r}}}\delta_a \qquad (7.19)$$

and differentiating with respect to $\beta$

$$\frac{\partial\delta_r}{\partial\beta} = -\frac{C_{n_{\beta\,(Fixed)}}}{C_{n_{\delta_r}}} - \frac{C_{n_{\delta_a}}}{C_{n_{\delta_r}}}\frac{\partial\delta_a}{\partial\beta} \qquad (7.20)$$

The subscript "fixed" is added as a reminder that Equation 7.20 is an expression for the static directional stability of an aircraft if the rudder is <u>not</u> free to float.

Equation 7.20 can be further simplified by discarding the terms that are usually the smallest contributors to the expression. As we have already discovered $C_{n_\beta}$ and $C_{n_{\delta_r}}$ are both usually large terms and normally dominate in the static directional equation of motion. On the other hand, if the aircraft flight control system is properly designed, $C_{n_{\delta_a}}$ should be zero or slightly negative. Therefore, if we assume that $C_{n_{\delta_a}}$ is significantly smaller than the other coefficients in the equation, then we are left with the following flight test relationship:

$$\frac{\partial \delta_r}{\partial \beta} = f \left[ - \frac{C_{n_\beta}}{C_{n_{\delta_r}}} \right] \tag{7.21}$$

Since $C_{n_{\delta_r}}$ is a known quantity once an aircraft is built, then $\partial\delta_r/\partial\beta$ can be taken as a direct indication of the rudder fixed static directional stability of an aircraft. Moreover, $\partial\delta_r/\partial\beta$ can be easily measured in flight.

Since $C_{n_\beta}$ has to be positive in order to have positive directional stability and $C_{n_{\delta_r}}$ is positive by definition, $\partial\delta_r/\partial\beta$ must be negative to obtain positive static directional stability.

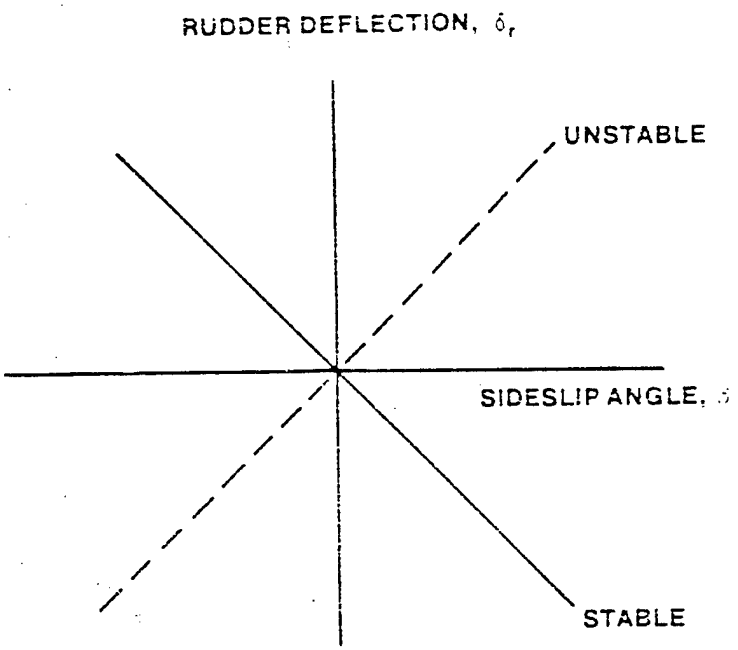


FIGURE 7.22. RUDDER DEFLECTION $\delta_r$ VS SIDESLIP

7.3.9 Rudder Free Directional Stability (Flight Test Relationship)

On aircraft with reversible control systems, the rudder is free to float in response to its hinge moments, and this floating can have large effects on the directional stability of the airplane. In fact, a plot of $\partial\delta_r/\partial\beta$ may be stable while an examination of the rudder free static directional stability reveals the aircraft to be unstable. Thus, if the rudder is free to float, there will be a change in the tail contribution to static directional stability. To analyze the nature of this change, recall that hinge moments are produced by the pressure distribution caused by angle of attack and control surface deflection.

Consider a conventional (tail-to-the-rear) aircraft with a reversible rudder. Figure 7.23 depicts the hinge moment on this rudder due to angle of attack only (i.e., $\delta_r = 0$). Note that $\alpha_r$ is positive with the relative wind from the right.

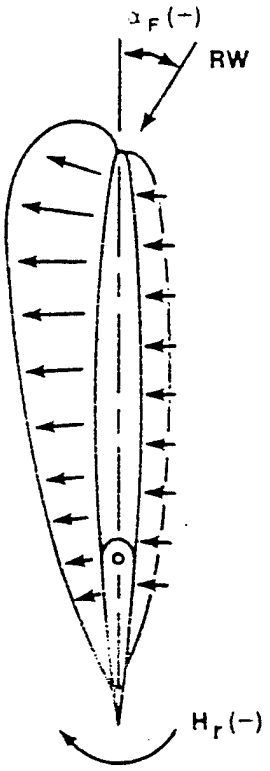


FIGURE 7.23. HINGE MOMENT DUE TO RUDDER ANGLE OF ATTACK

If the rudder control were released in this case, the hinge moment, $H_r$, would cause the rudder to rotate trailing edge left (TEL). This, in turn, would create a moment which would cause the nose of the aircraft to yaw to the left. Since our convention defines positive as a right yaw and anything that contributes to a right yaw is also defined as positive, then the hinge moment which causes the rudder to deflect TEL is NEGATIVE. Conversely, a positive $H_r$ would cause the rudder to deflect TER.

Figure 7.24 depicts the hinge moment due to rudder deflection. This condition assumes $\alpha_r = 0$.

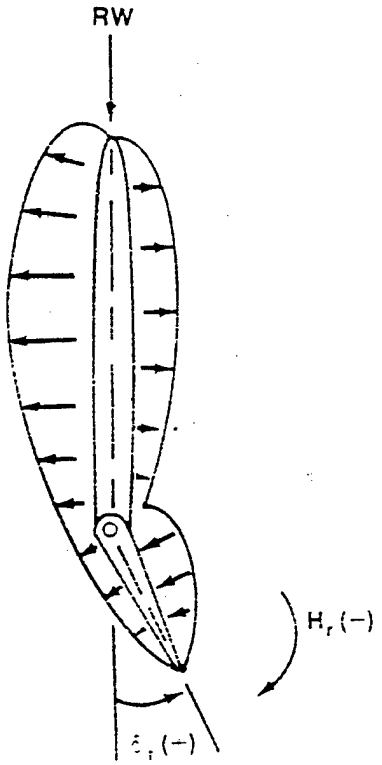


FIGURE 7.24. HINGE MOMENT DUE TO RUDDER DEFLECTION (TER)

This pressure distribution causes a hinge moment which tries to force the deflected surface back to its original position; that is, it tries to deflect the rudder TEL. We have already discovered that this moment is negative.

Combining the aerodynamic hinge moments for a given rudder deflection and a given rudder angle of attack, we find

$$H_r = \cancel{H_{r_0}}^{0} + \frac{\partial H_r}{\partial \alpha_F} \alpha_F + \frac{\partial H_r}{\partial \delta_r} \delta_r \qquad (7.22)$$

In coefficient form

$$C_h = C_{h_{\alpha_F}} \alpha_F + C_{h_{\delta_r}} \delta_r \qquad (7.23)$$

In the rudder free case, when the vertical tail is placed at some angle of attack, $\alpha_F$, the rudder will start to "float." However, as soon as it deflects, restoring moments are set up, and an equilibrium floating angle will be reached where the floating tendency is just balanced by the restoring tendency. At this point $\Sigma H_r = 0$ which implies $C_h = 0$ (see Figure 7.25).

Therefore,

$$C_{h_{\alpha_F}} \alpha_F + C_{h_{\delta_r}} \delta_{r_{(Float)}} = 0 \qquad (7.24)$$

or

$$C_{h_{\alpha_F}} \alpha_F = - C_{h_{\delta_r}} \delta_{r_{(Float)}} \qquad (7.25)$$

Thus,

$$\delta_{r_{(Float)}} = - \frac{C_{h_{\alpha_F}}}{C_{h_{\delta_r}}} \alpha_F \qquad (7.26)$$

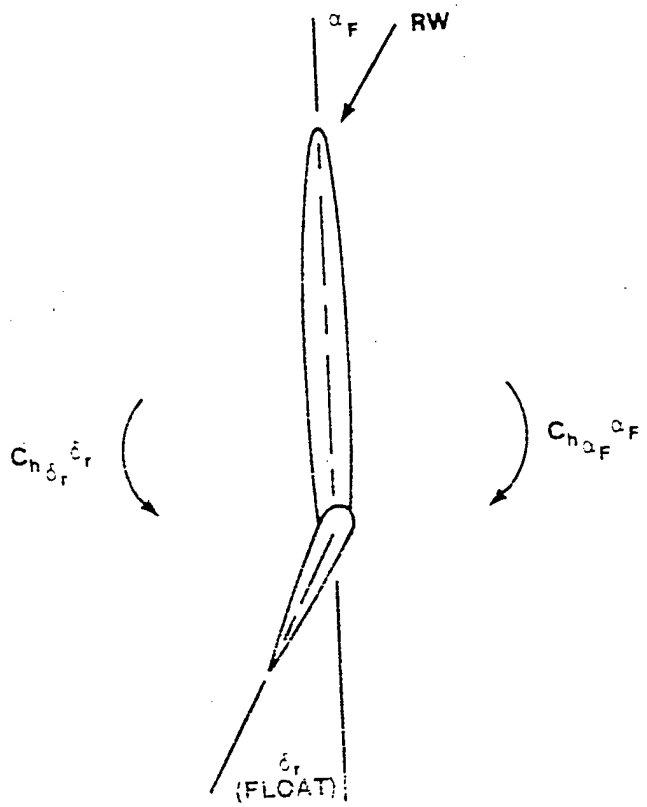


FIGURE 7.25. HINGE MOMENT EQUILIBRIUM (TEL)

With this background, it is now possible to develop a relationship that expresses the static directional stability of an aircraft with the rudder free to float.

Recall that

$$C_{n_F} = V_v \, a_F \, \alpha_F \qquad (7.27)$$

and that

$$\alpha_F = \beta - \sigma \text{ (rudder fixed)} \tag{7.28}$$

But for rudder free, another factor $(\partial\alpha_F/\partial\delta_r)\delta_r$ must be added to account for the $\Delta\alpha_F$ which will result from a floating rudder.

Therefore,

$$\alpha_F = \beta - \sigma + \frac{\partial\alpha_F}{\partial\delta_r}\,\delta_{r_{(Float)}} \tag{7.29}$$

Substituting into Equation 7.27

$$C_{n_F} = V_v\, a_F \left[\beta - \sigma + \frac{\partial\alpha_F}{\partial\delta_r}\,\delta_{r_{(Float)}}\right] \tag{7.30}$$

$$C_{n_{\beta_{(Free)}}} = \frac{\partial C_{n_F}}{\partial\beta} = V_v\, a_F \left[1 - \frac{\partial\sigma}{\partial\beta} + \tau\,\frac{\partial\delta_{r_{(Float)}}}{\partial\beta}\right] \tag{7.31}$$

where $\tau = \partial\alpha_F/\partial\delta_r$ = rudder effectiveness

$$C_{n_{\beta_{(Free)}}} = V_v\, a_F \left[1 - \frac{\partial\sigma}{\partial\beta}\right]\left[1 + \tau\,\frac{\partial\delta_{r_{(Float)}}}{\partial\beta}\,\frac{1}{1 - \frac{\partial\sigma}{\partial\beta}}\right] \tag{7.32}$$

Recalling that $\alpha_F = \beta - \sigma$, then $\partial\alpha_F/\partial\beta = 1 - \partial\sigma/\partial\beta$

$$C_{n_{\beta(Free)}} = V_v \, a_F \left[1 - \frac{\partial \sigma}{\partial \beta}\right] \left[1 + \tau \frac{\partial \delta_{r_{(Float)}}}{\partial \beta} \left[\frac{\partial \beta}{\partial \alpha_F}\right]\right] \qquad (7.33)$$

$$C_{n_{\beta(Free)}} = V_v \, a_F \left[1 - \frac{\partial \sigma}{\partial \beta}\right] \left[1 + \tau \frac{\partial \delta_{r(Float)}}{\partial \alpha_F}\right] \qquad (7.34)$$

Recall that

$$\delta_{r_{(Float)}} = - \frac{C_{h_{\alpha_F}}}{C_{h_{\delta_r}}} \alpha_F \qquad (7.35)$$

Therefore,

$$\frac{\partial \delta_{r(Float)}}{\partial \alpha_F} = - \frac{C_{h_{\alpha_F}}}{C_{h_{\delta_r}}} \qquad (7.36)$$

Thus, from Equation 7.34

$$(-)\ (-) \quad (+) \quad 1 - (+)\ \frac{(-)}{(-)} = (+) \text{ for tail to rear aircraft}$$

$$C_{n_{\beta\ (Free)}} = V_v \quad a_F \left[1 - \frac{\partial \sigma}{\partial \beta}\right] \left[1 - \tau \frac{C_{h_{\alpha_F}}}{C_{h_{\delta_r}}}\right] \qquad (7.37)$$

It can be seen that this expression differs from Equation 7.15, the expression for rudder fixed directional stability by the term $[1 - \tau C_{h_\alpha} / C_{h_{\delta_r}}]$. Since this term will always result in a quantity less than one, it can be stated that the effect of rudder float is to reduce the slope of the static directional stability curve.

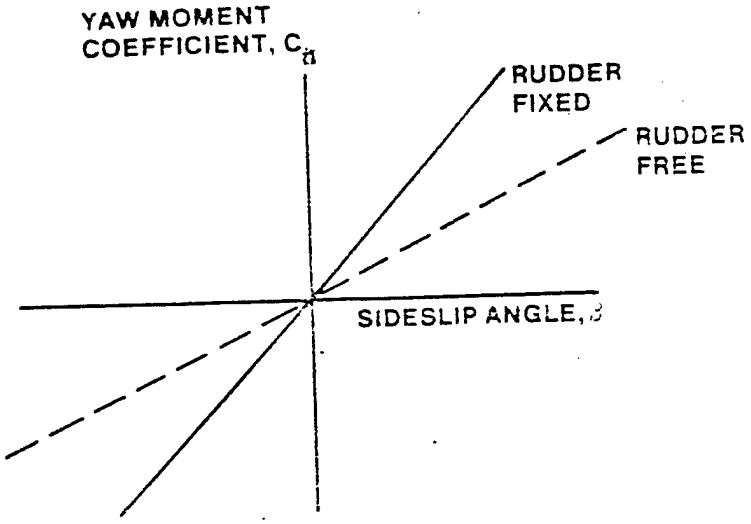


FIGURE 7.26. EFFECT OF RUDDER FLOAT ON DIRECTIONAL STABILITY

While Equation 7.37 is theoretically interesting, it does not contain parameters that are easily measured in flight. It is necessary, therefore, to develop an expression that will be useful in flight test work.

We have already seen that in a steady straight sideslip $\Sigma N = 0$. Therefore it follows that $\Sigma N_{Hinge\ Fin} = 0$. But we have also discovered that for a free floating system, as angle of attack is placed on the vertical fin, the rudder will tend to float and try to cancel some of this angle of attack until an equilibrium is reached. In a sideslip, therefore, the pilot must apply rudder force to oppose the aerodynamic hinge moment in order to keep the rudder deflected the desired amount to maintain the required $\beta$. This rudder force exerted by the pilot, $F_r$, acts through a moment arm and various gearing mechanisms, both of which are accounted for by some constant K.

Thus, in a steady straight sideslip

$$\Sigma N_{Hinge\ Pin} = F_r \cdot K + H_r = 0 \tag{7.38}$$

or

$$F_r = - G \cdot H_r \tag{7.39}$$

where

$$G = 1/K \text{ (definition)}$$

Recalling coefficient format

$$H_r = C_h\ q_r\ S_r\ c_r \tag{7.40}$$

From Equation 7.23

$$H_r = q_r\ S_r\ c_r \left[ C_{h_{\alpha_F}}\ \alpha_F + C_{h_{\delta_r}}\ \delta_r \right] \tag{7.41}$$

Thus, Equation 7.39 becomes

$$F_r = - Gq_r\ S_r\ c_r \left[ C_{h_{\alpha_F}}\ \alpha_F + C_{h_{\delta_r}}\ \delta_r \right] \tag{7.42}$$

Applying Equation 7.24

$$F_r = - Gq_r\ S_r\ c_r \left[ - C_{h_{\delta_r}}\ \delta_{r_{(Float)}} + C_{h_{\delta_r}}\ \delta_r \right] \tag{7.43}$$

$$F_r = - Gq_r\ S_r\ c_r\ C_{h_{\delta_r}} \left[ \delta_r - \delta_{r_{(Float)}} \right] \tag{7.44}$$

The difference between where the pilot pushes the rudder, $\delta_r$, and the amount it floats, $\delta_{r_{(Float)}}$, is the free position of the rudder, $\delta_{r_{(Free)}}$ (Figure 7.27).

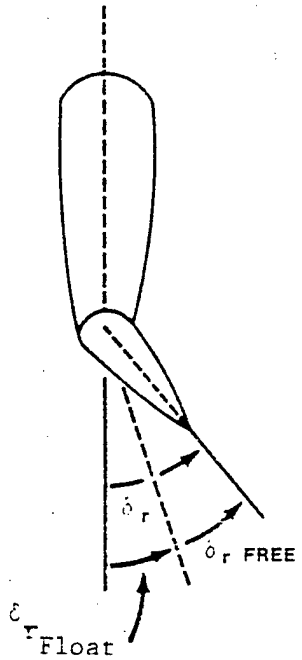


FIGURE 7.27 $\delta_{r_{Float}}$ VS $\delta_{r_{Free}}$

Therefore,

$$F_r = - Gq_r S_r c_r C_{n_{\dot{\delta}_r}} \delta_{r_{(Free)}} \tag{7.45}$$

$$\frac{\partial F_r}{\partial \beta} = - Gq_r S_r c_r C_{n_{\dot{\delta}_r}} \frac{\partial \delta_{r_{(Free)}}}{\partial \beta} \tag{7.46}$$

From Equation 7.21 it can be shown that

$$\frac{\partial \delta_{r_{(Free)}}}{\partial \beta} = - \frac{C_{n_{\beta_{(Free)}}}}{C_{n_{\delta_r}}} \tag{7.47}$$

Thus,

$$\frac{\partial F_r}{\partial \beta} = \underset{(+)}{G}\ \underset{(+)}{q_r}\ \underset{(+)}{S_r}\ \underset{(+)}{c_r}\ \underset{(-)}{\frac{C_{h_{\delta_r}}}{C_{n_{\delta_r}}}}\ \underset{(+)}{C_{n_{\beta_{(Free)}}}} \qquad (7.48)$$

Therefore,

$$\frac{\partial F_r}{\partial \beta} = (-) \text{ for stability}$$

This equation shows that the parameter, $\partial F_r/\partial \beta$, can be taken as an indication of the rudder free static directional stability of an aircraft since all terms are either constant or set by design, except $C_{n_{\beta_{(Free)}}}$. Further, this equation constitutes a flight test relationship because $\partial F_r/\partial \beta$ can be readily measured in flight.

An analysis of the components of Equation 7.48 reveals that for static directional stability (i.e., $C_{n_\beta} = +$), the sign of $\partial F_r/\partial \beta$ should be negative (Figure 7.28).

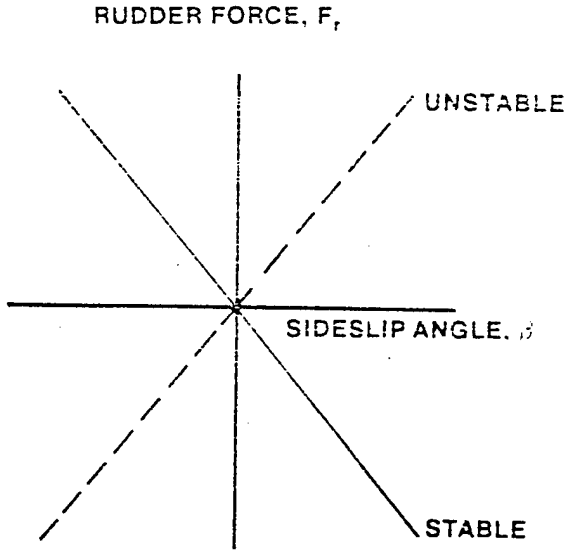


FIGURE 7.28. RUDDER FORCE VS SIDESLIP

## 7.4 STATIC LATERAL STABILITY

In our discussion of directional stability, the wings of the aircraft have been considered at some arbitrary angle to the vertical (angle of bank, $\phi$), usually taken as zero, with no concern for the aerodynamic problem of holding this angle or for bringing the airplane into this attitude.

The problem of holding the wings level or of maintaining some angle of bank is one of control over the rolling moments about the airplane's longitudinal axis. The major control over the rolling moments is the ailerons, while secondary control can be obtained through control over the sideslip angle. Recalling the stability derivatives which contribute to static lateral stability, we see both of these factors present.

$$C_l = C_{l_\beta}\beta + C_{l_{\dot\beta}}\frac{\dot\beta b}{2U_o} + C_{l_p}\frac{pb}{2U_o} + C_{l_r}\frac{rb}{2U_o} + C_{l_{\delta_a}}\delta_a + C_{l_{\delta_r}}\delta_r \qquad (7.6)$$

It can be seen that the rolling moment coefficient, $C_l$, is not a function of bank angle, $\phi$. In other words, a change in bank angle will produce no change in rolling moment. In fact, $\phi$ produces no moment at all. Thus, $C_{l_\phi} = 0$, and although it is analogous to $C_{m_\alpha}$ and $C_{n_\beta}$, it contributes nothing to lateral static stability analysis.

Bank angle, $\phi$, does have an indirect effect on rolling moment. As the aircraft is rolled into a bank angle, a component of aircraft weight will act along the Y-axis and will thus produce an unbalanced force (Figure 7.29). This unbalanced force in the Y direction, $F_y$, will produce a sideslip, $\beta$, and as seen from Equation 7.6, this will influence the rolling moment produced.

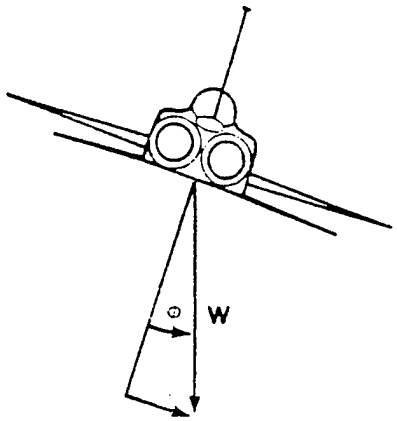


FIGURE 7.29. SIDE FORCE PRODUCED BY BANK ANGLE

Each stability derivative in Equation 7.6 will be discussed, and its contribution to aircraft stability will be analyzed. Table 7.2 summarizes these stability derivatives.

TABLE 7.2
LATERAL STABILITY AND CONTROL DERIVATIVES

| DERIVATIVE | NAME | SIGN FOR A STABLE AIRCRAFT | CONTRIBUTING PARTS OF AIRCRAFT |
|---|---|---|---|
| $C_{l_\beta}$ | Dihedral Effect | (-) | Wing, Tail |
| $C_{l_{\dot\beta}}$ | Lag Effects | (+) | Wing, Tail |
| $C_{l_p}$ | Roll Damping | (-) | Wing, Tail |
| $C_{l_r}$ | Cross-Coupling | (+) | Wing, Tail |
| $C_{l_{\delta_a}}$ | Lateral Control Power | (+) | Lateral Control |
| $C_{l_{\delta_r}}$ | Roll due to Rudder | (-) | Rudder |

### 7.4.1 $C_{l_\beta}$ Dihedral Effect

$C_{l_\beta}$, which is commonly referred to as "dihedral effect," is a measure of the initial tendency of an aircraft to roll when disturbed in sideslip. Although the static lateral stability of an aircraft is a function of all the derivatives in Equation 7.6, $C_{l_\beta}$ is the dominant term.

The algebraic sign of $C_{l_\beta}$ must be negative for stable dihedral effect (Figure 7.30). Consider an aircraft in wings level flight. If disturbed in bank to the right, the aircraft will develop a right sideslip (+β). If $C_{l_\beta}$ is negative, a rolling moment to the left (-) will result, and the initial tendency will be to return toward equilibrium.

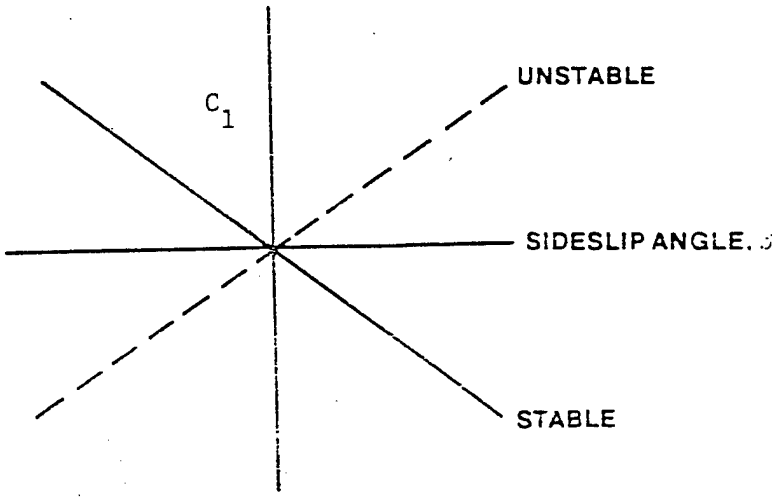


FIGURE 7.30. ROLLING MOMENT COEFFICIENT $C_l$ VS SIDESLIP

It is possible to have too much or too little dihedral effect. High values of dihedral effect give good spiral stability. If an aircraft has a large amount of dihedral effect, the pilot is able to pick up a wing with top rudder. This also means that in level flight, a small amount of sideslip will cause the aircraft to roll, and this can be annoying to the pilot. This is known as a high $\phi/\beta$ ratio. In multi-engine aircraft, an engine failure will

normally produce a large sideslip angle. If the aircraft has a great deal of dihedral effect, the pilot must supply an excessive amount of aileron force and deflection to overcome the rolling moment due to sideslip. Still another detrimental effect of too much dihedral effect may be encountered when the pilot rolls an aircraft. If an aircraft, in rolling to the right, tends to yaw to the left, the resulting sideslip, together with stable dihedral effect, creates a rolling moment to the left. This effect could significantly reduce the maximum roll rate available. The pilot wants a certain amount of dihedral effect, but not too much. The end result is usually a design compromise.

Both the wing and the tail contribute to $C_{l_\beta}$. The various effects on $C_{l_\beta}$ can be classified as "direct" or "indirect." A direct effect actually produces some increment of $C_{l_\beta}$, while an indirect effect merely alters the value of the existing $C_{l_\beta}$.

The discrete wing and tail effects that will be considered are classified as shown in Table 7.3.

TABLE 7.3.
EFFECTS ON $C_{l_\beta}$

| DIRECT | INDIRECT |
|---|---|
| Geometric Dihedral | Aspect Ratio |
| Wing Sweep | Taper Ratio |
| Wing-Fuselage Interference | Tip Tanks |
| Vertical Tail | Wing Flaps |

7.4.1.1 Geometric Dihedral. Geometric dihedral, $\gamma$, is defined as shown in Figure 7.31, and is positive (dihedral) when the chord lines of the wingtip are above those at the wing root, and is negative (anhedral) when the tip chord lines are below the wing roots.

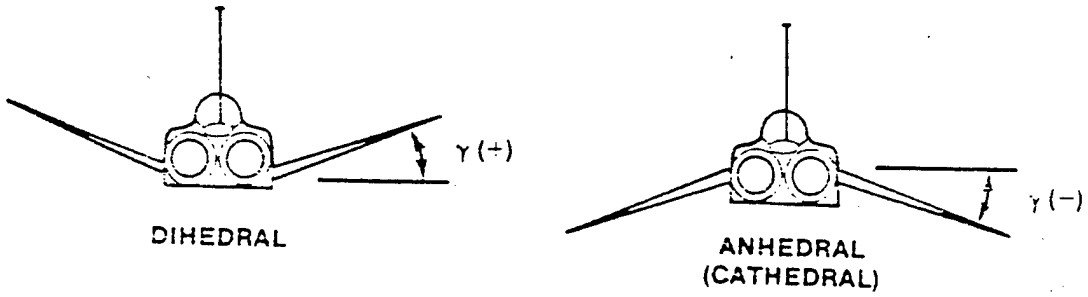


FIGURE 7.31. GEOMETRIC DIHEDRAL

To understand the effect of geometric dihedral on static lateral stability, consider Figure 7.32.

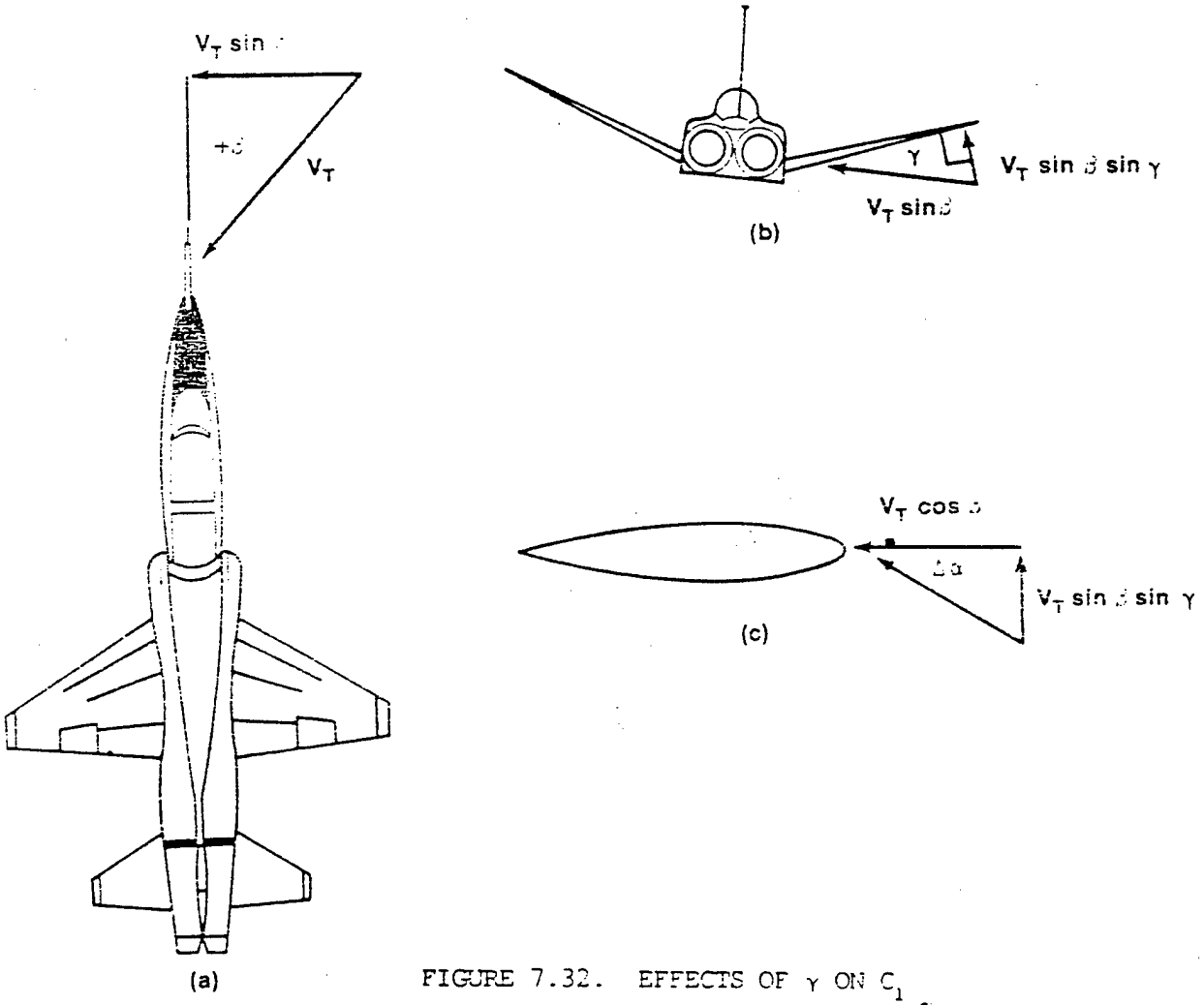


FIGURE 7.32. EFFECTS OF γ ON $C_{l_\beta}$

It can be seen that when an aircraft is placed in a sideslip, positive geometric dihedral causes the component, $V_T \sin\beta \sin\gamma$ to be added to the lift producing component of the relative wind, $V_T \cos\beta$. Thus, geometric dihedral causes the angle of attack on the upwind wing to be increased by $\Delta\alpha$. To find this $\Delta\alpha$

$$\tan \Delta\alpha = \frac{V_T \sin\beta \sin\gamma}{V_T \cos\beta} = \tan\beta \sin\gamma \qquad (7.49)$$

Making the small angle assumption,

$$\Delta\alpha = \tan\beta \sin\gamma \qquad (7.50)$$

Conversely, the angle of attack on the downwind wing will be reduced. These changes in angle of attack tend to increase the lift on the upwind wing and decrease the lift on the downwind wing, thus producing a roll away from the sideslip. In Figure 7.32, a positive sideslip ($+\beta$) will increase the angle of attack on the upwind (right) wing, thus producing a roll to the left. Therefore, it can be seen that this effect produces a stable, or negative, contribution to $C_{l_\beta}$.

7.4.1.2 Wing Sweep. The wing sweep angle, $\Lambda$, is measured from a perpendicular to the aircraft x-axis at the forward wing root, to a line connecting the quarter chord points of the wing. Wing sweep back is defined as positive.

Aerodynamic theory shows that the lift of a yawed wing is determined by the component of the free stream velocity normal to wing. That is, $L = 1/2\ C_L \rho V_N^2 S$ where, $V_N$ is the normal velocity.

As was previously shown in our discussion of $C_{n_{\beta_{wing}}}$, and as can be seen from Figure 7.33, the normal component of free stream velocity on the upwind wing on a swept wing aircraft is

$$V_N = V_T \cos(\Lambda - \beta) \qquad (7.51)$$

Conversely, on the downwind wing,

$$V_N = V_T \cos(\Lambda + \beta) \qquad (7.52)$$

Therefore, $V_N$ is greater on the upwind wing. This causes the upwind wing to produce more lift and creates a roll away from the direction of the sideslip. In other words, a right sideslip will produce a roll to the left. Thus, aft wing sweep makes a stable contribution to $C_{l_\beta}$ and produces the same effect as positive geometric dihedral.

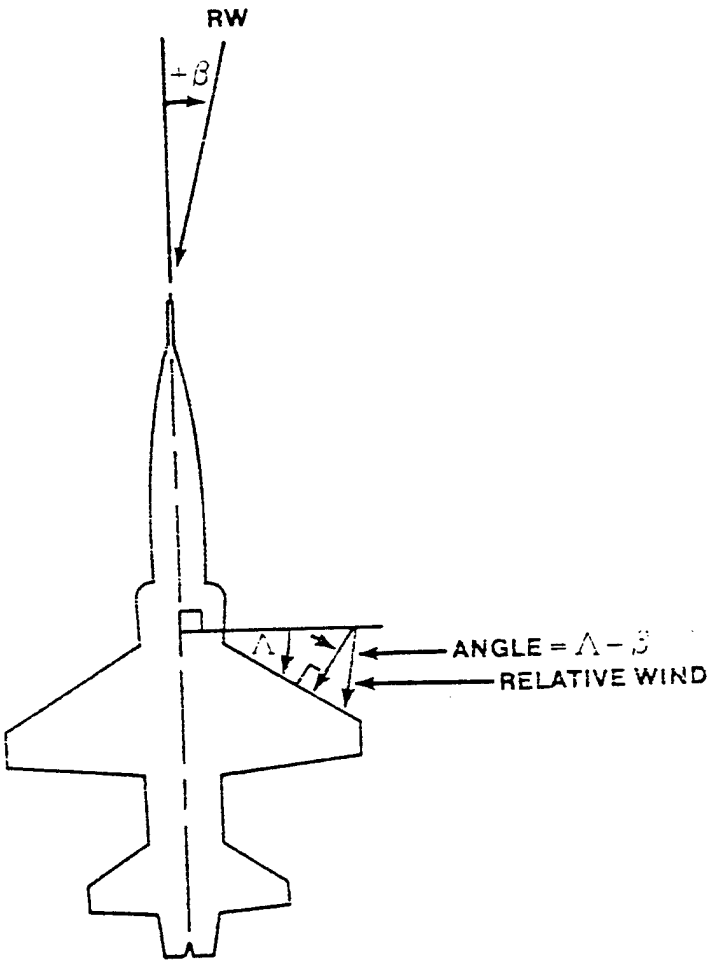


FIGURE 7.33. NORMAL VELOCITY COMPONENT ON SWEPT WING

To fully appreciate the effect of wing sweep on static lateral stability, it will be necessary to develop an equation relating the two.

$$L_{(\text{Upwind Wing})} = (1/2)\, C_L \frac{S}{2} \rho V_N^2 \tag{7.53}$$

$$L_{(\text{Upwind Wing})} = (1/2) C_L \frac{S}{2} \rho [V_T \cos (\Lambda - \beta)]^2 \tag{7.54}$$

Similarly,

$$L_{(\text{Downward Wing})} = (1/2) C_L \frac{S}{2} \rho [V_T \cos (\Lambda + \beta)]^2 \tag{7.55}$$

Thus,

$$\Delta L = (1/2) C_L \frac{S}{2} \rho [V_T \cos (\Lambda - \beta)]^2 - (1/2) C_L \frac{S}{2} \rho [V_T \cos (\Lambda + \beta)]^2 \tag{7.56}$$

$$\Delta L = (1/2) C_L \frac{S}{2} \rho V_T^2 [\cos^2 (\Lambda - \beta) - \cos^2 (\Lambda + \beta)] \tag{7.57}$$

Applying a trigonometric identity,

$$[\cos^2 (\Lambda - \beta) - \cos^2 (\Lambda + \beta)] = \sin 2\Lambda \sin 2\beta \tag{7.58}$$

Making the assumption of a small sideslip angle,

$$\sin 2\Lambda \sin 2\beta = 2\beta \sin 2\Lambda \tag{7.59}$$

Therefore, Equation 7.57 becomes

$$\Delta L = (1/2) C_L \frac{S}{2} \rho V_T^2 \, 2\beta \sin 2\Lambda = (1/2) C_L S \rho V_T^2 \beta \sin 2\Lambda \tag{7.60}$$

The rolling moment produced by this change in lift is

$$L \text{ (Rolling Moment)} = - \Delta L \quad Y \tag{7.61}$$

Where Y is the distance from the wing cp to the aircraft cg. The minus sign arises from the fact that Equation 7.60 assumes a positive sideslip, $+\beta$, and for an aircraft with stable dihedral effect, this will produce a negative rolling moment

$$C_l = \frac{L \text{ (Rolling Moment)}}{q_w S_w b_w} \tag{7.62}$$

$$C_l = - \frac{Y C_L S \rho V_T^2 \beta \sin 2\Lambda}{\rho V_T^2 Sb} = - \frac{C_L Y \beta}{b} \sin 2\Lambda \tag{7.63}$$

$$\frac{\partial C_l}{\partial \beta} = C_{l_\beta} = - \frac{Y}{b} C_L \sin 2\Lambda = - \text{CONST } (C_L \sin 2\Lambda) \tag{7.64}$$

where the constant will be on the order of 0.2. Equation 7.64 should not be used above $\Lambda = 45°$ because highly swept wings are subject to leading edge separation at high angles of attack, and this can result in reversal of the dihedral effect. Therefore, it is best to use empirical results above $\Lambda = 45°$.

Equation 7.64 shows that at low speeds (high $C_L$) sweepback makes a large contribution to stable dihedral effect. However, at high speeds (low $C_L$) sweepback makes a relatively small contribution to stable dihedral effect (Figure 7.34).

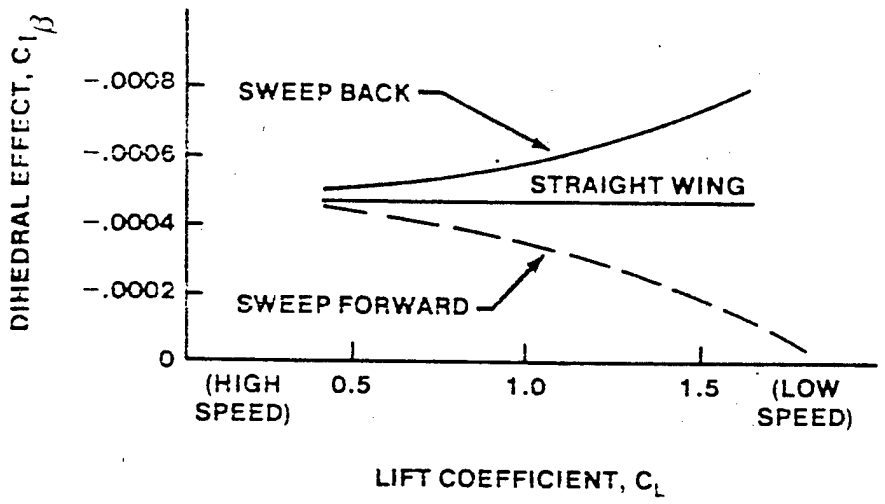


FIGURE 7.34. EFFECTS OF WING SWEEP AND LIFT COEFFICIENT ON DIHEDRAL EFFECT, $C_{l_\beta}$

For forward swept wings, the sweep becomes more destabilizing at slow speeds and less destabilizing at high speeds. For angles of sweep on the order of 45°, the wing sweep contribution to $C_{l_\beta}$ may be on the order of $-C_L/5$. For large values of $C_L$, this is a very large contribution, equivalent to nearly 10° of geometric dihedral

Since the effect of sweepback varies with $C_L$, becoming extremely small at high speeds, it can help keep the proper ratio of $C_{l_\beta}$ to $C_{n_\beta}$ at high speeds and reduce poor Dutch roll characteristics at these speeds.

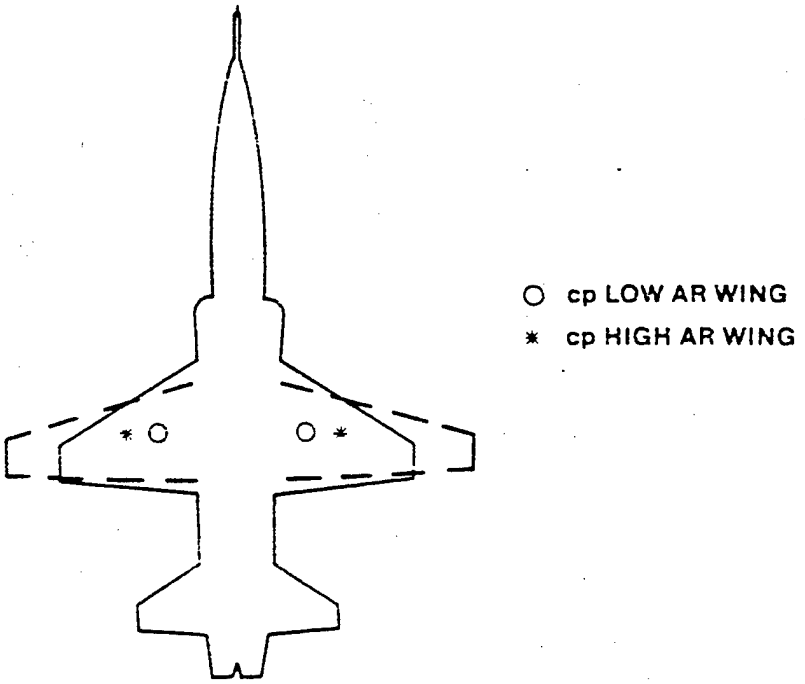


FIGURE 7.35. CONTRIBUTION OF ASPECT RATIO TO DIHEDRAL EFFECT

7.4.1.3 Wing Aspect Ratio. The wing aspect ratio exerts an indirect contribution to dihedral effect. On a high aspect ratio wing, the center of pressure is further from the cg than on a low aspect ratio wing. This results in high aspect ratio planforms having a longer moment arm and thus, greater rolling moments for a given asymmetric lift distribution (Figure 7.35). It should be noted that aspect ratio, in itself, does not create dihedral effect.

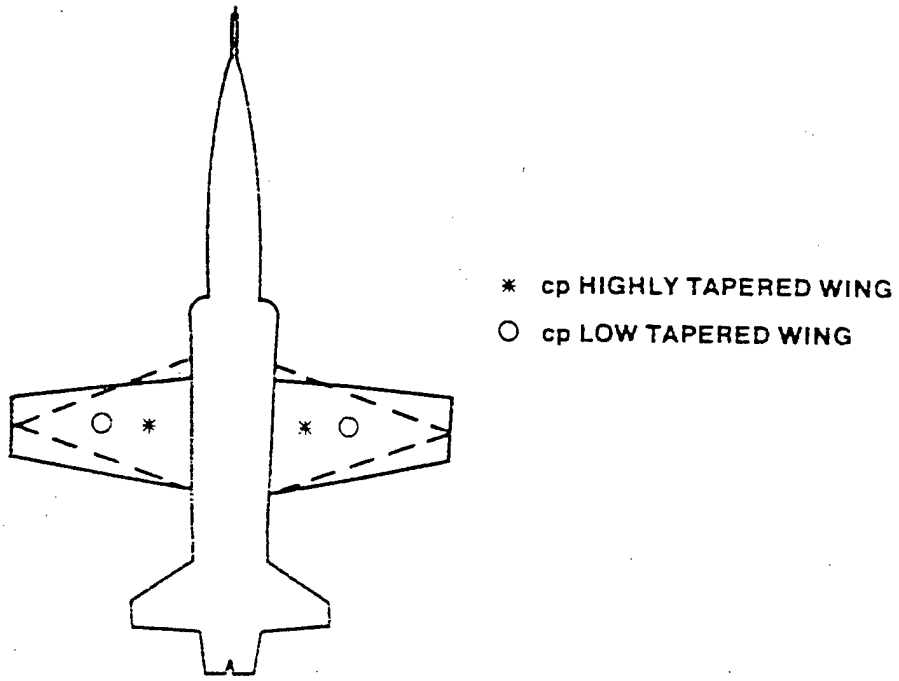


FIGURE. 7.36. CONTRIBUTION OF TAPER RATIO TO DIHEDRAL EFFECT

7.4.1.4 Wing Taper Ratio. Taper ratio, $\lambda$, is the ratio of the tip chord to the root chord and is a measure of how fast the wing chord shortens. Therefore, the lower the taper ratio, the faster the chord shortens. On highly tapered wings, the center of pressure is closer to the aircraft cg than on untapered wings. This results in a shorter moment arm and thus, less rolling moment for a given asymmetric lift distribution (Figure 7.36). Taper ratio does not create dihedral effect but merely alters the magnitude of the existing dihedral effect. Thus it has an indirect contribution to dihedral effect.

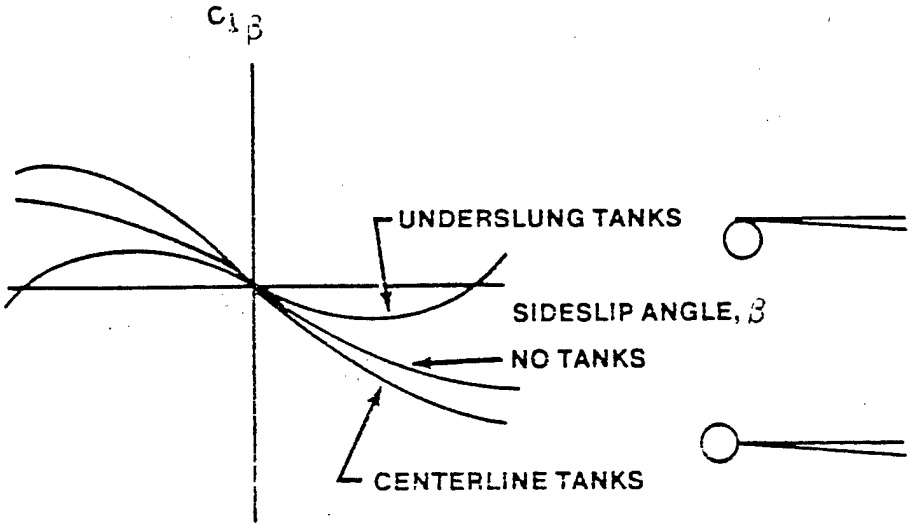


FIGURE 7.37. EFFECT OF TIP TANKS ON DIHEDRAL EFFECT, $C_{l_\beta}$ OF F-80

7.4.1.5 Tip Tanks. Tip tanks, pylon tanks, or other external stores will generally exert an indirect influence on $C_{l_\beta}$. Unfortunately, the effect of a given external store configuration is hard to predict analytically, and it is usually necessary to rely on empirical results. To illustrate the effect of various external store configurations, data for the F-80 are presented in Figure 7.37. The data are for an F-80 in cruise configuration, 230 gallon centerline tip tanks, and 165 gallon underslung tanks. These data show that the centerline tanks increase dihedral effect while the underslung tanks reduce stable dihedral effect considerably.

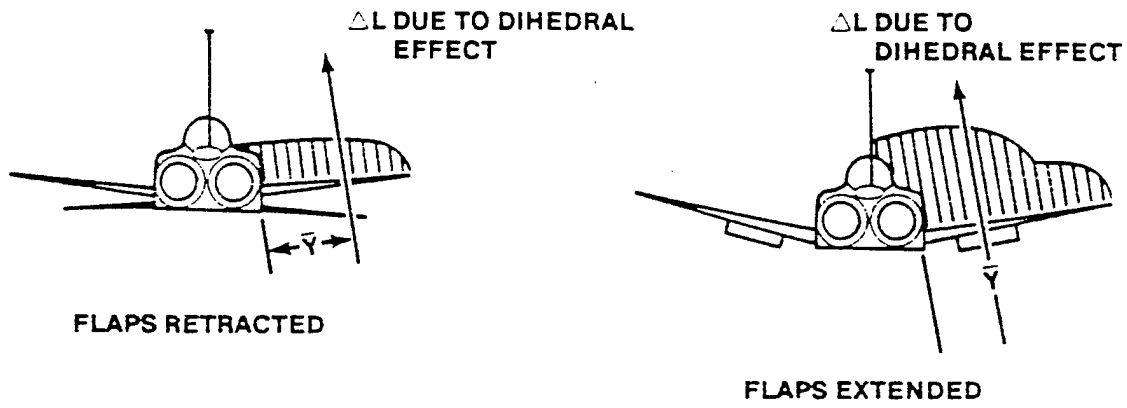


FIGURE 7.38. EFFECT OF FLAPS ON WING LIFT DISTRIBUTION

7.4.1.6 Partial Span Flaps. Partial span flaps indirectly affect static lateral stability by shifting the center of lift of the wing, thus changing the effective moment arm Y. If the partial span flap is on the inboard portion of the wing (as is usually the case), then it will shift the center of lift inboard and reduce the effective moment arm. Therefore, although the values of ΔL remain the same, the rolling moment will decrease. This in turn has a detrimental effect on $C_{l_\beta}$ (Figure 7.38). The higher the effectiveness of the flaps in increasing the lift coefficient, the greater will be the change in span lift distribution and the more detrimental will be the effect of the inboard flaps. Therefore, the decrease in lateral stability due to flap extension may be large.

Extended flaps may also cause a secondary, and generally small, variation in the effective dihedral. This secondary effect depends upon the planform of the flaps themselves. If the shape of the wing gives a sweepback to the leading edge of the flaps, a slight stabilizing dihedral effect results when the flaps are extended. If the leading edges of the flaps are swept forward, flap extension causes a slight destabilizing dihedral effect. These effects are produced by the same phenomenon that produced a change in $C_{l_\beta}$ with wing sweep.

7.4.1.7 Wing-Fuselage Interference. For a complete analysis of dihedral effect, account must be taken of the various interference effects between parts of the aircraft. Of these, probably the most important is wing-fuselage interference-more precisely, the change in angle of attack of the wing near the root due to the flow pattern about the fuselage in a sideslip. To illustrate this, consider a cylindrical body yawed with respect to the relative wind.

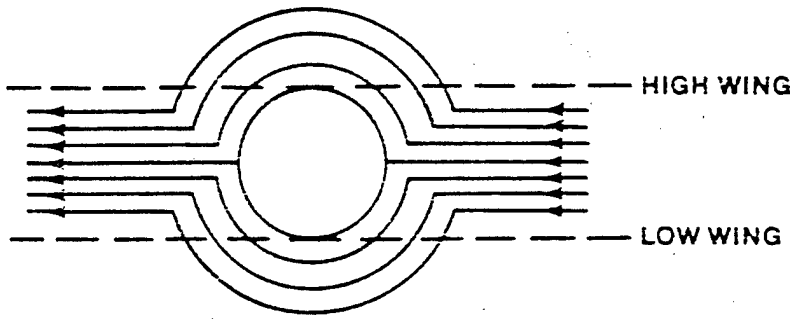


FIGURE 7.39. FLOW PATTERN ABOUT A FUSELAGE IN SIDESLIP

The fuselage induces vertical velocities in a sideslip which, when combined with the mainstream velocity, alters the local angle of attack of the wing. When the wing is located at the top of the fuselage (high-wing), then the angle of attack will be increased at the wing root, and a positive sideslip will produce a negative rolling moment; i.e., the dihedral effect will be enhanced. Conversely, when the aircraft has a low wing, the angle of attack at the root will be decreased, and the dihedral effect will be diminished. Generally, this explains why high-wing airplanes often have little or no geometric dihedral, whereas low-wing aircraft may have a great deal of geometric dihedral.

The magnitude of this effect is dependent upon the fuselage length ahead of the wing, its cross-sectional shape, and the planform and location of the wing.

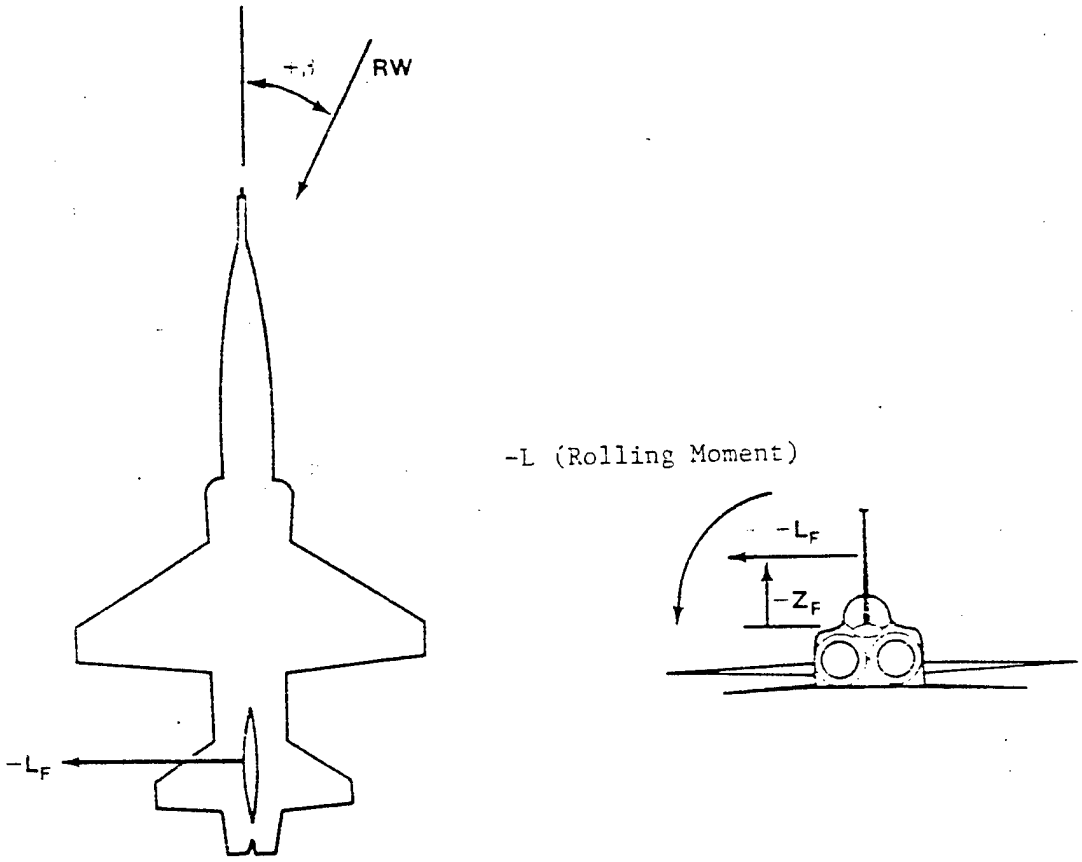


FIGURE 7.40. ROLLING MOMENT CREATED BY VERTICAL TAIL AT A POSITIVE ANGLE OF SIDESLIP

7.4.1.8 Vertical Tail. As we have already discovered in our $C_{n_\beta}$ discussion when the sideslip angle is changed, the angle of attack of the vertical tail is changed. This change in angle of attack produces a lift force on the vertical tail. If the center of pressure of the vertical tail is above the aircraft cg, this lift force will produce a rolling moment.

In the situation depicted in Figure 7.40, the negative rolling moment was created by a positive sideslip angle, thus, the vertical tail contributes a stable increment to dihedral effect. This contribution can be quite large. In fact, it can be the major contribution to $C_{l_\beta}$ on aircraft with large vertical tails such as the T-38. This effect can be calculated in the same manner yawing moments were calculated in the directional case.

Assuming a positive sideslip angle,

$$L_F(\text{Rolling Moment}) = -Z_F L_F \tag{7.65}$$

$$L_F(\text{Rolling Moment}) = -Z_F \bar{k} \times -L_F \bar{j} = -Z_F L_F \bar{i}$$

Since

$$C_{l_F} = \frac{L\ (\text{Rolling Moment})}{q_w S_w b_w}$$

then

$$C_{l_F} = \frac{-Z_F L_F}{q_w S_w b_w} \tag{7.66}$$

but

$$L_F = C_{L_F} q_F S_F$$

Therefore,

$$C_{l_F} = \frac{-Z_F\ C_{L_F}\ q_F\ S_F}{q_w S_w b_w} \tag{7.67}$$

Define $\bar{V}_F$ as

$$V_F = \frac{S_F Z_F}{S_w b_w} \tag{7.68}$$

Assume that for a jet aircraft

$$q_F = q_w \tag{7.69}$$

And Equation 7.67 becomes

$$C_{l_F} = -C_{L_F} V_F = -a_F \alpha_F V_F \tag{7.70}$$

Knowing

$$\alpha_F = (\beta - \sigma)$$

$$C_{l_F} = -a_F V_F (\beta - \sigma) \tag{7.71}$$

$$(-)(-) \quad (+) \quad = \quad (-) \text{ Tail on top}$$

$$C_{l_\beta}\Big|_{\substack{\text{Vertical} \\ \text{tail}}} = \frac{\partial C_{l_F}}{\partial \beta} = -a_F V_F \left[1 - \frac{\partial \sigma}{\partial \beta}\right] \tag{7.72}$$

$$(-)(+) \quad (+) \quad = \quad (+) \text{ Tail on bottom}$$

Equation 7.72 reveals that a vertical tail contributes a stable increment to $C_{l_\beta}$, whereas a ventral fin [$V_F$ = (+)] would contribute an unstable increment to $C_{l_\beta}$. Also, if the lift curve slope of the vertical tail is increased, by end plating for example, the stable dihedral effect would be greatly increased. For example, the F-104 has a high horizontal stabilizer that acts as an end plate on the vertical tail, and this increases the stable dihedral effect. In fact, the increase is so large that it is necessary to add negative geometric dihedral to the wings to maintain a reasonable value of stable dihedral effect.

### 7.4.2 $C_{l_{\delta_a}}$ LATERAL CONTROL POWER

Lateral control is normally achieved by altering the lift distribution so that the total lift on the two wings differs, thereby creating a rolling moment. This is done by destroying lift on one wing by a spoiler, or by altering the lift on both wings with ailerons (Figure 7.41).

Many modern aircraft designs use differential deflections of the horizontal stabilizers for roll control. When the pilot makes a roll input, the horizontal stabilizer on one side will deflect trailing edge down, while the stabilizer on the other side deflects trailing edge up. The difference in lift on the two sides of the stabilizer results in a rolling moment.

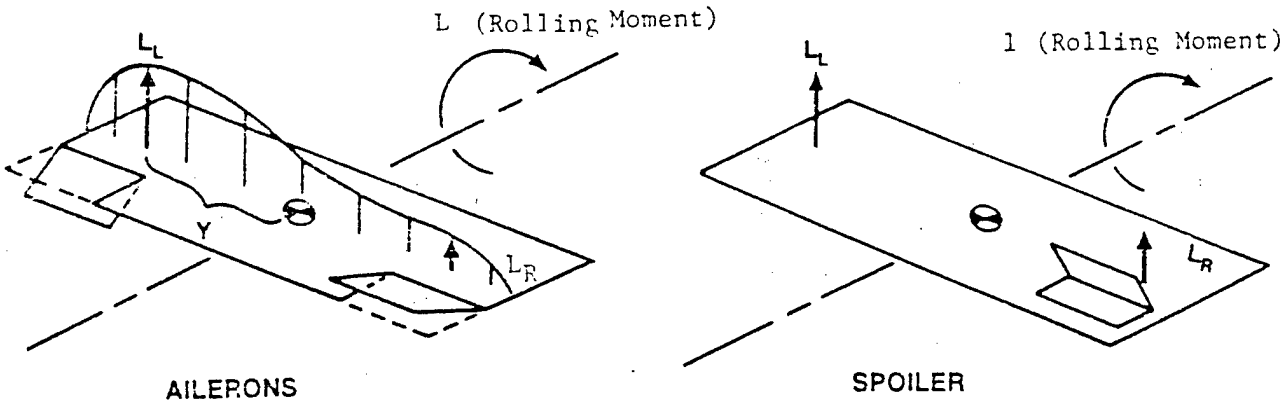


FIGURE 7.41. LATERAL CONTROL

This discussion will be limited to the use of ailerons as the means of lateral control. A measure of aileron power is the rolling moment created by a given aileron deflection. A positive deflection of either aileron, $+\delta_a$, is defined as one which produces a positive rolling moment, (right wing down). $C_{l_{\delta_a}}$ is positive by definition. Total aileron deflection is defined as the sum of the two individual aileron deflections. Thus,

$$\delta_{a_{Total}} = \delta_{a_{Left}} + \delta_{a_{Right}} \tag{7.73}$$

The assumption will be made that the wing cp shift due to aileron deflection will not alter the value of $C_{l_\beta}$. The distance from the x-axis to the cp of the wing will be labeled Y. When the ailerons are deflected, they produce a change in lift on both wings. This total change in lift, $\Delta L$, produces a rolling moment, L.

$$L(\text{Rolling Moment}) = L_L\, Y - L_R\, Y = (L_L - L_R)\, Y = \Delta L\ Y \tag{7.74}$$

Since

$$L = C_L\, q\, S$$

then

$$\Delta L = \frac{\partial C_L}{\partial \alpha}\ \Delta\alpha\ q\ S \tag{7.75}$$

therefore

$$L(\text{Rolling Moment}) = \frac{\partial C_{L_a}}{\partial \alpha_a} \Delta\alpha_a \, q_a \, S_a \, Y \tag{7.76}$$

where the "a" subscripts refer to "aileron" values.

But

$$\frac{\partial C_{L_a}}{\partial \alpha_a} = a_a \tag{7.77}$$

therefore

$$L(\text{Rolling Moment}) = a_a \, \Delta\alpha_a \, q_a \, S_a \, Y \tag{7.78}$$

Recalling

$$C_l = \frac{L \text{ (Rolling Moment)}}{q_w \, S_w \, b_w}$$

then

$$C_l = \frac{a_a \, \Delta\alpha_a \, S_a \, Y}{S_w \, b_w} \left[\frac{q_a}{q_w}\right]^1 \tag{7.79}$$

If we let $\Delta\alpha_a = \delta_{a_{Left}} + \delta_{a_{Right}} = \delta_{a_{Total}}$

then

$$C_l = \frac{a_a \, \delta_{a_{Total}} \, S_a \, Y}{S_w \, b_w} \tag{7.80}$$

and

$$\frac{\partial C_l}{\partial \delta_a} = C_{l_{\delta_a}} = a_a \left[\frac{S_a}{S_w}\right] \left[\frac{Y}{b}\right] \tag{7.81}$$

Thus, from Equation 7.81 the lateral control power is a function of the aileron airfoil section ($a_a$), the area of the aileron in relation to the area of the wing $S_a/S_w$, and the location of the wing cp ($Y/b$).

### 7.4.3 $C_{l_p}$ Roll Damping

The forces generated when an airplane is rolling about its x-axis, at some roll rate, p, produce rolling moments which tend to oppose the motion. Thus the algebraic sign of $C_{l_p}$ is usually negative.

The primary contributors to roll damping are the wings and the tail. The wing contribution to $C_{l_p}$ arises from the change in wing angle of attack that results from the rolling velocity. It has already been shown that the downgoing wing in a rolling maneuver experiences an increase in angle of attack. This increased $\alpha$ tends to develop a rolling moment that opposes the original rolling moment. However, when the wing is near the aerodynamic stall, a rolling motion may cause the downgoing wing to exceed the stall angle of attack. In this case, the local lift curve slope may fall to zero or even reverse sign. The algebraic sign of the wing contribution to $C_{l_p}$ may then become positive. This is what occurs when a wing "autorolls," as in spinning (Figure 7.42).

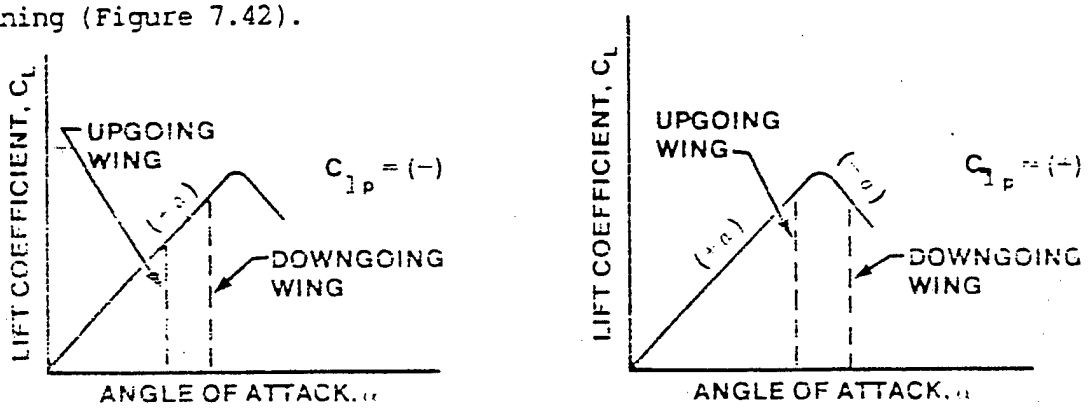


FIGURE 7.42. HIGH AOA EFFECTS ON $C_{l_p}$

The vertical tail contribution to $C_{l_p}$ arises from the fact that when the aircraft is rolled, the angle of attack on the vertical tail is changed. This change in angle of attack develops a lift force which opposes the original rolling moment. This contribution to a negative $C_{l_p}$ is the same regardless of whether the tail is above (conventional tail) or below (ventral fin) the aircraft roll axis.

### 7.4.4 $C_{l_r}$ Rolling Moment Due to Yaw Rate

The primary contributions to $C_{l_r}$ come from two sources, the wings and the vertical tail (Figure 7.43).

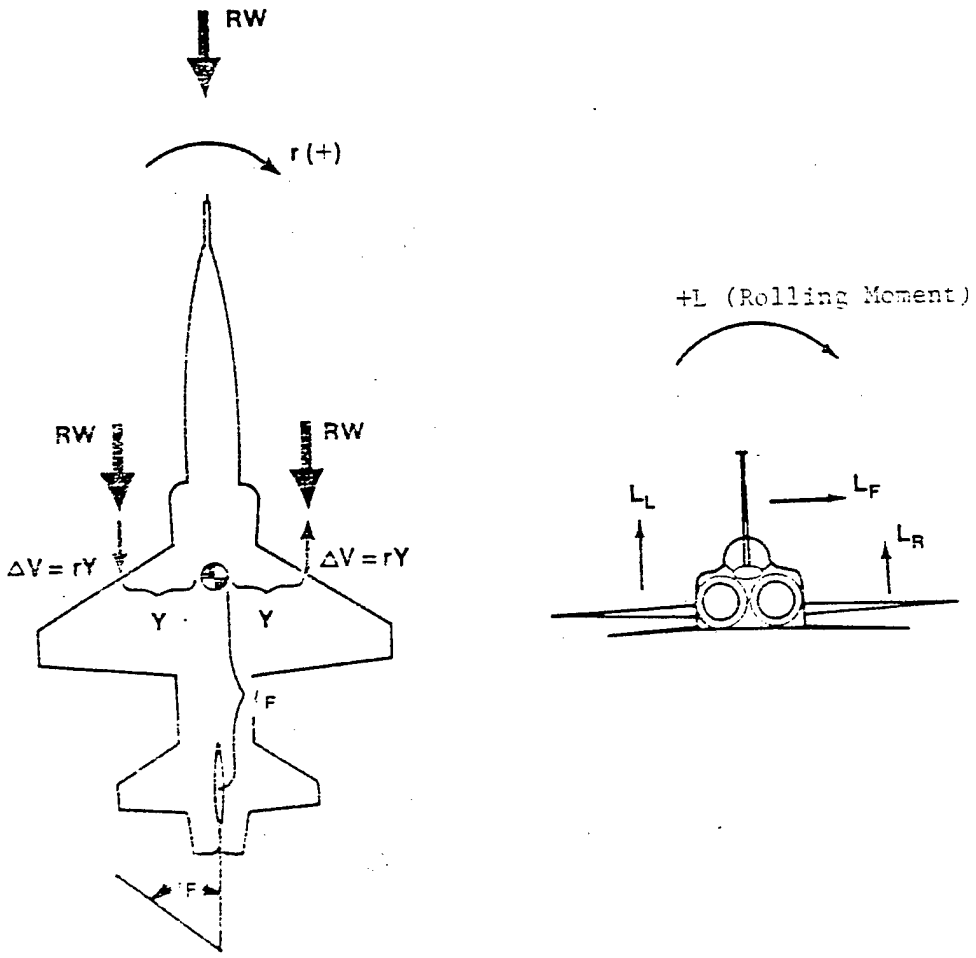


FIGURE 7.43. $C_{l_r}$ CONTRIBUTORS

As the aircraft yaws, the velocity of the relative wind is increased on the advancing wing to produce more lift and thus produces a rolling moment. A right yaw would produce more lift on the left wing and thus a rolling moment to the right. Thus, the algebraic sign of the wing contribution to $C_{l_r}$ is positive.

The tail contribution to $C_{l_r}$ arises from the fact that as the aircraft is yawed, the angle of attack on the vertical tail is changed. The lift force thus produced, $L_F$, will create a rolling moment if the vertical tail cp is above or below the cg. For a conventional vertical tail, the sign of $C_{l_r}$ will be positive, while for a ventral fin the sign will be negative.

### 7.4.5 $C_{l_{\delta_r}}$ Rolling Moment Due to Rudder Deflection

When a rudder is deflected it creates a lift force on the vertical tail. If the cp of the vertical tail is above or below the aircraft cg a rolling moment will result. Refer to Figure 7.44.

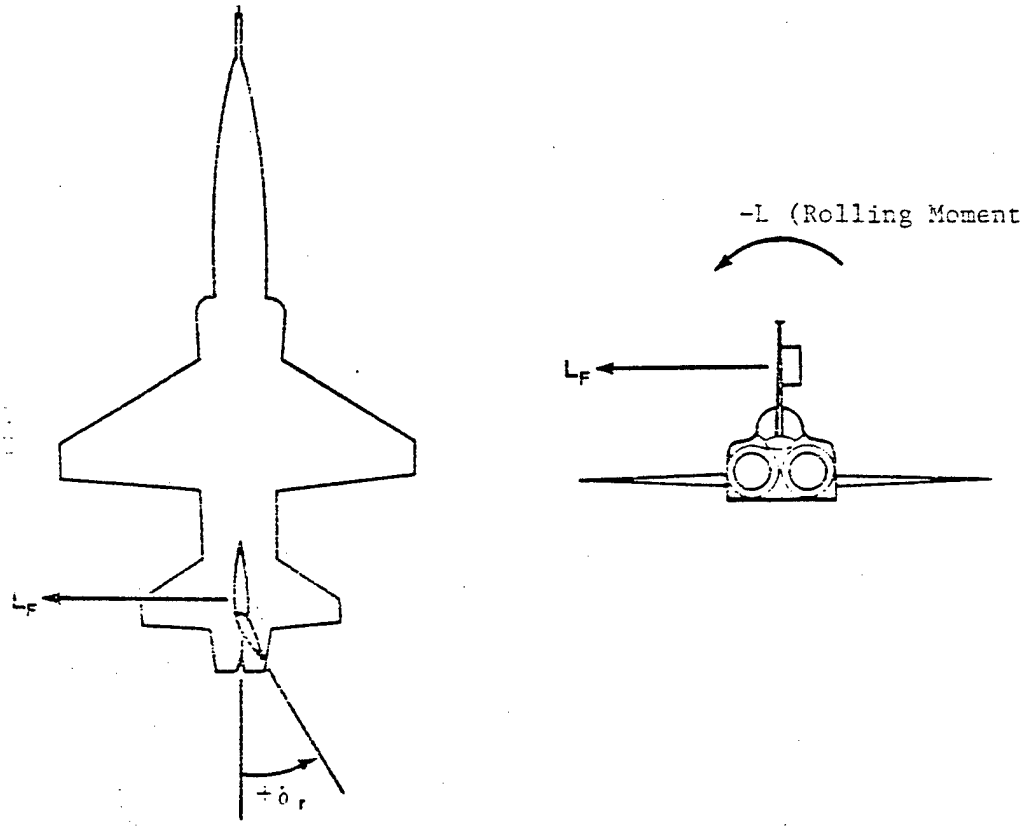


FIGURE 7.44. LIFT FORCE DEVELOPED AS A RESULT OF $\delta_r$

It can be seen that if the cp of the vertical tail is above the cg, as with a conventional vertical tail, the sign of $C_{l_{\delta_r}}$ will be negative. However, with a rudder mounted on a ventral fin, the sign would be positive.

The effects of $C_{l_{\delta_r}}$ and $C_{l_\beta}$ are opposite in nature. When the rudder is deflected to the right, initially, a rolling moment to the left is created due to $C_{l_{\delta_r}}$. However, as sideslip develops due to the rudder deflection, dihedral effect, $C_{l_\beta}$, comes into play and causes a resulting rolling moment to the right. Therefore, when a pilot applies right rudder to pick up a left wing, he initially creates a rolling moment to the left and, finally, to the right (Figure 7.45).

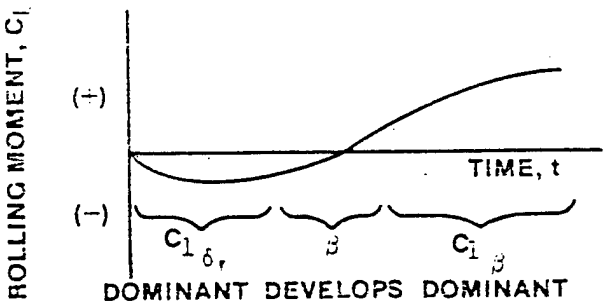


FIGURE 7.45. TIME EFFECTS ON ROLLING MOMENT DUE TO $C_{l_{\delta_r}}$ and $C_{l_\beta}$ CAUSED BY + $\delta_r$

7.4.6 $C_{l_{\dot\beta}}$ Rolling Moments Due to Lag Effects in Sidewash

In the discussion of $C_{n_{\dot\beta}}$, it was pointed out that during an increase in $\beta$, the angle of attack of the vertical tail will be less than it will finally be in steady state condition. If the cp of the vertical tail is displaced from the aircraft cg, this change in $\alpha_T$ due to lag effects will alter the rolling moment created during the $\beta$ build up period. Because of lag effects, $C_{l_T}$ will be less during the $\beta$ build up period than at steady state. Thus, for a conventional vertical tail, the algebraic sign of $C_{l_{\dot\beta}}$ is positive.

Again, it should be pointed out that there is widespread disagreement over the interpretation of data concerning lag effects in sidewash and that the foregoing is only one basic approach to a complex problem.

7.4.7 High Speed Consideration of Static Lateral Stability

Most of the contributions to $C_l$ are due to $L_{wing}$, $\Delta L_{wing}$ or $L_{vertical\ tail}$. As airspeed affects these parameters, it also affects static lateral stability.

7.4.7.1 $C_{l_\beta}$. Generally, $C_{l_\beta}$ is not greatly affected by Mach. However, in the transonic region the increase in the lift curve slope of the vertical tail increases this contribution to $C_{l_\beta}$ and usually results in an overall increase in $C_{l_\beta}$ in the transonic region.

7.4.7.2 $C_{l_{\delta_a}}$. Because of the decrease in the lift curve slope of all aerodynamic surfaces in supersonic flight, lateral control power decreases as Mach increases supersonically.

Aeroelasticity problems have been quite predominant in the lateral control system, since in flight at very high dynamic pressures the wing torsional deflections which occur with aileron use are considerable and cause noticeable changes in aileron effectiveness (Figure 7.46). At high dynamic pressures, dependent upon the given wing structural integrity, the twisting deformation might be great enough to nullify the effect of aileron deflection and the aileron effectiveness will be reduced to zero. Since at speeds above the point where this phenomenon occurs, rolling moments are created which are opposite in direction to the control deflection, this speed is termed "aileron reversal speed."

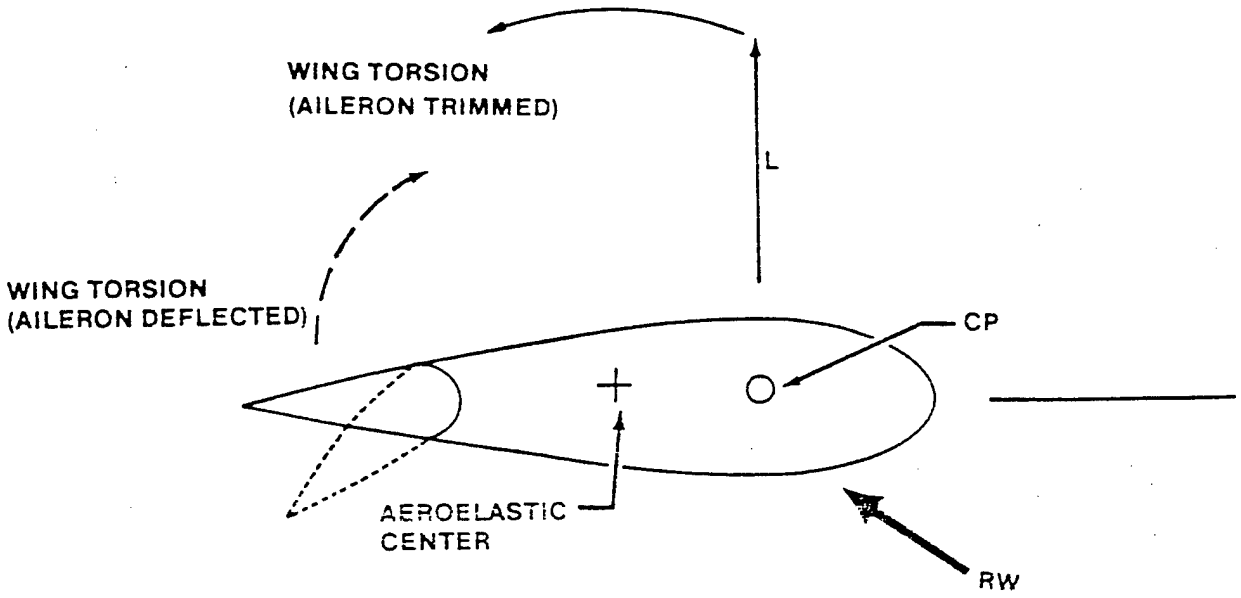


FIGURE 7.46. AEROELASTIC EFFECTS

In order to alleviate this characteristic, the wing must have a high torsional stiffness which presents a significant design problem in sweptwing aircraft. For an aircraft design of the B-47 type, it is easy to visualize how aeroelastic distortion might result in a considerable reduction in lateral control capability at high speeds. In addition, lateral control effectiveness at transonic Mach may be reduced seriously by flow separation effects as a result of shock formation. However, modern high-speed fighter designs have been so successful in introducing sufficient rigidity into wing structures and employing such design modifications as split ailerons, inboard ailerons, spoiler systems etc., that the resulting high control power coupled with the low $C_{l_p}$ of low aspect ratio planforms, has resulted in the lateral control becoming an accelerating device rather than a rate control. That is to say, a steady state rolling velocity is normally not reached prior to attaining the desired bank angle. Consequently, many high speed aircraft have a type of differential aileron system to provide the pilot with much more control surface during approach and landings and to restrict the degree of control in other areas of flight.

Spoiler controls are quite effective in reducing aeroelastic distortions since the pitching moment changes due to spoilers are generally smaller than those for a flap type control surface. However, a problem associated with

spoilers is their tendency to reverse the roll direction for small stick inputs during transonic flight. This occurs as a result of re-energizing the boundary layer by a vortex generator effect for very small deflections of the spoiler, which can reduce the magnitude of the shock induced separation and actually increase the lift on the wing. This difficulty can be eliminated by proper design.

7.4.7.3 $C_{l_p}$. Since "damping" requires the development of lift on either the wing or the tail, it depends on the value of the lift curve slope. Thus, as the lift curve slope of the wing and tail decreases supersonically, $C_{l_p}$ decreases. Also, since most supersonic designs make use of low aspect ratio surfaces, $C_{l_p}$ will tend to be less for these designs.

7.4.7.4 $C_{l_r}$ and $C_{l_{\delta_r}}$. Both of these derivatives depend on the development of lift and will decrease as the lift curve slope decreases supersonically.

7.4.7.5 $C_{l_{\dot{\beta}}}$. Data on the supersonic variation of this derivative is sketchy, but it probably will not change significantly with Mach.

Variation of all the $C_l$ component derivatives with Mach is illustrated in Figure 7.47.

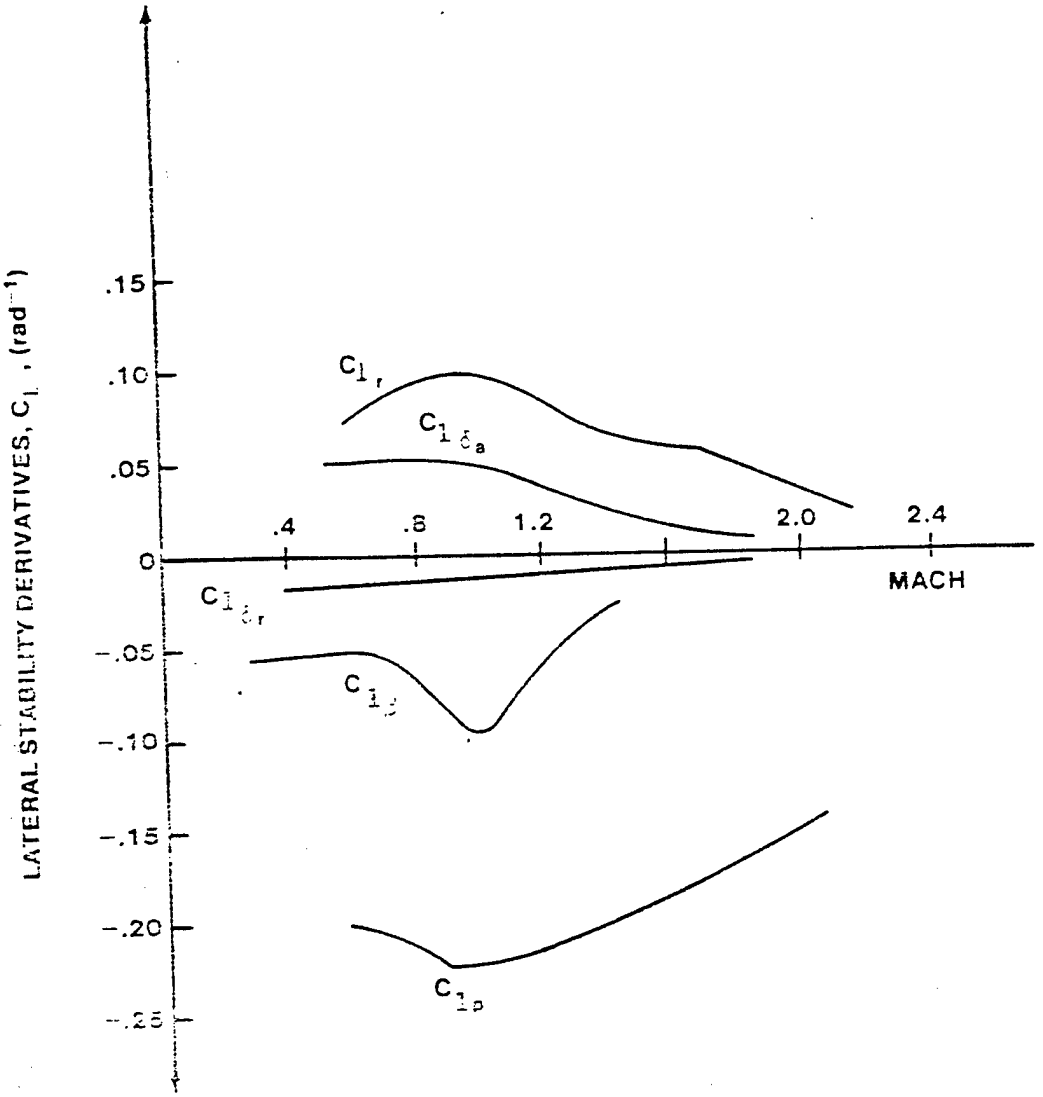


FIGURE 7.47. CHANGES IN LATERAL STABILITY DERIVATIVES WITH MACH (F-4C)

7.4.8 Controls Fixed Static Lateral Stability (Flight Test Relationship)

Having discussed the lateral stability derivatives, we are now ready to develop a parameter which can be measured in flight to determine the static lateral stability of an aircraft. As in the directional stability case, the maneuver that will be flown will be steady straight sideslip (reference Figure 7.21). Recalling the static lateral equation of motion and the fact that in a steady straight sideslip $p = q = r = \dot{\beta} = \dot{p} = \dot{r} = \dot{v} = \Sigma G = \Sigma F_y = 0$, then

$$C_{l_\beta}\beta + C_{l_{\dot\beta}}\frac{\dot\beta b}{2U_o}^{0} + C_{l_p}\frac{pb}{2U_o}^{0} + C_{l_r}\frac{rb}{2U_o}^{0} + C_{l_{\delta_a}}\delta_a + C_{l_{\delta_r}}\delta_r = C_l^{0}$$

Thus

$$C_{l_\beta}\beta + C_{l_{\delta_a}}\delta_a + C_{l_{\delta_r}}\delta_r = 0 \tag{7.82}$$

Solving for $\delta_a$

$$\delta_a = -\frac{C_{l_\beta}}{C_{l_{\delta_a}}}\beta - \frac{C_{l_{\delta_r}}}{C_{l_{\delta_a}}}\delta_r \tag{7.83}$$

and differentiating with respect to $\beta$

$$\frac{\partial\delta_a}{\partial\beta} = -\frac{C_{l_{\beta\,(\text{Fixed})}}}{C_{l_{\delta_a}}} - \frac{C_{l_{\delta_r}}}{C_{l_{\delta_a}}}\frac{\partial\delta_r}{\partial\beta}$$

Disregarding the term that is usually the smallest contributor to the expression, $C_{l_{\delta_r}}$, we arrive at the following flight test relationship:

$$\frac{\partial\delta_a}{\partial\beta} = f\left[-\frac{C_{l_\beta}}{C_{l_{\delta_a}}}\right] \tag{7.84}$$

Since $C_{l_{\delta_a}} = a_a\,(S_a/S_w)(Y/b)$, all of which are known and fixed by design, then the only dominant variable remaining is $C_{l_\beta}$. Therefore $\partial\delta_a/\partial\beta$ can be taken as a direct measure of the static lateral stability of an aircraft, controls fixed.

Since $C_{l_\beta}$ has to be negative in order to have lateral stability and $C_{l_{\delta_a}}$ is positive by definition, then $\partial\delta_a/\partial\beta$ should have a positive slope as shown in Figure 7.48.

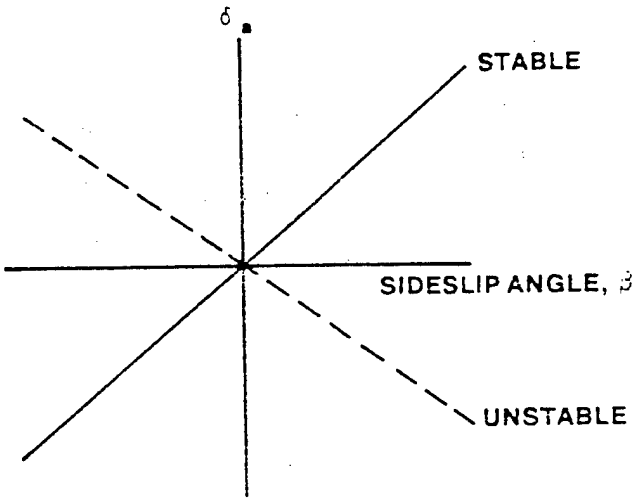


FIGURE 7.48. AILERON DEFLECTION $\delta_a$ VERSUS SIDESLIP ANGLE

7.4.9 Controls Free Static Lateral Stability (Flight Test Relationship)

On aircraft with reversible control systems, the ailerons are free to float in response to their hinge moments. Using the same approach as in the directional case, it is possible to derive an expression that will relate the "aileron free" static lateral stability to parameters that can be easily measured in flight. For the discussion of aileron hinge moments, a change in angle of attack on a wing will be defined as positive if it causes a positive rolling moment. This may be contrary to the sign convention used in the longitudinal case.

In a steady straight sideslip, $\Sigma L = 0$ which implies that $\Sigma L_{Hinge\ Pin} = 0$. Now if moments are summed about the aileron hinge pin, then a pilot must apply aileron forces to oppose the aerodynamic hinge moment in order to keep the ailerons deflected the required amount to maintain $\Sigma L_{Hinge\ Pin} = 0$. This aileron force, $F_a$, acts through a moment arm and gearing mechanism, both accounted for by some constant K.

Thus in steady straight flight

$$\Sigma L_{Hinge\ Pin} = F_a K + H_a = 0 \qquad (7.85)$$

where $H_a$ = the aileron hinge moment. Or

$$F_a = -GH_a \tag{7.86}$$

where G = 1/K (definition).

Recalling coefficient format,

$$C_h = \frac{H_a}{(1/2\ \rho\ V_T^2)\ S_a\ c_a} \tag{7.87}$$

Thus

$$H_a = C_h\ (1/2\ \rho\ V_T^2)\ S_a\ c_a \tag{7.88}$$

But we have already shown from Equation 7.23 that

$$C_h = C_{h_{\alpha_a}}\ \alpha_a + C_{h_{\delta_a}}\ \delta_a \tag{7.89}$$

Therefore,

$$H_a = (1/2\ \rho\ V_T^2)\ S_a\ c_a\ \left[C_{h_{\alpha_a}}\ \alpha_a + C_{h_{\delta_a}}\ \delta_a\right] \tag{7.90}$$

Thus Equation 7.86 becomes

$$F_a = -G\ (1/2\ \rho\ V_T^2)\ S_a\ c_a\ \left[C_{h_{\alpha_a}}\ \alpha_a + C_{h_{\delta_a}}\ \delta_a\right] \tag{7.91}$$

Recalling that for a floating control surface

$$C_{h_{\alpha_a}} \alpha_a = - C_{h_{\delta_a}} \delta_{a(\text{Float})} \tag{7.92}$$

Therefore

$$F_a = - G (1/2 \rho V_T^2) S_a c_a C_{h_{\delta_a}} [\delta_a - \delta_{a(\text{Float})}] \tag{7.93}$$

The difference between where the pilot pushes the aileron, $\delta_a$, and the amount it floats, $\delta_{a_{(\text{Float})}}$, is the free position of the aileron, $\delta_{a_{(\text{Free})}}$.

Therefore,

$$F_a = - G (1/2 \rho V_T^2) S_a c_a C_{h_{\delta_a}} \delta_{a_{(\text{Free})}} \tag{7.94}$$

Differentiating with respect to $\beta$

$$\frac{\partial F_a}{\partial \beta} = - G (1/2 \rho V_T^2) S_a c_a C_{h_{\delta_a}} \frac{\partial \delta_{a_{(\text{Free})}}}{\partial \beta} \tag{7.95}$$

From Equation 7.84, it can be shown that

$$\frac{\partial \delta_{a_{(\text{Free})}}}{\partial \beta} = - \frac{C_{l_{\beta_{(\text{Free})}}}}{C_{l_{\delta_a}}} \tag{7.96}$$

Thus

$$\frac{\partial F_a}{\partial \beta} = \underset{(+)}{G} \; \underset{(+)}{(1/2\ \rho\ V_T^2)} \; \underset{(+)(+)}{S_a\ c_a\ \frac{C_{h_{\delta_a}}}{C_{l_{\delta_a}}}\ C_{l_\beta}(\text{Free})} = \underset{\text{for stability}}{(+)} \qquad (7.97)$$

This equation shows that the parameter $\partial F_a/\partial\beta$ can be taken as an indication of the aileron free static lateral stability of an aircraft since all terms are either constant or set by design, except $C_{l_\beta}$. More importantly, $\partial F_a/\partial_\beta$ can be readily measured in flight.

An analysis of Equation 7.97 reveals that for stable dihedral effect, a plot of $\partial F_a/\partial\beta$ would have a positive slope (Figure 7.49).

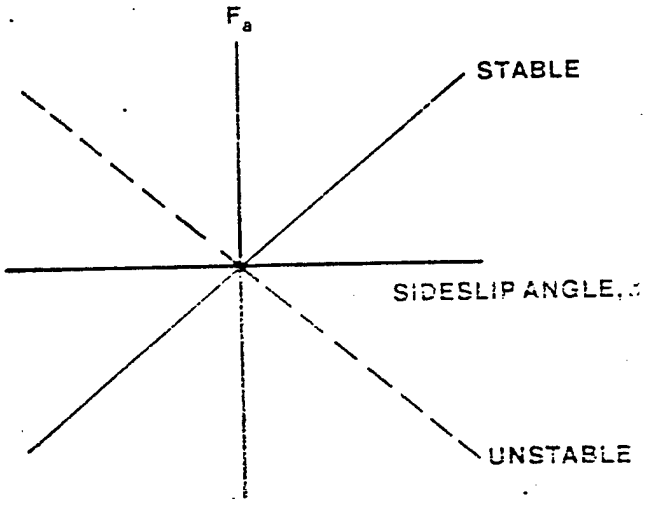


FIGURE 7.49. AILERON FORCE $F_a$ VERSUS SIDESLIP ANGLE

## 7.5 ROLLING PERFORMANCE

Now that we have shown how aileron force and deflection can be used as a measure of the stable dihedral effect of an aircraft, it is necessary to consider how these parameters affect the rolling capability of the aircraft. For example, full aileron deflection may produce excellent rolling characteristics on certain aircraft; however, because of the large aileron forces required, the pilot may not be able to fully deflect the ailerons, thus making the overall rolling performance unsatisfactory. Thus, it is necessary to evaluate the rolling performance of the aircraft.

The rolling qualities of an aircraft can be evaluated by examining the parameters $F_a$, $\delta_a$, p and $(pb/2U_0)$. Although the importance of the first three parameters is readily apparent, the parameter $(pb/2U_0)$ needs some additional explanation.

Mathematically $pb/2U_0$ is a nondimensional parameter where p = roll rate (rad/sec); b = wing span (ft); and $U_0$ = velocity (ft/sec).

Physically $pb/2U_0$ may be described as the helix angle that the wing tip of a rolling aircraft describes (Figure 7.50). In addition, the $pb/2U_0$ that can be produced by full lateral control deflection is a measure of the relative lateral control power available.

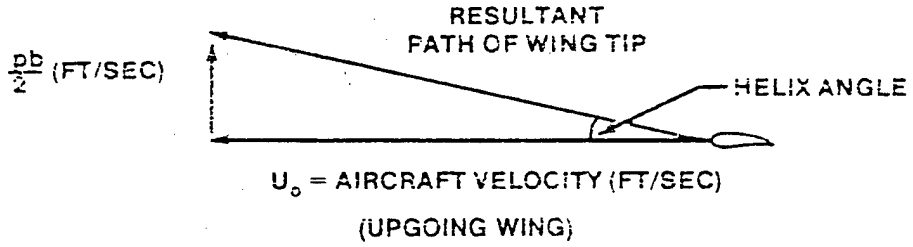


FIGURE 7.50. WING TIP HELIX ANGLE (UPGOING WING)

It can be seen that

$$\tan(\text{Helix Angle}) = \frac{pb}{2U_0} \qquad (7.98)$$

Assuming small angles

$$\text{Helix Angle} = \frac{pb}{2U_0} \tag{7.99}$$

This angle also represents the change in angle of attack of a rolling wing (Figure 7.51).

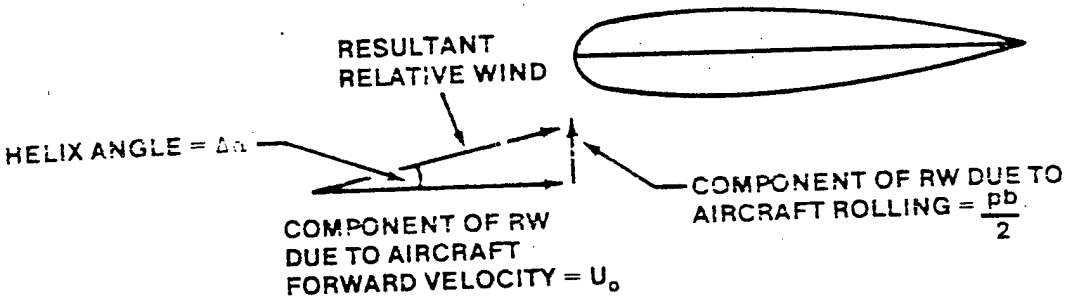


FIGURE 7.51. WIND FORCES ACTING ON A DOWNGOING WING DURING A ROLL

This figure shows that the angle of attack of the downgoing wing is increased due to the roll rate. This implies increased lift opposite the direction of roll on the downgoing wing and, conversely, decreased lift in the direction of roll on the upgoing wing due to decreased $\alpha$. This is essentially the same effect as $C_{l_p}$. Thus $pb/2U_0$ represents a damping term.

With the foregoing discussion as background, we are now ready to discuss the effect of $F_a$, $\delta_a$, p, $pb/2U_0$ on roll performance through the flight envelope of an aircraft.

From Equation 7.94 it can be seen that

$$F_a = f\left[V_T^2,\ \delta_{a_{(Free)}}\right] \tag{7.100}$$

$$\delta_{a_{(Free)}} = f\,(F_a,\ 1/V_T^{\,2}) \tag{7.101}$$

To derive a functional relationship for $(pb/2U_0)$, it is necessary to start with the basic lateral equations of motion,

$$C_l = C_{l_\beta}\beta + C_{l_{\dot\beta}}\frac{\dot\beta b}{2U_o} + C_{l_p}\frac{pb}{2U_o} + C_{l_r}\frac{rb}{2U_o} + C_{l_{\delta_a}}\delta_a + C_{l_{\delta_r}}\delta_r \tag{7.102}$$

and examine the effect of roll terms only, i.e., assume that the roll moment developed is due to the interaction of moments due to $\delta_a$ and roll damping only. Therefore, Equation 7.102 becomes

$$C_l = C_{l_p}\left[\frac{pb}{2U_0}\right] + C_{l_{\delta_a}}\delta_a \tag{7.103}$$

For the maximum steady state roll rate, $C_l = 0$, and Equation 7.103 becomes

$$C_{l_p}\left[\frac{pb}{2U_0}\right] + C_{l_{\delta_a}}\delta_a = 0 \tag{7.104}$$

$$\frac{pb}{2U_0} = -\frac{C_{l_{\delta_a}}\delta_a}{C_{l_p}} \tag{7.105}$$

$$p = \frac{-C_{l_{\delta_a}}\delta_a}{C_{l_p}}\left[\frac{2}{b}\right]U_o \tag{7.106}$$

$$\frac{pb}{2U_0} = f(\delta_a) \tag{7.107}$$

But we have already shown that $\delta_a = f(F_a, 1/V_T^2)$ therefore,

$$\frac{pb}{2U_0} = f(F_a, 1/V_T^2) \tag{7.108}$$

From equation 7.106

$$p = f(U_0, \delta_a) \tag{7.109}$$

and since

$$\delta_a = f(F_a, 1/V_T^2)$$

then

$$p = f(F_a, 1/V_T) \tag{7.110}$$

assuming

$$U_0 = V_T \text{ (i.e., no sideslip)}$$

To summarize, the rolling performance of an aircraft can be evaluated by examining the parameters, $F_a$, $\delta_a$, p, and $(pb/2U_0)$. Functional relationships have been developed in order to look at the variance of these parameters below Mach or aeroelastic effect. These functional relationships are

$$F_a = f(V_T^2, \delta_a) \tag{7.111}$$

$$\delta_a = f(F_a, 1/V_T 2) \tag{7.112}$$

$$\frac{pb}{2U_0} = f(\delta_a) = f(F_a, 1/V_T^2) \tag{7.113}$$

$$p = f(V_T, \delta_a) = f(F_a, 1/V_T) \tag{7.114}$$

These relationships are expressed graphically in Figure 7.52 for a case in which the pilot desires the maximum roll rate at all airspeeds.

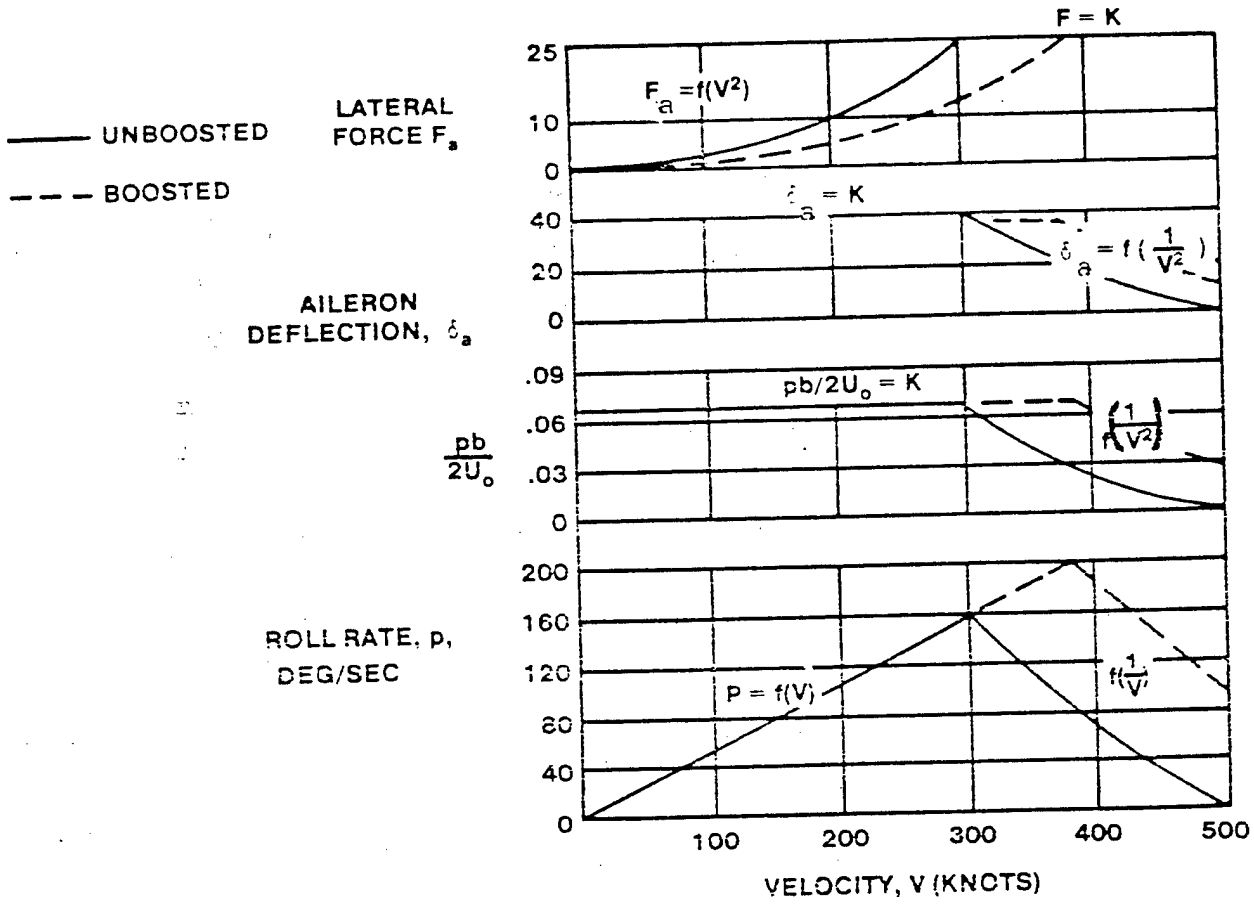


FIGURE 7.52. ROLLING PERFORMANCE

As indicated in Equation 7.111, the force required to hold a constant aileron deflection will vary as the square of the airspeed. The force required by the pilot to hold full aileron deflection will increase in this manner until the aircraft reaches $V_{MAX}$ or until the pilot is unable to apply any more force. In Figure 7.52, it is assumed that the pilot can supply a maximum of 25 pounds force and that this force is reached at 300 knots. If the speed is increased further, the aileron force will remain at this 25 pound maximum value. The curve of aileron deflection versus airspeed shows that the pilot is able to maintain full aileron deflection out to 300 knots. Inspection of Equation 7.112 shows that if aileron force is constant beyond 300 knots, then aileron deflection will be proportional to $(1/V_T^2)$. Equation 7.113 shows that $(pb/2U_0)$ will vary in the same manner as aileron deflection. Inspection of Equation 7.114 shows that the maximum roll rate available will increase linearly as long as the pilot can maintain maximum aileron

deflection, up to 300 knots in this case. Beyond this point, the maximum roll rate will fall off hyperbolically. That is, above 300 knots, p is proportional to $1/V_T$. It follows, then, that at high speeds the maximum roll rate may become unacceptably low. One method of combating this problem is to increase the pilot's mechanical advantage by adding boosted or fully powered ailerons.

By boosting the controls, the pilot can maintain full aileron deflection with less physical effort on his part. Thus, $F_a$ = 25 pounds will be delayed to a higher airspeed. The net effect is a shift of the $F_a$, $\delta_a$ and $pb/2U_0$ curves and a resulting increase in p (reference Figure 7.52 dashed lines).

Many modern aircraft have irreversible flight control systems. These systems allow an aircraft to be designed for a specific aileron force at full deflection, regardless of the airspeed. This allows the pilot to hold full deflection at high speeds, resulting in a constant helix angle and increasing roll rate at higher airspeeds. This change in performance is still limited by Mach effects and aeroelasticity.

## 7.6 LATERAL-DIRECTIONAL STATIC STABILITY FLIGHT TESTS

The lateral-directional characteristics of an aircraft are determined by two different flight tests: the steady straight sideslip test and the aileron roll test. The tests do not measure lateral and directional characteristics independently. Rather, each test yields information concerning both the lateral and the directional characteristics of the aircraft. The requirements of the MIL-STD-1797A will be discussed.

### 7.6.1 Steady Straight Sideslip Flight Test

The steady straight sideslip is a common maneuver which requires the pilot to balance the forces and moments generated on the airplane by a sideslip with appropriate lateral and directional control inputs and bank angle. Since these control forces and positions and bank angles are at least indicative of the sign (if not the magnitude) of the generated forces and moments (and therefore of the associated stability derivatives), the steady straight sideslip is a convenient flight test technique.

All equations relating to the static directional stability of an aircraft were developed under the assumption that the aircraft was in a "steady straight sideslip." This is the maneuver used in the sideslip test. First, trim the aircraft at the desired altitude and airspeed. Apply rudder to develop a sideslip. In order to maintain "straight" flight (constant ground track), bank the aircraft in the direction opposite that of the applied rudder. In Figure 7.53 the aircraft is in a steady sideslip. The moment created by the rudder, $N_{\delta_r}$, must equal the moment created by the

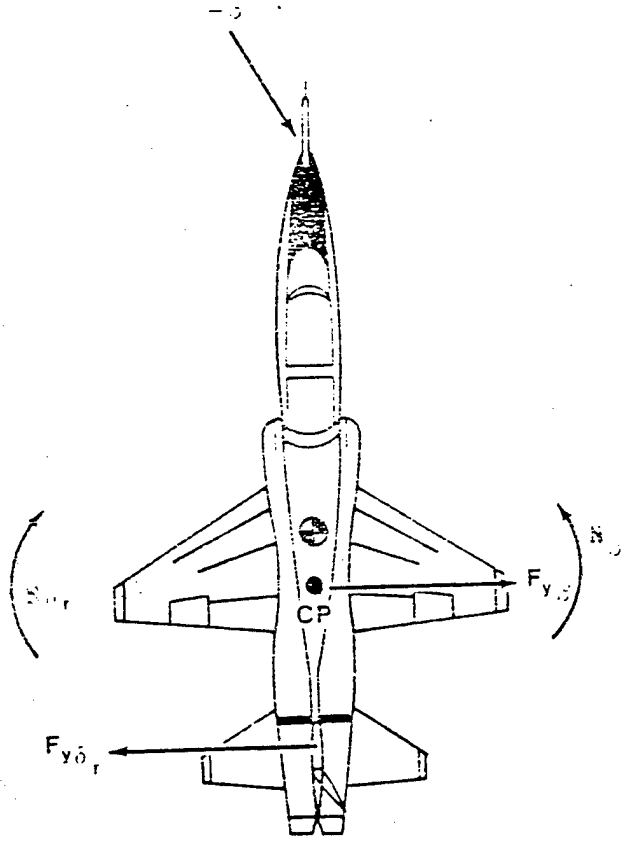


FIGURE 7.53. STEADY SIDESLIP

aerodynamic forces acting on the aircraft, $N_\beta$ . In this condition the side forces are unbalanced. $F_{y_\beta}$, will always be greater than $F_{y_{\delta_r}}$ . Thus, in the case depicted, the aircraft will accelerate, or turn, to the right. In order to stop this turn, it is necessary to bank the aircraft, in this case to the left (Figure 7.54). The bank allows a component of aircraft weight, W sin $\phi$, to act in the y direction and balance the previously unbalanced side forces. Thus, the pilot establishes a "straight sideslip." By holding this condition constant with respect to time or varying it so slowly in a continuously stabilized condition that rate effects are negligible, he establishes a "straight sideslip" - the condition that was used to derive the flight test relationships in static directional stability theory.

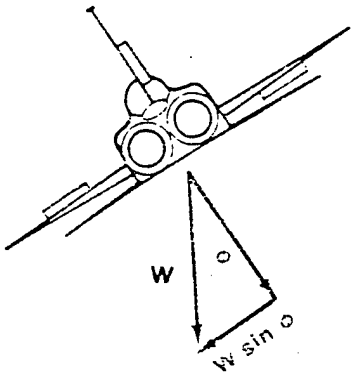


FIGURE 7.54. STEADY STRAIGHT SIDESLIP

MIL-STD-1797A, Paragraph 4.6.1.2 outlines the sideslip tests that must be performed in an aircraft. The specification recommended guidance states that sideslips be tested to full rudder pedal deflection, 250 pounds of rudder pedal force, or maximum aileron deflection, whichever occurs first. Often side slips must be discontinued prior to reaching these limits due to controllability or structural problems.

The following MIL-STD-1797A paragraphs apply to sideslip tests: 4.2.8.6.4, 4.5.5, 4.5.8.2, 4.5.8.5, 4.5.9.5.2, 4.5.9.5.4, 4.6.1.2., 4.6.6, 4.6.7, 4.6.7.6, 4.5.9.4 and 4.6.7.11. In addition, paragraphs 4.6.7.2 and 4.5.9.5 apply to steady turns.

One property of basic importance in the sideslip test is the directional stiffness of an aircraft or its static directional stability. To review, the static directional stability of an aircraft is defined by the initial tendency of the aircraft to return to or depart from its equilibrium angle of sideslip when disturbed from the equilibrium condition. In order to determine if the aircraft possesses static directional stability, it is necessary to determine how the yawing moments change as the sideslip angle is changed. For positive directional stability, a plot of $C_{n_\beta}$ must have a positive slope (Figure 7.55).

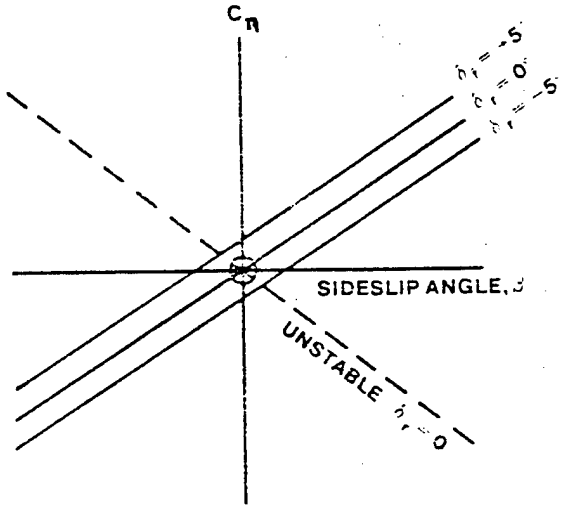


FIGURE 7.55. WIND TUNNEL RESULTS OF YAWING MOMENT COEFFICIENT $C_n$ VERSUS SIDESLIP ANGLE

Plots like those presented in Figure 7.55 are obtained from wind tunnel data. The aircraft model is placed at various angles of sideslip with various angles of rudder deflection, and the unbalanced moments are measured. However it is impossible to determine from flight tests the unbalanced moments at varying angles of sideslip. It was shown in static directional theory, however, that the rudder deflection required to fly in a steady straight sideslip is an indication of the amount of yawing moment tending to return the aircraft to or remove it from its original trimmed angle of sideslip. A plot is made of rudder deflection required versus sideslip angle in order to determine the sign of the rudder fixed static directional stability, $C_{n_\beta}$.

The control fixed stability parameter, $\partial\delta_r/\partial\beta$, for a directionally stable aircraft has a negative slope as shown in Figure 7.56. Paragraph 4.6.1.2, recommended guidance requires that right rudder pedal deflection ($+\delta_r$) accompany left sideslips ($-\beta$). Further, for angles of sideslip between $\pm 15°$, a plot of $\partial\delta_r/\partial\beta$ should be essentially linear. For larger sideslip angles, an increase in $\beta$ must require an increase in $\delta_r$. In other words, the slope of $\partial\delta_r/\partial\beta$ cannot go to zero.

Drastic changes occur in the transonic and supersonic speed regions. In the transonic region where the flight controls are most effective, a small $\delta_r$ may give a large $\beta$ and thus $\partial\delta_r/\partial\beta$ may appear less stable. However, as speed increases, control surface effectiveness decreases, and $\partial\delta_r/\partial\beta$ will increase in slope. This apparent change in $C_{n_\beta}$ is due solely to a change in control surface effectiveness and can give an entirely erroneous indication of the magnitude of the static directional stability if not taken into account.

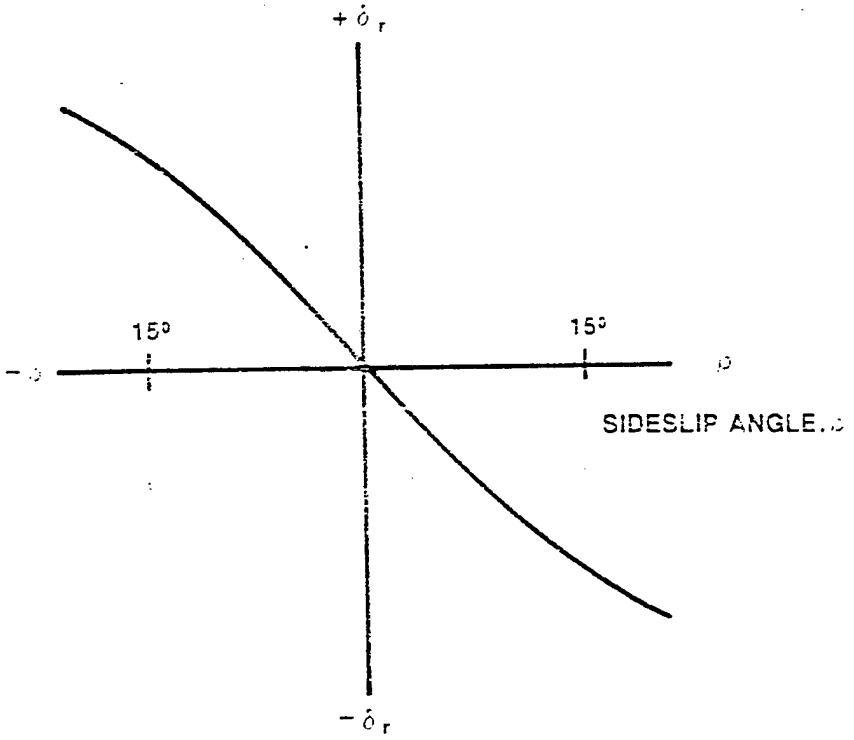


FIGURE 7.56. RUDDER DEFLECTION $\delta_r$ VERSUS SIDESLIP

A plot of rudder force required versus sideslip, $\partial F_r/\partial\beta$, is an indication of the rudder-free static directional stability of an aircraft. A plot of $\partial F_r/\partial\beta$ must have a negative slope for positive rudder-free static directional stability. Paragraph 4.6.1.2 recommends that a plot of $\partial F_r/\partial\beta$ be essentially linear between $\pm 10°$ of $\beta$ from the trim condition. At greater angles of sideslip, an increase in rudder force is required for an increase in sideslip.

These requirements are depicted in Figure 7.57.

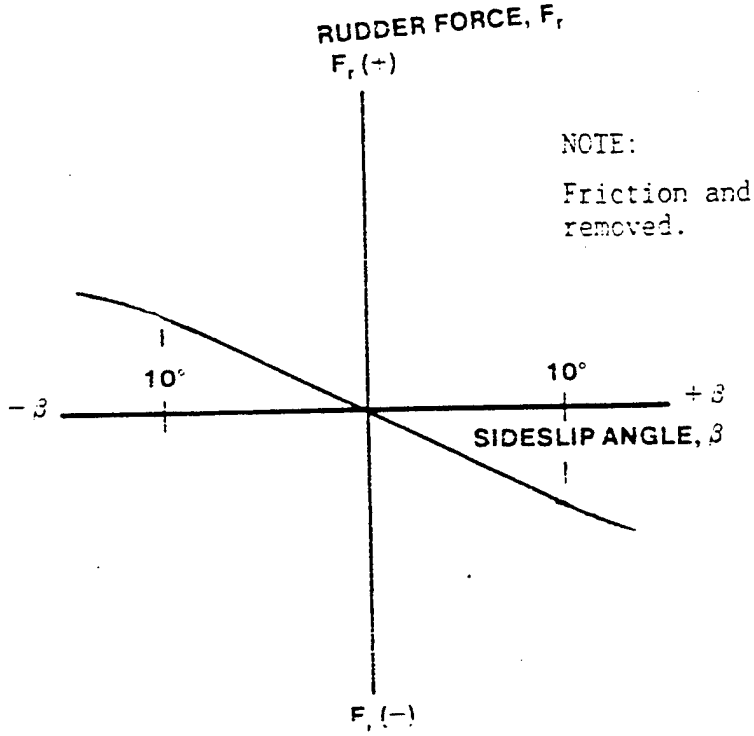


FIGURE 7.57. CONTROL FREE SIDESLIP DATA

The control force information in Figure 7.57 is acceptable as long as the algebraic sign of $F_r/\beta$ is negative.

Static lateral characteristics are also investigated during the sideslip test. It was shown in the theory of static lateral stability that $\partial\delta_a/\partial\beta$ may be taken as an indication of the control-fixed dihedral effect of an aircraft, $C_{l_{\beta(Fixed)}}$. For stable dihedral effect, it was shown that a plot of $\partial\delta_a/\partial\beta$

must have a positive slope. Right aileron control deflection shall accompany right sideslips and left aileron control shall accompany left sideslips. A plot of $\partial\delta_a/\partial\beta$ for stable dihedral effect is presented in Figure 7.58.

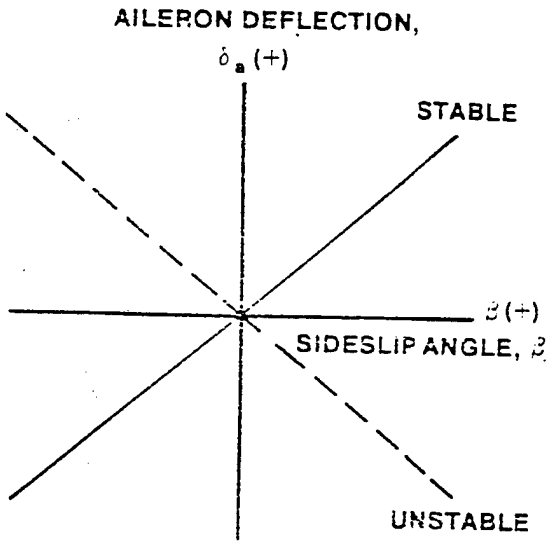


FIGURE 7.58. CONTROL FIXED SIDESLIP DATA

Recommended guidance from paragraphs 4.5.8.2 and 4.5.9.5.4 limits the amount of stable dihedral effect an aircraft will exhibit by specifying that no more than 75% of roll control power available to the pilot, and no more than 10 lbs of roll stick force or 20 lbs of roll wheel force are required for sideslip angles which may be experienced in service employment.

Theoretical discussion of control free dihedral effect revealed that $\partial F_a/\partial\beta$ gives an indication of $C_{l_{\beta(Free)}}$, and that for stable dihedral effect $\partial F_a/\partial\beta$ is positive (Figure 7.59). Paragraph 4.5.5 recommends that left aileron force should be required for left sideslips and that a plot of $\partial F_a/\partial\beta$ should be essentially linear for all of the mandatory sideslips tested.

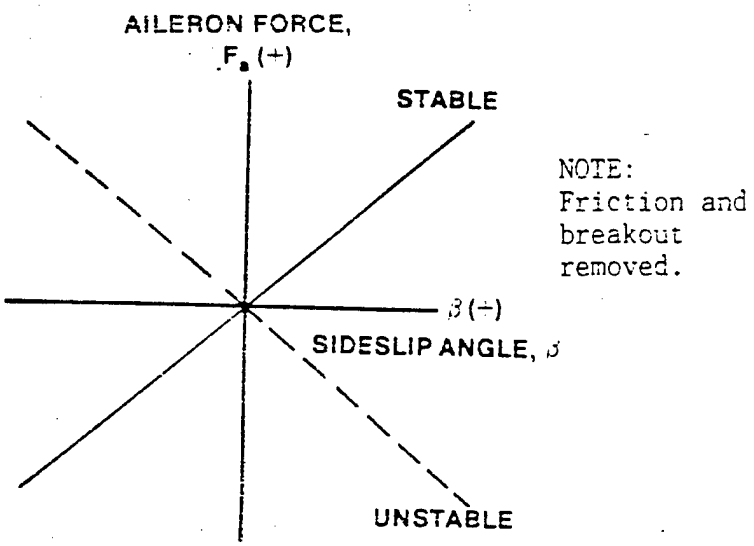


FIGURE 7.59. CONTROL FREE SIDESLIP DATA

Paragraph 4.5.5 does permit an aircraft to exhibit negative dihedral effect in wave-off conditions as long as no more than 50% of available roll control or 10 lbs of aileron control force is required in the negative dihedral direction.

Paragraph 4.5.5 also states that "an increase or no change in right bank angle shall accompany an increase in right sideslip....."

A longitudinal trim change will most likely occur when the aircraft is sideslipped. Paragraph 4.2.8.6.4 recommends limits on the allowable magnitude of this trim change. It is preferred that an increasing pull of force accompany an increase in sideslip angle and that the magnitude and direction of the trim change should be similar for both left and right sideslips. The specification also limits the magnitude of the control force accompanying the longitudinal trim change depending on the type of controller in the aircraft (stick or wheel). A plot of elevator force versus sideslip angle that complies with MIL-STD-1797Ais presented in Figure 7.60.

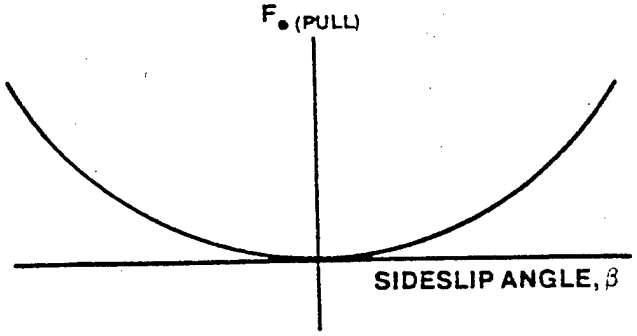


NOTE:
Friction and breakout removed.

FIGURE 7.60. ELEVATOR FORCE, $F_e$ VERSUS SIDESLIP ANGLE

EXAMPLE DATA

Sample data plots of sideslip test results are presented in Figures 7.61 and 7.62.

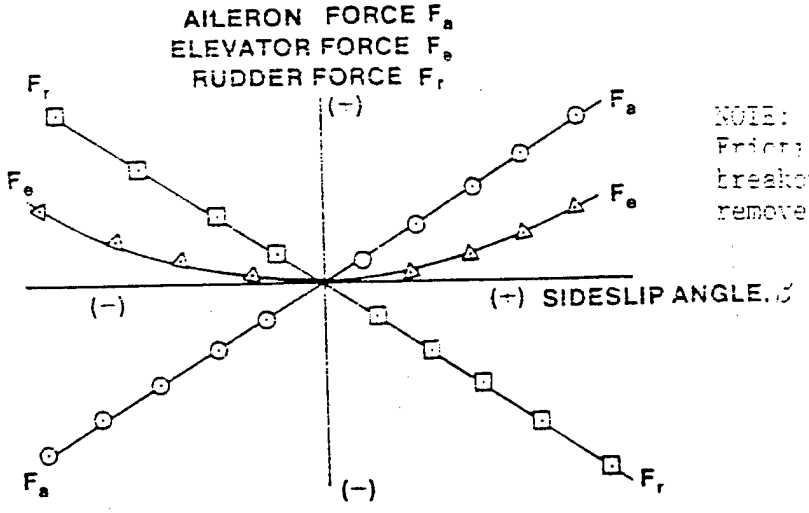


NOTE:
Friction and breakout removed.

FIGURE 7.61. STEADY STRAIGHT SIDESLIP CHARACTERISTICS CONTROL FORCES VERSUS SIDESLIP

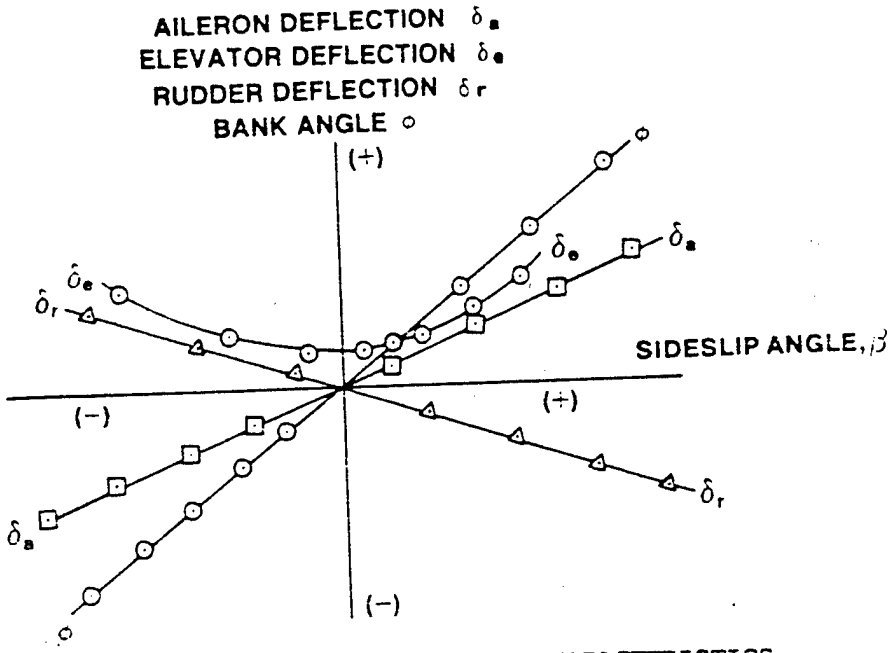


FIGURE 7.62. STEADY STRAIGHT SIDESLIP CHARACTERISTICS CONTROL DEFLECTION AND BANK ANGLE VERSUS SIDESLIP

7.6.2 Aileron Roll Flight Test

The aileron roll flight test technique is used to determine the rolling performance of an aircraft and the yawing moments generated by rolling. Roll coupling is another important aircraft characteristic normally investigated by using the aileron roll flight test technique. The roll coupling aspect of the aileron roll test will not be investigated at the USAF Test Pilot School. However, the theoretical aspects of roll coupling will be covered in Chapter 9.

To accomplish the aileron roll flight test, trim the aircraft at the desired altitude and airspeed. Then, abruptly place the lateral control to a particular control deflection (1/4, 1/2, 3/4, or full) with a step input. Normally, the desired control deflection is obtained by using some mechanical restrictor such as a chain stop. With the lateral control at the desired deflection, roll the aircraft through a specified increment of bank. For control deflections less than a maximum, the aircraft is normally rolled through 90° of bank. Because of the higher roll rates obtained at full control deflection, it is usually desirable to roll the aircraft through 360° of bank. To facilitate aircraft control when rolling through a bank angle change of 90°, start the roll from a 45° bank angle. During the roll, an automatic data recording system may be used to record the following

information: aileron position, aileron force, bank angle, sideslip and roll rate. Aileron rolls are normally conducted in both directions to account for roll variations due to engine gyroscopic effects. Aileron rolls are performed with rudders free, with rudders fixed, and are coordinated with $\beta = 0$ throughout roll.

Exercise caution in testing a fighter type airplane in rolling maneuvers. The stability of the airplane in pitch and yaw is lower while rolling. The incremental angles of attack and sideslip that are attained in rolling can produce accelerations which are disturbing to the pilot and can also cause critical structural loading. The stability of an airplane in a rolling maneuver is a function of Mach, roll rate, dynamic pressure, angle of attack, configuration, and control deflections during the maneuver.

The most important design requirement imposed upon ailerons or other lateral control devices is the ability to provide sufficient rolling moments at low speeds to counteract the effects of vertical asymmetric gusts tending to roll the airplane. This means, in effect, that the ailerons must provide a minimum specified roll rate and a rolling acceleration such that the required rate of roll can be obtained within a specified time, even under loading conditions that result in the maximum rolling moment of inertia (e.g., full tip tanks). The steady roll rate and the minimum time required to reach a particular change in bank angle are the two parameters presently used to indicate rolling capability. Pilot opinion surveys reveal that time to roll a specified number of degrees provides the best overall measure of rolling performance.

The following is a complete list of MIL-STD-1797A paragraphs that apply to aileron roll tests: 4.5.1.1, 4.5.1.4, 4.5.3, 4.5.8.1, 4.5.9.1, 4.5.9.2, 4.6.2, 4.6.7.1, 4.5.3, 4.5.9.3 and 4.5.9.5.1.

The minimum rolling performance recommended for an aircraft is outlined in MIL-STD-1797A, paragraph 4.5.8.1. This rolling performance is expressed as a function of time to reach a specified bank angle, with tables of specified values for different aircraft Classes and Flight Phases. Paragraph 4.5.9.2 specifies the maximum and minimum aileron control forces allowed in meeting the roll requirements.

Paragraph 4.6.7.1 specifies the maximum rudder force permitted for coordinating the required rolls.

In addition to examining time required to bank a specified number of degrees and aileron forces, $F_a$, it is necessary to examine the maximum roll rate, $p_{max}$, to get a complete picture of the aircraft's rolling performance. Therefore, in any investigation of aircraft rolling performance, the maximum roll rate obtained at maximum lateral control displacement is normally plotted versus airspeed.

Paragraph 4.5.3 states that there should be no objectionable nonlinearities in the variation of rolling response with roll control deflection or force. Sensitivity or sluggishness in response to small control deflections or force shall be avoided. To investigate this area, it is necessary to observe the roll response to aileron deflections less than maximum-such as 1/4 and 1/2 aileron deflections (Figure 7.63).

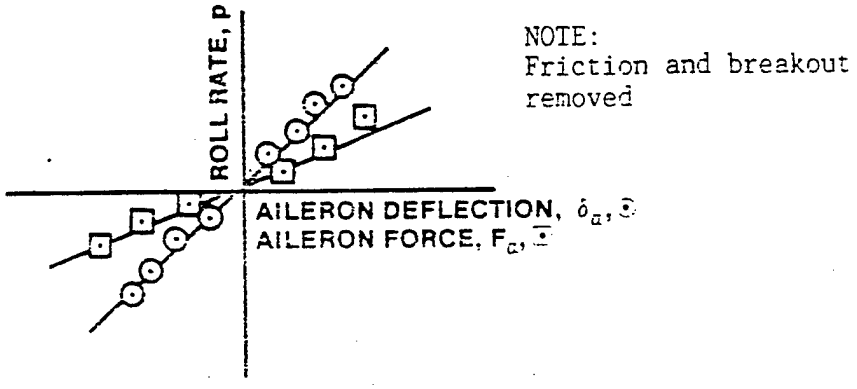


FIGURE 7.63. LINEARITY OF ROLL RESPONSE

Turn coordination requirements are spelled out in Paragraph 4.5.9.5.1 and 4.6.7.2 for steady turning maneuvers.

The other area of prime interest in the aileron roll flight test is the amount of sideslip that is developed in a roll and the phasing of this sideslip with respect to the roll rate. Associated with this characteristic is the roll rate oscillation. These factors influence the pilot's ability to accomplish precise tracking tasks.

### 7.6.3 Demonstration Flight

To unify all that has been said concerning the sideslip and aileron roll flight test techniques, a complete description of a demonstration mission is presented in the Flying Qualities Phase Planning Guide.

## PROBLEMS

7.1. Answer the following questions True (T) or False (F).

T F The primary source of directional instability is the aircraft fuselage.

T F Ailerons usually produce proverse yaw.

T F The tail contribution to $C_{n_r}$ is the dominant damping factor.

T F In a steady straight sideslip p = 0.

7.2. The aircraft shown in the following diagram is undergoing a design study to improve static directional stability. The Contractor has recommended the addition of surfaces A, B, C, D, and E. However, the System Program Office (SPO) isn't too impressed and wants the following questions answered by the Flight Test Center. With the wings in position 1 or 2 determine if the following contributions to $C_{n_\beta}$ are stabilizing (+) or destabilizing (-):

| | POSITION 1 | POSITION 2 |
|---|---|---|
| a. Vertical Tail | | |
| b. Area E (Ventral) | | |
| c. Canopy Area | | |
| d. Area B (Dorsal) | | |
| e. Area A | | |
| f. Area C | | |

g. Area D

h. Wing

i. Fuselage

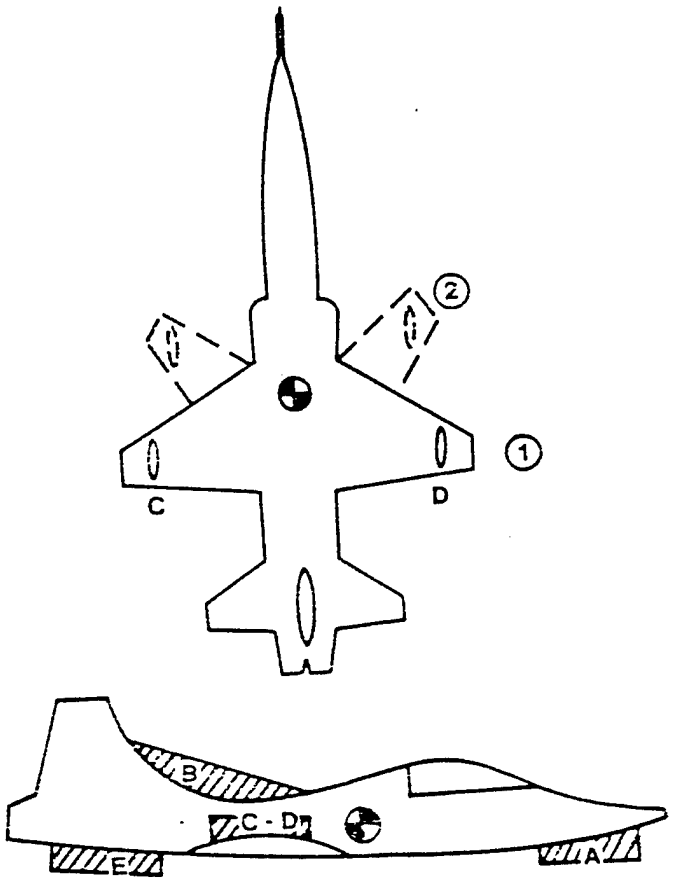


7.3. Lateral-Directional Static Stability is a function of what variables?

7.4. Sketch a curve ($C_n$ versus $\beta$) for an aircraft with stable static directional qualities and show the effect on this curve of adding a dorsal.

7.5. Does fuselage sidewash ($\sigma$) have a stabilizing or destabilizing effect on $C_{n_\beta}$? Why?

7.6. How would you design a flying wing with no protuberances in the Z direction so that it has directional stability?

7.7. What effect do straight wings have on $C_{n_\beta}$? Why?

7.8. How does increasing wing sweep ($\Lambda$) effect $C_{n_\beta}$? Why?

7.9. What effect will increasing AR have on $C_{n_\beta FIN}$? Why?

7.10. What is the sign of a left rudder deflection for a tail to the rear aircraft? For a right rudder deflection? Why?

7.11. What would the sign of $\tau$ be for a tail to the rear aircraft? Why?

7.12. For a tail to the rear aircraft, draw an airfoil showing the pressure distribution caused by $+ \alpha_F$. What is the sign of $H_r$?

What is the sign of $\partial C_h / \partial \alpha_F$. Why? Sketch a plot of $C_h$ versus $\alpha_F$.

7.13. For a tail to rear aircraft, draw an airfoil showing the pressure distribution caused by $\delta_r$. What is the sign of $H_r$ ?

What is the sign of $\partial C_h / \partial \delta_r$? Why? Sketch a plot of $C_h$ versus $\delta_r$.

7.14. Knowing $\delta_{r_{FLOAT}} = -\left[C_{h_{\alpha_F}} / C_{h_{\delta_r}}\right] \alpha_F$ for a tail to the rear aircraft, determine which direction the rudder will float for $- \alpha_F$.

7.15. Knowing $C_{n_{\beta_{(FREE)}}} = V_v a_F \left[1 - \frac{\partial \sigma}{\partial \beta}\right] \left[1 - \tau \frac{C_{h_{\alpha_F}}}{C_{h_{\delta_r}}}\right]$,

how does float effect $C_{n_\beta}$ for a tail to the rear aircraft? Tail to front?

HINT: You should be able to answer Questions 7.10 - 7.14 for a tail to front aircraft.

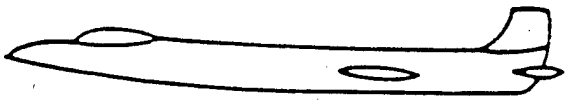

7.16. Go-Fast Inc. of Mojave has completed a preliminary design on a new Mach 3.0 fighter. The chief design engineer is concerned that the aircraft may not have sufficient directional stability. List <u>three</u> design changes/additions which would help ensure directional stability.

7.17. You are flying an F-15 Eagle on a sideslip data mission. You establish a steady straight sideslip and record +5° of $\beta$. You record the following data on your DAS: $\delta_e = -6.25°$, $\delta_a = +8.0°$, $F_e = +6.8$ lbs, $F_a = +3.7$ lbs, $F_r = -12.3$ lbs.

You had hoped to make a plot of $\partial\delta_r/\partial\beta$, but in true TPS fashion the rudder gage failed to work. The following is wind tunnel data for the F-15:

All data dimensions ($deg^{-1}$)

$C_{n_\beta} = +0.006$ $C_{n_r} = -0.460$ $C_{n_{\delta_r}} = +0.003$

$C_{n_{\delta_a}} = +0.001$ $C_{n_p} = +0.002$ $C_{n_{\dot{\beta}}} = -0.0006$

a. Determine the value of $\delta_r$ at your test point.

b. Assuming that at $\beta = 0$ both $\delta_r$ and $F_r$ are $= 0$, does the aircraft exhibit static directional stability rudder Fixed and rudder Free? Sketch plots of $\delta_r$ vs $\beta$ and $F_r$ vs $\beta$.

7.18. Given the following swing-wing fighter:

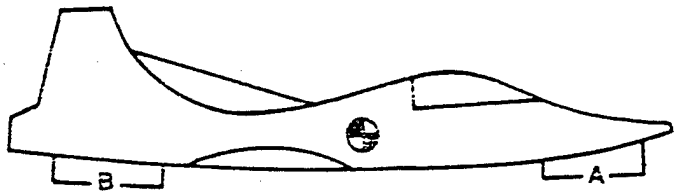


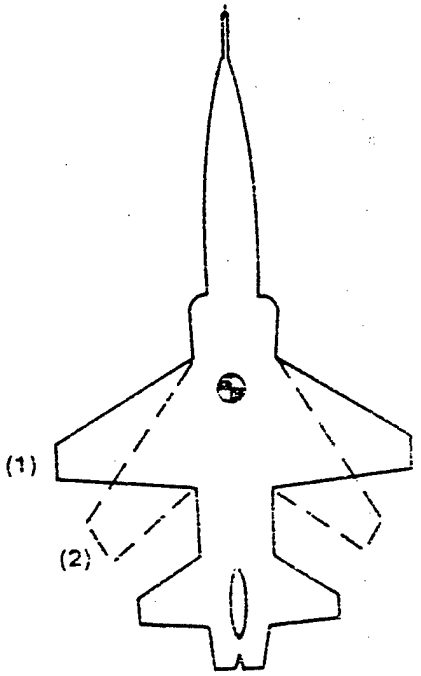


With wings in Position (1), what is the sign of $C_{l_\beta}$ for the following components?

a. Wing

b. Wing-Fuselage Interference

c. Vertical Tail
d. Area B (Ventral)
e. Area A
f. Canopy

7.19. What is the effect on $C_{l_{\beta_{wing}}}$ of sweeping the wings to Position (2)?

7.20. What is the sign of $C_{l_r}$ for the following?

a. Vertical Tail
b. Area B
c. Area A
d. Canopy

7.21. What is the sign of $C_{l_{\delta_r}}$ ?

7.22. What is the sign of $C_{l_p}$ for the following?

a. Vertical Tail
b. Area B
c. Area A
d. Canopy

7.23. For this swing wing fighter

$$C_{l_\beta} = -0.0020 \quad (\text{deg}^{-1})$$

$$C_{l_{\dot{\beta}}} = +0.0006$$

$$C_{l_p} = -0.0046$$

$$C_{l_r} = +0.0018$$

$$C_{l_{\delta_r}} = -0.0005$$

$$C_{l_{\delta_a}} = +0.0010$$

You run a steady straight sideslip test and measure $\beta = + 5°$ and $\delta_r = - 10°$. What was your aileron deflection? Does the aircraft exhibit stick-fixed static lateral stability?

7.24. For an aircraft in a right roll, show the pressure distributions that cause $C_{h_\alpha}$ and $C_{h_{\delta_a}}$ on the right wing. Determine the sign of both.

7.25. Assuming an unboosted reversible flight control system, sketch a curve of ($F_a$, $\delta_a$, $pb/2U_0$, p) versus velocity and explain the shape of each for a maximum rate roll. Show the effect of boosting the system.

7.26. Answer each of the following questions True (T) or False (F).

T F High wings make a negative contribution to $C_{l_\beta}$.

T F Taper ratio only affects the magnitude of $C_{l_\beta}$ but does not provide any asymmetric lift distribution.

T F $C_{l_{\beta_{fin}}}$ is increased if the fin area ($S_F$) is decreased.

T F $C_{l_r}$ and $C_{l_{\delta_r}}$ are cross derivatives.

T F $C_{l_\beta}$ is a significant factor in determining aircraft lateral stability.

BIBLIOGRAPHY

1. Perkins, C. D., and Hage, R. E., Airplane Performance Stability and Control, John Wiley & Sons., New York NY, 1949.

2. Perkins, C. D., Editor, Flight Testing, Volume II, Stability and Control, North Atlantic Treaty Organization, Pergamon Press, New York NY, 1962.

3. Anon., Military Standard, Flying Qualities of Piloted Aircraft, MIL-STD-1797A, Department of Defense, Washington DC 20402, 30 Jan 90.